



The impact of climate change and climate variability on coastal wetland ecosystem dynamics

Faeza Fortune

Submitted in fulfilment of the academic requirement for the
degree of Master of Arts in the Faculty of Arts at the
University of the Western Cape



Preface

The research described in this thesis was carried out at the Department of Geography, Environmental Studies and Tourism, University of the Western Cape, from January 2016 to December 2018, under the supervision of Dr SE Grenfell.

Declaration

The research presented in this thesis is my own work that has not been submitted in any form to another University. The references used in this study have been duly acknowledged in the text and presented by means of a complete reference list. The thesis has been checked for plagiarism by my supervisor via submission to Turnitin.



Acknowledgements

I would like to thank the following people and originations for their support and contributions to this research:

My supervisor, Dr SE Grenfell, thank you for your unconditional supervision, support, encouragement and friendship. Thank you for sharing your enthusiasm and love for research.

The National Research Fund (NRF) Alliance for Collaboration on Climate and Earth System Science (ACCESS), for funding my research.

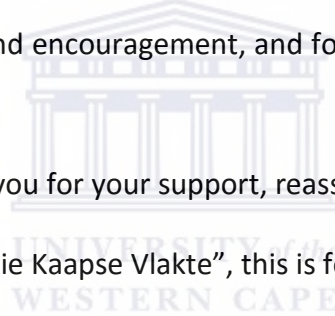
The Agricultural Research Council (ARC) for providing their rainfall data.

The UWC Institute for Water Studies for allowing me to use their lab.

To the staff of the Department of Geography, Environmental Studies and Tourism, thank you for the constant reaffirmation and encouragement, and for making the department feel like home.

To my family and friends, thank you for your support, reassurance and constant motivation.

To my Cape Flats Community, “Die Kaapse Vlakte”, this is for us.



Abstract

This thesis investigates the influence of climate change and climatic variability on wetland ecosystems (coastal and inland wetlands) on the Agulhas coastal plain. Firstly, this research examines coastal wetland ecosystem resilience to sea level rise by modelling sea level rise trajectories for the Droë River wetland. The rate of sediment accretion was modelled relative to IPCC sea level rise estimates for multiple RCP scenarios. For each scenario, inundation by neap and spring tide and the 2-, 4- and 8-year recurrence interval water level was modelled over a period of 200 years. When tidal variation is considered, the rate of sediment accretion exceeds rising sea levels associated with climate change, resulting in no major changes in terms of inundation. When sea level rise scenarios were modelled in conjunction with the recurrence interval water levels, flooding of the coastal wetland was much greater than current levels for the 1 in 4 and 1 in 8 year events. The study suggests that for this wetland, variability of flows may be a key factor contributing to wetland resilience.

Secondly, the thesis examines the variability of open wetland water surface areas and their relation to rainfall to determine wetland hydrological inputs for the Nuwejaars wetland system and respective wetlands. A remote sensing approach was adopted, Landsat 5 TM and 8 OLI multispectral imagery were used to detect changes of water surfaces for the period 1989 to 2017. Water surfaces were enhanced and extracted using the Modified Normalized Difference Water Index of Xu (2006). The coefficient of variation of wetland water surface area was determined. The variability ranges from low to high for respective wetlands. A correlation analysis of wetland water surfaces and local and catchment rainfall for the preceding 1, 3, 6, 9, 12 and 24 months was undertaken. The preceding month and associated inputs explains the annual variability of surface waters. The study suggests that, the variability of wetland water surface area are related to variations to water inputs and groundwater, as well as variations in water outputs such as evapotranspiration and an outlet channel.

Key words: wetlands, resilience, sea level rise, sediment accretion, water surface area variability, rainfall variability, wet climatic phase.

Contents

Preface	ii
Declaration	iii
Acknowledgements	iv
Abstract	v
Contents	vi
List of Tables	ix
List of Figures	x
Acronyms and Abbreviations	xiv
Chapter 1: Introduction	1
1.1 Background to research.....	1
1.2 Research aim and objectives	2
1.3 Background to study area.....	2
1.4 Structure of thesis.....	4
Chapter 2: Literature Review	5
2.1 Global climate change and climatic variability	5
2.2 Climate Variability in southern Africa	6
2.2.1 The influence of climatic oscillations on wetland ecosystems	8
2.3 Methods for estimating wetland response to external environmental changes.....	9
2.3.1 Inundation modelling approaches of coastal wetlands: static versus hydrodynamic modelling	9
2.3.2 The application of remote sensing techniques in coastal wetlands.....	12
Chapter 3: Coastal wetland resilience to climate change: modelling inundation responses to rising sea levels	16
3.1 Introduction	16

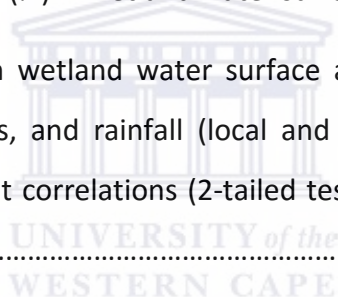
3.2 Materials and Methods.....	18
3.2.1 Data collection	18
3.2.2 Data analysis	26
3.3 Results.....	28
3.3.1 Sediment accretion rates	28
3.3.2 Sediment accretion rates and sea level rise outputs.....	29
3.4 Discussion.....	42
3.4.1 Coastal wetland resilience: sediment accretion versus sea level rise	42
3.4.2 Coastal wetlands in balance: the impact of flow variability	44
Chapter 4: Inland wetlands on a hydrological continuum: variations in hydrological inputs determined using a remote sensing approach	47
4.1 Introduction	47
4.2 Materials and Methods.....	49
4.2.1 Study site.....	49
4.2.2 Data collection	51
4.2.3 Data analysis	53
4.2.3.2 Statistical analysis of rainfall and wetland water surface area	55
4.3 Results.....	56
4.3.1 Rainfall variability of two rainfall stations	56
4.3.2 Variability in wetland water surface	58
4.3.3 Wetland water surface area and rainfall correlations	69
4.4 Discussion.....	76
4.4.1 Understanding the variability of wetland water surface area.....	76
4.4.2 Implications for wetland management and rehabilitation.....	78
4.4.3 A potential monitoring tool	80

Chapter 5: Discussion and conclusion	82
5.1 Wetlands in dry climates: the influence of wet cycles	82
5.2 Wetland management in variable landscapes: local versus catchment management.....	83
5.3 Conclusion.....	84
5.3.1 Recommendations	84
References	86



List of Tables

Table 3.1: The tide levels below are mean heights for MSL, MHWN, MHWS and HAT tides....	25
Table 3.2: The water level station for the Heuningnes River is located downstream, in the De Mond Nature Reserve. It is attached to the footbridge which extend across the river and is operated by the Department of Water and Sanitation.....	25
Table 4.1: Hydrogeomorphic characteristics of the Nuwejaars wetland ecosystems.....	50
Table 4.2: Landsat 5 TM and Landsat 8 OLI specifications.....	52
Table 4.3: Specifications of ARC rainfall stations.....	53
Table 4.4: The MNDWI equation for Landsat 5 TM and Landsat 8 OLI.....	54
Table 4.5: Coefficient of Variation (%) in wetland water surface area (ha).....	59
Table 4.6: Correlations between wetland water surface area for the Nuwejaars Wetland System and respective wetlands, and rainfall (local and catchment) for 1 to 24 months preceding image date. Significant correlations (2-tailed test) are in italics (0.01 confidence) and bold (0.05 confidence).....	69



List of Figures

- Figure 1.1: The location of the Agulhas Coastal Plain, along the south-western cape coast of southern Africa (insert map a). The large map indicates the relative elevation (m) of the Agulhas Coastal Plain, derived from a STRM digital elevation model (map b). The wetlands are located on the south-eastern region of the plain and is extensively surrounded by agriculture activities.....3
- Figure 2.1: Global mean sea level rise and precipitation change projection for 2081- 2100 relative to 1986-2005 (Church et al, 2013 and Hartmann et al., 2013).....6
- Figure 2.2: Spectral reflectance signatures of water, built-up land and vegetation (Xu, 2006).13
- Figure 3.1: Location of the Droë River wetland (i.e. study site) adjacent to the Heuningnes Estuary indicated by the large map (Figure 3.1a). The Droë River is located on an abandoned channel of the Kars River, which now flows into the Heuningnes River toward the west. The inset map of Figure 3.1b indicates the position of the bulk density plots, astroturf mats, the ^{210}Pb sediment core as well as the area of the detailed DGPS survey.....19
- Figure 3.2: Astroturf mats were installed across the Droë River wetland to measure the rate of short-term sediment accretion.....20
- Figure 3.3: Bulk density samples were collected at various homogenous sites within the wetland. Sampling sites were stratified by vegetation community within the wetland, *Sarcocornia perennis* or *Sarcocornia littorea* (left), salt tolerant samphire's, grass and creeping herbs (middle) and *Phragmites australis* (right).....20
- Figure 3.4: How a differential GPS works (ESRI, 2018). The base station receiver is setup precisely at a known position. The location of the receiver is computed based on a number of satellites e.g. GLONASS satellites. The difference in base station position is calculated and corrected in real-time relative to the rover GPS receiver.....22
- Figure 3.5: A detailed DGPS survey was conducted within the wetland. The survey captures the morphology of the wetland, in some areas, the old river course can be seen.....22

Figure 3.6: Extent of the LiDAR dataset across the Agulhas Plain (Cape Nature, 2017).....	23
Figure 3.7: IPCC RCP global mean sea level rise projections corrected to Hartebeeshoek 94 datum.....	24
Figure 3.8: Sediment accretion and sea level rise model iteration workflow summary.....	27
Figure 3.9: The Pb ²¹⁰ activity profile of the wetland core (left) and variability in sediment accretion rates as calculated from sediment deposited on recovered astroturf mats.....	29
Figure 3.10: Low accretion rate scenario for Inundation levels associated with the astroturf accretion rate: Mean High Water Neap (MHWN) and Mean High Water Spring (MHWS) tide model predictions for respective Representative Concentration Pathway (RCP) scenarios, a). RCP 2.6 (low emission scenario) b). RCP4.5 (intermediate emission scenario) c). RCP 6.0 (intermediate emission scenario) and d). RCP 8.5 (high emission scenario).....	31
Figure 3.11: High accretion rate scenario for Inundation levels associated with the Pb ²¹⁰ accretion rate: Mean High Water Neap (MHWN) and Mean High Water Spring (MHWS) tide model predictions for respective Representative Concentration Pathway (RCP) scenarios, a). RCP 2.6 (low emission scenario) b). RCP4.5 (intermediate emission scenario) c). RCP 6.0 (intermediate emission scenario) and d). RCP 8.5 (high emission scenario).....	32
Figure 3.12: Low accretion rate scenario comparing water levels at different recurrence interval model for the astroturf accretion rate: predictions for RCP 2.6 (low emission scenario), a). 1 in 2 years b). 1 in 4 years and c). 1 in 8 years.....	33
Figure 3.13: Low accretion rate scenario comparing water levels at different recurrence interval model for the astroturf accretion rate: predictions for RCP 4.5 (intermediate emission scenario), a). 1 in 2 years b). 1 in 4 years and c). 1 in 8 years.....	34
Figure 3.14: Low accretion rate scenario comparing water levels at different recurrence interval model for the astroturf accretion rate: predictions for RCP 6.0 (intermediate emission scenario), a). 1 in 2 years b). 1 in 4 years and c). 1 in 8 years.....	35

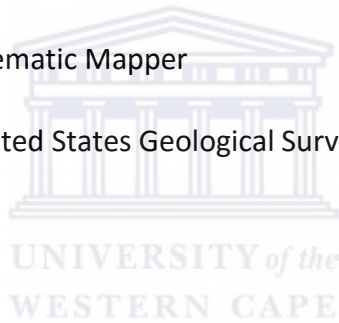
Figure 3.15: Low accretion rate scenario comparing water levels at different interval model for the astroturf accretion rate: predictions for RCP 8.5 (high emission scenario), a). 1 in 2 years b). 1 in 4 years and c). 1 in 8 years.....	36
Figure 3.16: High emission scenario comparing water levels at different recurrence intervals based on the Pb ²¹⁰ accretion rate. Predictions for RCP 2.6 (low emission scenario), a). 1 in 2 years b). 1 in 4 years and c). 1 in 8 years.....	37
Figure 3.17: High accretion rate scenario comparing water levels at different water level recurrence interval model for the ²¹⁰ Pb accretion rate: predictions for RCP 4.5 (intermediate emission scenario), a). 1 in 2 years b). 1 in 4 years and c). 1 in 8 years.....	38
Figure 3.18: High accretion rate scenario comparing water levels at water level recurrence interval model for the ²¹⁰ Pb accretion rate: predictions for RCP 6.0 (intermediate emission scenario), a). 1 in 2 years b). 1 in 4 years and c). 1 in 8 years.....	39
Figure 3.19: High accretion rate scenario comparing water levels at different water level recurrence interval model for the ²¹⁰ Pb accretion rate: predictions for RCP 8.5 (high emission scenario), a). 1 in 2 years b). 1 in 4 years and c). 1 in 8 years.....	40
Figure 3.20: Conceptual model of coastal wetland resilience and the feedbacks between flow variability, sea level rise and wetland accretion rates.....	45
Figure 4.1: The location of Nuwejaars wetland system (map a), near the southernmost tip of Africa (insert map b). These wetlands are characterized by large areas of open surface water, some are interlinked to the Nuwejaars River system and other are isolated endorheic pans/depression. Insert map c indicates the locations of local (Prinskraal) and catchment (Jonaskraal) rainfall stations relative to the wetlands.....	49
Figure 4.2: MNDWI iteration summary for Landsat 5 TM and Landsat 8 OLI for the period 1989 – 2017.....	54
Figure 4.3: Precipitation record presented for Prinskraal, indicating monthly mean precipitation, annual precipitation, seasonality and inter-annual variability.....	57

Figure 4.4: Precipitation record presented for Jonaskraal, indicating monthly mean precipitation, annual precipitation, seasonality and inter-annual variability.....	58
Figure 4.5: Variations in wetland water surface area for the Nuwejaars Wetland System (period 1989 -2017).....	60
Figure 4.6: Variations in wetland water surface area for Waskraalvlei (period 1989 -2017)....	61
Figure 4.7: Variations in wetland water surface area for Die Anker (period 1989 -2017).....	62
Figure 4.8: Variations in wetland water surface area for Varkvlei (period 1989 -2017).....	63
Figure 4.9: Variations in wetland water surface area for Rondepan (period 1989 -2017).....	64
Figure 4.10: Variations in wetland water surface area for Voëlvlei (period 1989 -2017).....	65
Figure 4.11: Variations in wetland water surface area for Soutpan (period 1989 -2017).....	66
Figure 4.12: Variations in wetland water surface area for Langpan (period 1989 -2017).....	67
Figure 4.13: Variations in wetland water surface area for Soetendalsvlei (period 1989 -2017).....	68
Figure 4.14: Percentage of variation in wetland water surface area for the preceding 1 - 24 months.....	69
Figure 4.15: The continuum of wetlands on the Agulhas coastal plain and their associated wetland hydrological inputs and outputs.....	78

Acronyms and Abbreviations

AOGCM	Atmosphere Globe Circulation Model
ARC	Agricultural Research Council
CMIP5	Coupled Model Intercomparison Project 5
CV	Coefficient of Variation
DEM	Digital Elevation Model
DGPS	Differential Global Positioning System
DTM	Digital Terrain Model
ENSO	El Niño-Southern Oscillation
ETM+	Enhanced Thematic Mapper Plus
GIS	Geographic Information System
GLONASS	Global Navigation Satellite System
GPS	Global Positioning System
HAT	Highest Astronomical Tide
IPCC	Intergovernmental Panel on Climate Change
LiDAR	Light Detecting and Ranging
LLD	Land Levelling Datum
MHWN	Mean High Water Neap
MHWS	Mean High Water Spring
MIR	Middle Infrared
MNDWI	Modified Normalized Difference Water Index
MODIS	Moderate Resolution Imaging Spectroradiometer

MSL	Mean Sea Level
NDWI	Normalized Difference Water Index
NDVI	Normalized Difference Vegetation Index
NIR	Near infrared
OLI	Operational Land Imager
RCP	Representative Concentration Pathway
SANPARKS	South African National Parks
SMA	Special Management Unit
STRM	Shuttle Radar Topography Mission
SWIR	Shortwave Infrared
TM	Thematic Mapper
USGS	United States Geological Survey





UNIVERSITY *of the*
WESTERN CAPE

Chapter 1: Introduction

1.1 Background to research

Wetland ecosystems (i.e. coastal and inland wetlands) are often referred to as the 'kidneys of the earth' (Mitsch and Gosselink, 2015). These inherently dynamic and complex ecosystems are extremely vulnerable to changes in environmental conditions which are largely driven by land use changes. According to Zedler and Kerher (2005) approximately 50% of wetland ecosystems have already been lost and degraded as result of landuse changes, particularly through the conversion of wetlands to agricultural lands. In addition to the threats posed by land use changes, growing international and regional recognition has been placed on the influence of anthropogenic induced climate change on the structural and functional attributes of wetland ecosystems (Mitsch and Gosselink, 2015). Growing scientific evidence suggests with certainty that the earth's climate is changing at an unsettling pace with global temperatures rising, glaciers melting, rising sea levels and exacerbated changes in weather and climate (IPCC, 2013). The current degree of change associated with the anthropogenic warming of the earth through sea level rise and exacerbated variations in rainfall patterns, are projected to result in a cascade of effects on human livelihoods and their well-being, and natural ecosystems such as wetlands (Mitsch and Gosselink, 2015).

In order to prevent further loss and degradation, regional and international impetus initiated by international agencies such as the Ramsar convention and local agencies such as the South African National Biodiversity Institute (SANBI), has placed emphasis regaining lost wetland ecosystems and better conservation. Focus has thus been placed on optimizing the services provided by these ecosystem for human livelihoods; to regain lost and degraded services through prioritization and effective rehabilitation strategies; and to ultimately facilitate sustainable wetland management and conservation (Euliss et al., 2008). Co-operative management and rehabilitation requires not only a deep understanding of how and why wetlands function, but equally important is understanding how wetlands will respond to climate change, particularly wetlands in marginal climate settings.

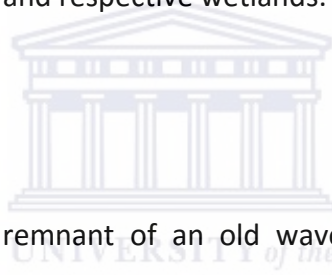
1.2 Research aim and objectives

Aim:

This research aims to investigate wetlands response to climate change and climatic variability, in order to understand how wetlands change and adapt in marginal climates, on the Agulhas Coastal Plain, South Africa.

Objectives:

1. Determine sediment accretion to model and predict coastal wetland resilience to sea level rise and inundation for the Droë River coastal wetland.
2. Examine and compare the relationship between rainfall and variations of wetland water surface area for the Nuwejaars River system and respective wetlands.
3. Determine and understand the influence of rainfall on wetland hydrological inputs for the Nuwejaars River system and respective wetlands.



1.3 Background to study area

The Agulhas coastal plain is a remnant of an old wave-cut platform, stretching across 270 000 ha, bounded by the Cape Fold Mountains ranges in the north and the Atlantic and Indian oceans in the south (Kraaji et al., 2008). Nestled in these coastal lowlands, towards the south-eastern region of the plain, is a variety of interlinked and isolated wetland ecosystems known as the Nuwejaars wetland system. These include a unique diversity of depressions (i.e. pan), vleis, lakes, valley-bottom and floodplain wetlands. These wetlands are either isolated or are associated with the Nuwejaars River, of which the Kars River is a tributary. The combined Kars and Nuwejaars River is called the Heuningnes River and flows out to sea at an estuary which is known locally as De Mond. This region is situated in a winter rainfall zone (Schulze, 1997), characterised by a Mediterranean climate with hot dry summers and cold wet winters. Strong westerly and easterly winds prevail all year round with annual rainfall ranging between 400 and 600 mm/yr, with most rainfall occurring between the months of May and October (Bertsky 2013).

The Agulhas Plain is a unique and diverse ecologically sensitive region, serving as a storehouse for a variety of endemic, rare and endangered species (i.e. terrestrial and wetland vegetation, bird, freshwater, estuarine and marine species). This region is renowned for its conservation value, housing the Cape Floristic Region which is an internationally recognized Biodiversity Hotspot; the Heuningnes Estuary and De Hoop Vlei which are Ramsar Wetlands of International Importance; and Soetendalsvlei which is the second largest lacustrine wetland in South Africa (Kraaji et al., 2008). These wetland systems together with the Overberg Wheatbelt provide excellent habitat for a variety of bird species, particularly species such as the Blue Crane (*Anthropoides paradiseus*), Denham’s Bustard (*Neotis denhami*), the endangered Cape Vulture (*Gyps coprotheres*) and many more (United Nations, 2013).

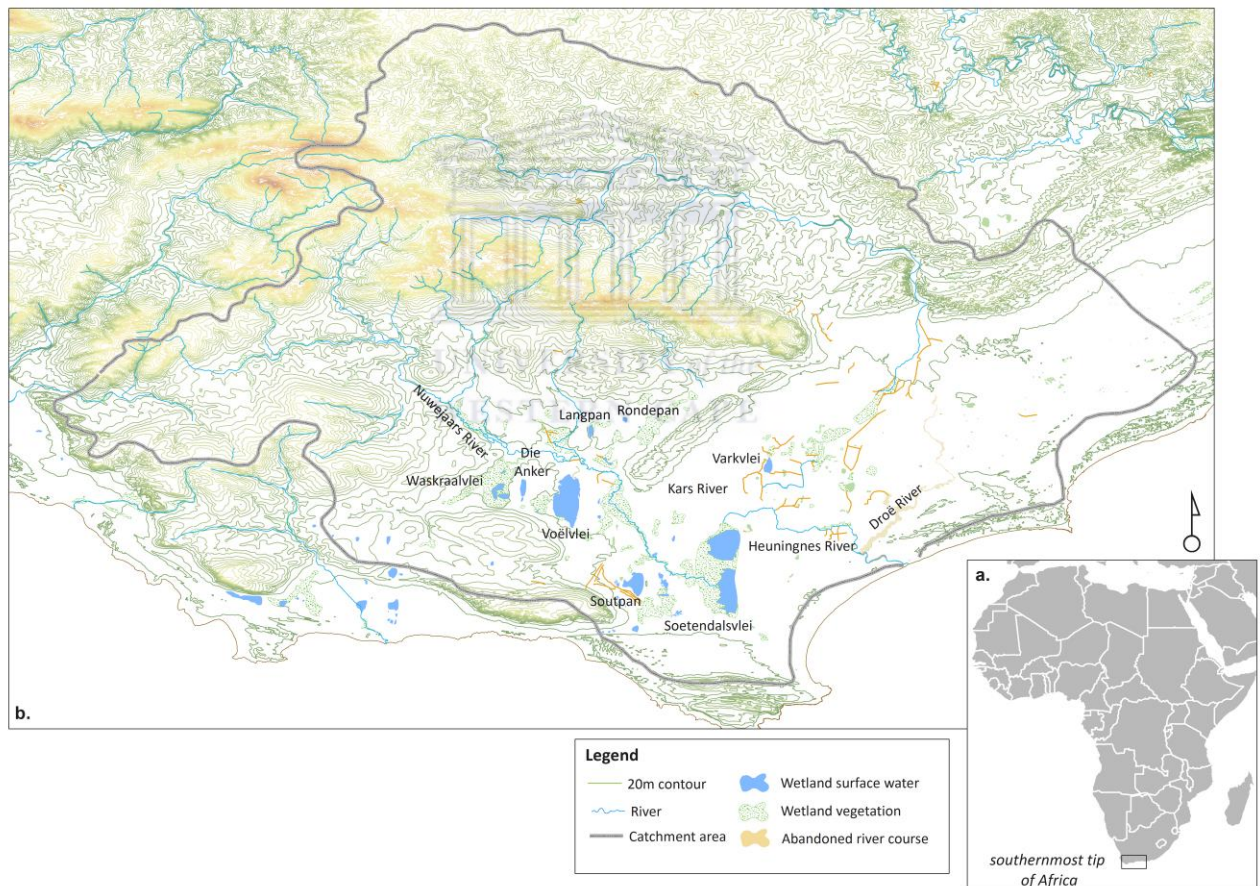


Figure 1.1: The location of the Agulhas Coastal Plain, along the south-western cape coast of southern Africa (insert map a). The large map indicates the catchment topography and location of the wetlands towards the south-eastern region of the Agulhas Coastal Plain (map b).

The Agulhas region is used extensively for the cultivation of wheat and canola, as well as livestock farming. Agriculture is one of the major anthropogenic pressures threatening the sustainability of fynbos, wetland and river ecosystems within this region (Kraaji et al, 2008). Conservation and rehabilitation efforts have been implemented across the plain. These efforts have persisted under authorities such as South African National Parks (SANPARKS), Cape Nature, Working for Wetlands, Working for Water and private landowners, i.e. the Nuwejaars Wetland Special Management Area (SMA).

1.4 Structure of thesis

The overall structure of the thesis follows the general formatting principles of a standard thesis. However, Chapters 3 and 4 are presented in a manuscript format as they are intended for publication. Portions of Chapter 3 have been included in a manuscript accepted to *Anthropocene Coasts*, along with contributions from Dr S Grenfell and F Mamphoka. The work presented here is all my own. Chapter 4 is being formatted for submission to *Wetlands Ecology and Management* in 2019. The content and design of the thesis takes the reader from a broad scale literature review on the future of wetlands in a climatically changing world, techniques for modelling sea level rise, and the remote sensing of wetlands (Chapter 2). This is followed by a detailed micro scale focus on the Droë River wetland response and resilience to inundation and associated global mean sea level rise (Chapter 3) and then an exhaustive examination of wetland hydrologic dynamics using remote sensing on the Nuwejaars wetland system as a whole (Chapter 4). Chapters 3 and 4 contain a detailed literature review relevant to these chapters, as well as individual methods and discussion. This is in order to expedite publication following examination, although it results in some minor repetition. The thesis is then synthesized in a general overall discussion and conclusion in Chapter 5.

Chapter 2: Literature Review

2.1 Global climate change and climatic variability

Comprehensive observations of global climates are provided by paleoclimate reconstructions, remote sensing technology and direct measurements (IPCC, 2013). The evidence gathered suggests that the unprecedented warming of the earth's climate system is influenced by anthropogenic activities, while natural emissions from volcanoes and changes in solar irradiance (i.e. natural radiative forcing) are responsible for some perturbations (IPCC, 2013). Natural emissions are not responsible for a trend of increasing temperature, sea level rise and changes in weather and climate (IPCC, 2013).

Changes in climatic systems are inevitable, even under the influence of natural radiation forcing (IPCC, 2013). In addition to natural forcing, changes in climate can be influenced by natural variability in climatic systems such as the glacial-interglacial cycles and interannual variability such as the El Niño-Southern Oscillation (ENSO) (IPCC, 2013). However, as a result of increasing anthropogenic activities and greenhouse gas emissions, the natural variability exhibited in the presence of external influences has been exacerbated (IPCC, 2013 and Engelbrecht et al., 2015). As indicated by several sophisticated climatic models that have been developed to investigate past, current and future changes; global sea surface and land temperatures are rising, there are large scale changes in weather, climate and the hydrological cycle, glaciers are melting, and the rate of sea level rise is increasing (IPCC, 1990; 1996; 2001; 200; 2013).

According to Church et al., (2013), it is likely that global mean sea level will rise into and beyond the 21st century as indicated by all RCP scenarios, shown in Figure 2.1. The projected rates for global mean sea level rise for the period 2081 – 2100 relative to 1986 – 2005 will likely range between 0.26 m to 0.98 m for all Represented Concentration Pathway (RCP) scenarios (IPCC, 2013). Dominant factors contributing to sea level rise include ocean thermal expansion; melting glaciers and ice sheets (from Greenland and Antarctic), and changes in land surface water storage (e.g. rivers, wetlands, aquifers) influenced by climate change, climatic variability and human influences (IPCC, 2013). Concerning current changes related to

weather and climate, extreme events have increased since the 1950s (Hartmann et al., 2013). Some of the extreme events include frequent occurrence of heat waves in Europe, Asia, and Australia; increase in the frequency and intensity in rainfall and contrasting drought cycles across Africa and parts of Australia; and changes in the global hydrological cycle (Hartmann et al., 2013).

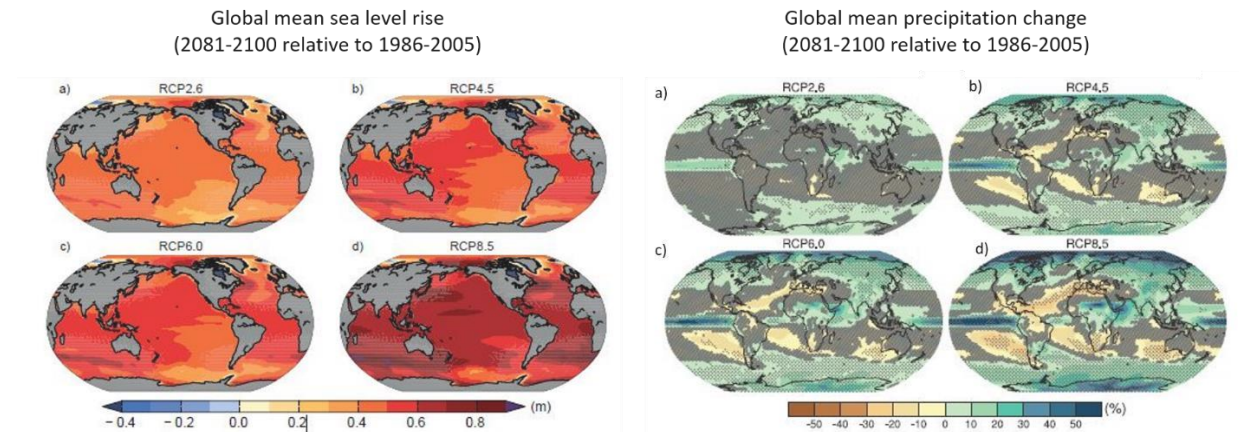


Figure 2.1: Global mean sea level rise and precipitation change projection for 2081- 2100 relative to 1986-2005 (from Church et al., 2013 and Hartmann et al., 2013).

2.2 Climate Variability in southern Africa

Southern Africa is a predominantly semi-arid region with high rainfall variability characterised by sporadic occurrences of drought and flood (Vogel, 2000; Engelbrecht et al., 2015). According to Tyson (1981), the long term variations in rainfall over Southern Africa can be partially explained in terms of variations in climatic oscillations. Climatic oscillations are recurring changes in annual rainfall, which may occur at regular intervals and may be investigated through long-term rainfall data (Tyson and Preston-Whyte, 2000). Ongoing research suggests that there are many notable oscillations patterns which influence rainfall variability in southern Africa (Kane, 2009; Pohl et al., 2010; Oettli et al., 2014). The most important and distinctive patterns are the 3 to 6 years, 10 to 12 years and 18-year oscillation (Vogel, 2000; Tyson et al., 2002; Dieppos et.al., 2015; Morioka et al., 2015). The most notable oscillations are the 3 to 6 and 18-year oscillations for the reason that studies are generally limited to 10-years of data which is insufficient to detect decadal oscillations (Dieppois et al., 2015).

The 18 year oscillation is spatially variable and predominant in the north-eastern, summer rainfall region of South Africa and extends into Zimbabwe and Botswana (Kane, 2009). Historical evidence of this oscillation were initially inferred by travel journals which were considered unreliable (Tyson and Preston-Whyte, 2000). Precipitation anomaly maps were then reconstructed and illustrated evidence of potential wet and periods (Tyson and Preston-Whyte, 2000). For example, the period 1825 to 1829 was characterized by desiccation and drought, followed by reports of rain and floods (see Tyson and Preston-Whyte, 2000). Nevertheless, meteorological evidence indicate a number of quasi- periodic oscillations since the 19th century (Tyson and Preston-Whyte, 2000). The occurrences of droughts and floods for the 18 year oscillation are anomalous in which rainfall generally exceeds the mean during 9 years and is below the mean for 9 years (Tyson and Preston-Whyte, 2000).

The 10 to 12 year oscillation predominantly affects the southern coastal region and the adjacent inland area (Kane, 2009). According to Vogel (2000), this oscillation accounts for over 30% of inter-annual rainfall variability along this region. The 3 to 6 year oscillation is associated with ENSO and is pervasive throughout southern Africa (Vogel, 2000; Reason et al., 2006). ENSO events are usually linked to drought and flood events in South Africa (Rouault and Richard, 2003; Malherbe et al., 2012). During an ENSO phase, the rainfall received is below average as the cloud bands move offshore of South Africa and with it the highest rainfall (Tyson and Preston-Whyte, 2000; Nel, 2009). (Tyson and Preston-Whyte, 2000). Conversely, during La Nina event, the region receives higher than average rainfall as the cloud band coverage extends across southern Africa, resulting in the frequent occurrence of flood events (Tyson and Preston-Whyte, 2000; Vogel, 2000; Nel, 2009).

This phenomenon is one of the leading factors influencing interannual variability in rainfall in southern Africa (Vogel, 2000), with a coefficient of variation exceeding 40% in the western region (Nel, 2009). According to Rouault and Richard (2003), the occurrences of droughts have increased considerably with different intensities, spatial extents and duration across South Africa since the late 1960, and wet years have been enhanced since the 1970s (Rouault and Richard, 2003). Since then, the southern African region has experienced eight severe droughts occurring in 1996, 1970, 1973, 1979, 1983, 1992, 1995 and most recently 2015 (Rouault and Richard, 2003;Baudoin et al., 2017). This is possibly as a result of climate change, however,

this is not fully understood and requires thorough investigations (Dai and Trenberth, 1998; Rouault and Richard, 2003).

2.2.1 The influence of climatic oscillations on wetland ecosystems

It is evident that droughts and floods are a recurring phenomenon in southern Africa. Some authors suggest that as a result of increasing greenhouse gas emissions investigated under low mitigation scenarios, the impact of climate change across southern Africa is projected to change annual and seasonal patterns in rainfall and temperature (Niang et al., 2014; Engelbrecht et al., 2015). These variations are known to have major consequences for human livelihoods (e.g. Smith and Rhiney, 2016; Ankrah, 2018; Biggs et al., 2018), food security (e.g. Murphy and Timbal, 2008; Krishnamurthy et al., 2012; Ding et al., 2017) and natural ecosystems such as wetlands (e.g. Short et al., 2016; Harvriil et al., 2018; Scheiter et al., 2018).

Wetlands are globally recognized as the earth's most valuable and productive ecosystems, providing a variety of ecosystem services to the biophysical environment and human livelihoods (Mitsch and Gosselink, 2015). Naturally, wetlands are complex and dynamic, their physical structure are shaped by movements of mass and their functional characteristics influenced by earth systems processes (Tooth and McCarthy, 2007; Ellery et al., 2009). As a result, these ecosystems are extremely sensitive to the influence of droughts and floods associated with climatic oscillations such as ENSO and the 18-year oscillation (see Drexler and Ewel, 2001; Short et al., 2016).

The influence of short-term climatic perturbations such as El Niño/La Niña and related events are largely associated with direct and indirect changes to the functioning of wetlands (House et al., 2016). During drought conditions rainfall is limited resulting in dramatic changes in wetland hydrology. For example, the decline in rainfall results in limited water inputs (e.g. direct precipitation, overland flow, throughflow and groundwater recharge). This alters surface waters in wetlands, often leading to temporary or permanent desiccation, thus causing shifts in wetland vegetation compositions and stress on fauna and avifauna (Vilina and Cofre, 2000; Drexler and Ewel, 2001; House et al., 2016). The hydrologic stress placed on groundwater have been widely documents (Candela et al., 2009;Tulbure and Brich, 2013), with concerns related to the pressure placed on groundwater during dry periods, particularly

by human activities (e.g. excessive abstraction of water from underground aquifer). Furthermore, flooding caused by excessive rainfall may replenish wetland waters and aquifers, but could possibly increase soil erosion and submerge flood-intolerant vegetation (Zhang et al., 2019).

Long-term climatic perturbation such as the 18-year oscillation and related drought and flood events have been well documented by McCarthy et al. (2000) in the Okavango Delta, Botswana. Their study indicated that flooding is influenced by local rainfall in the swamp and inflow from the catchment. The 18-year oscillation is evident in precipitation and discharge records at the Shakawe and Okavango catchment (McCarthy et al., 2000). However, it differs across the catchment, suggesting that there are two oscillations which are out of phase in terms of drought and flood cycles (McCarthy et al., 2000). These authors suggest that the out-of-phase relationship acts as a buffer against flooding within the Okavango wetland since the inflow into the wetland and local rainfall can compensate each other during drought and flood cycles (McCarthy et al., 2000).



2.3 Methods for estimating wetland response to external environmental changes

Optimal wetland management and rehabilitation requires an in-depth understanding of how wetlands function, by identifying key factors which influence their structure and function, and how they respond to external perturbations (Ellery et al., 2009). With this understanding, it would be possible to better understand certain wetland process and the changes associated with them, provide more reason to mitigate human disturbances and understand implications for management (Euliss et al., 2008). As such, the application of modelling (see Chapter 3) and remote sensing techniques (see Chapter 4) have become prevalent in wetland research.

2.3.1 Inundation modelling approaches of coastal wetlands: static versus hydrodynamic modelling

The vulnerability of coastal wetlands to the inevitable rate of sea level rise have caused global concerns (Titus, 1991; Nicholls et al., 1991; Nicholls, 2004; Kirwan et al., 2010; Mogensen and Rogers, 2018). The preparation of mitigation measures and identifying priority areas prone to inundation are facilitated by modelling the current and most importantly, the future impacts

of sea level rise (Kumbier et al., 2017; Mogensen and Rogers, 2018). The traditional static modelling (i.e. bathtub model) and in recent times, sophisticated hydrodynamic modelling approaches, are widely used to model the impact of sea level rise on coastal wetland ecosystems (e.g. Kumbier et al., 2017; Mogensen and Rogers, 2018).

Static modelling is a stationary approach based on a given elevation whereby areas below a certain water level (e.g. areas below mean sea level) are inundated of which the extent is influenced by hydrologic connectivity (Teng et al., 2017; Kumbier et al., 2017). This approach is non-variable and generally assumes that inundation occurs at specific sedimentation rates corresponding to sea level rise (Mogensen and Rogers, 2018). Many authors consider static modelling of low accuracy as it often results in implausible results which are attributed to over estimations of inundation extents (Kumbier et al., 2017; Mogensen and Rogers, 2018). This is largely due to the omission of other essential factors influencing coastal wetlands response to sea level rise, such as clastic deposition during fluvial inundation, effect of rough landscape flood extant and duration, bottom friction, organic matter deposition, flood attenuation by vegetation, etc. (Breilh et al., 2013; Ramirez et al., 2016; Jankowski et al., 2017). Despite this limitation, this approach is efficient, low cost as it requires minimal computational power, and it can be simulated in a Geographic Information System (GIS) (Kumbier et al., 2017).

According to Mogensen and Rogers (2018), recent modelling approaches are shifting towards hydrodynamic modelling in order to include the variability of factors influencing coastal wetland response to sea level rise. Ramirez et al. (2016) suggests that dynamic modelling accounts for processes which cannot be simulated in static models (e.g. varying water levels in wetlands from flood drivers, including storm surges and fluvial floods). However, dynamic modelling is extremely complex to setup and generally expensive (with the exception of the Delft3D model - open source), and requires large computing power, especially if modelling at high resolutions (Teng et al., 2017; Kumbier et al., 2017). Nevertheless, some author suggests that by increasing the complexity of dynamic models to reduce inaccuracies and uncertainties, model outputs in this regard may contain more errors and uncertainty (see Snowling and Kramer, 2001; Muller et al., 2011). Models with low complexity such as static models also contains errors and are considered less accurate (Teng et al., 2017). It is therefore under

debate as to which models are appropriate for investigating environmental systems that are influenced by a variety non-linear factors (Snowling and Kramer, 2001; Muller et al., 2011).

Despite the errors in both modelling approaches, major improvements in accuracy can be made, particularly when using static models. This however, is largely dependent on the type of data collected and the system being represented. According to Mogensen and Rogers (2018), integral to accurate modelling is the use of quality empirical data, particularly data that is unique to the system and study site. Thus, if inundation modelling is done at a high spatial resolution, it could improve the overall accuracy of the model outputs in static (e.g. Grenfell et al., 2016) and hydrodynamic modelling (e.g. Rodriguez et al., 2017).

As such, essential to fine scale modelling is a high resolution digital elevation model (DEM), in the case of modelling coastal wetlands and response to rising sea levels; current elevation is often used as a starting point for spatial modelling (Mogensen and Rogers, 2018). Topography is a key driver that influence coastal change. Therefore, high resolution and accurate elevation data is required. Recent advancements in the vertical accuracy and spatial resolution of digital elevation models has improved the accuracy and detail of the earth's surface (Gesch, 2009). According to Gesch (2009), considering the complex topographic nature of the world's coastal plains, high-resolution elevation datasets provide major advances in mapping and modelling the adverse effects of sea-level rise. Predictions provided by raster modelling approaches have in the past been limited by the coarse-resolution of digital elevation models (Poulter and Halpin, 2008).

Furthermore, essential to wetland responses and their ability to maintain resilience against sea level rise is dependent on the persistence of sediment accretion rates and the interconnected processes which influence their availability (see chapter 3) (Day et al., 1999; Morris et al., 2002; Mitsch and Gosselink, 2015; Martinez et al., 2017; Mogensen and Rogers, 2018). Sediment accretion and sea level rise estimates are therefore equally essential inputs. Sediment accretion rates can be derived from several methods, such as short-term accretion rates derived from surface elevation table (e.g. Jankowski et al., 2016) and astroturf mats (e.g. Lambert and Walling, 1987). Accretion rates can be derived from Pb210 radiometric dating (e.g. Appleby and Oldfield, 1978).

2.3.2 The application of remote sensing techniques in coastal wetlands

In the face of climate change, and recent growing recognition of wetlands as global key ecosystem providers, management of wetlands is becoming increasingly important (Millennium Ecosystem Assessment, 2005; Tooth, 2018). The impetus now is to prevent further loss and provide support to maintain the structural and functional integrity of wetlands. This is facilitated by local, regional and international bodies through environmental management, policies and legislation, and rehabilitation strategies. Essential to effective management is an in-depth understanding of the functional and structural dynamics of wetland ecosystems, particularly in highly variable environments.

Dues and Gloanguen (2013) suggests that characterizing environmental changes is the first step towards understanding the drivers of change, and with this, decision makers are better equipped to support effective management. Over the past five decades, remote sensing technology has proven to be an essential tool that provides indispensable spatial information about the earth's surface and features, the ocean and atmosphere (Jones et al, 2009; Guo et al., 2017). The spatial information provided is enhanced through a variety of spectral, spatial, temporal and radiometric resolutions (Campbell and Wynne, 2013; Guo et al., 2017). Thus serving as a unique platform to detect, monitor and characterize changes over time (Dues and Gloanguen, 2013). The remote sensing of wetlands and freshwater ecosystems has become popular given increasing anthropogenic and climatic pressures (Guo et al., 2017).

The accurate delineation and estimation of water features requires precise surface water extraction techniques (Dues and Gloanguen, 2013), which has become possible over the last decade with the development of several extraction techniques (Ji et al., 2009; Klemas, 2011; Li et al., 2013). General classification methods such as the maximum likelihood, decision tree and support vector machine classifications, are among the most commonly used methods for extracting surface waters (Li et al., 2013). However, these methods are principally based on the nature of features within a pixel, which depending on the complexity of the landscape, can lead to misclassification (i.e. over or under estimated surface water) (Li et al., 2013). This method is reliant on fieldwork to improve the accuracy of the classification, which in some instances can be time consuming (Rokni et al., 2014).

Single-band extraction techniques involves selecting a single band in which water is a strong reflector (e.g. near infrared band) following the application of a subjective threshold to extract water features (Dues and Gloanguen, 2013; Li et al., 2013; Rokni et al., 2014). The disadvantage of single-band methods is the increased likelihood of misclassification which is as a result of the subjective threshold estimation. Du et al. (2012) suggests that the classification method is generally more accurate than the single-band technique.

The multi-band extraction technique combines two spectral bands to accurately enhance the reflective nature of water by suppressing other features such as soil and vegetation, thus improving the extraction of surface water from wetlands (Li et al., 2013; Rokni et al., 2014). This technique takes full advantage of the spectral reflectance of water and absorption of vegetation in the green band (i.e. band 2), and the reflectance of vegetation and absorption of water in the near-infrared (NIR-band 4) and shortwave-infrared (SWIR-band 5) bands, respectively (see Figure 2.2) (McFeeters, 1996; Xu, 2006; Buma et al., 2018).

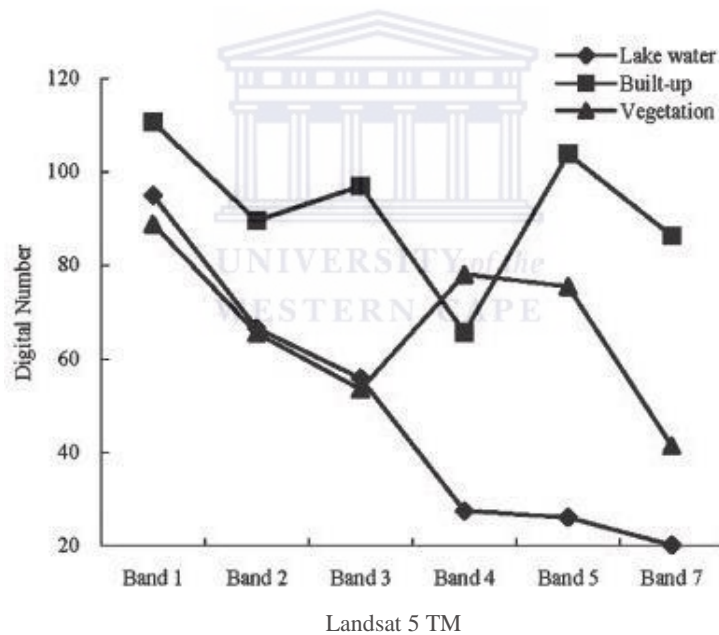


Figure 2.2: Spectral reflectance signatures of water, built-up land and vegetation (from Xu, 2006).

Through the adoption of this technique, a number of spectral water index methods such as McFeeters (1996) Normalized Difference Water Index (NDWI) and Xu’s (2006) Modified Normalized Difference Water Index (MNDWI) have been developed to enhance water and suppress soil, vegetation and built-up features. The NDWI developed by McFeeters (1996), is

based on the high reflective characteristics of water in the green band and vegetation in the NIR, and low reflectivity (i.e. high absorption) of water in the NIR and vegetation in the green band. McFeeters (1996) NDWI Equation (2.1) is defined as follows:

$$NDWI = \frac{\rho_{Green} - \rho_{NIR}}{\rho_{Green} + \rho_{NIR}} \quad (2.1)$$

where ρ_{Green} is the reflectance in the green band, and ρ_{NIR} is the reflectance in the near infrared band.

Through the computation of the NDWI, surface water is enhanced, producing positive values, and vegetation is suppressed, producing negative values, (Xu, 2006; Ning et al., 2015). However, the performance of the NDWI in images characterized by built-up features, are not effectively suppressed and are characterized by positive values (i.e. similar to water) (Xu, 2006; Ning et al., 2015). This is for the reason that the spectral signatures of built-up land are similar to the spectral signatures of water in the green band and NIR (see Figure 2.2), thus producing positive values for both water and built-up land (Xu, 2006; Ning et al., 2015).

The MNDWI proposed by Xu (2006) was adapted from the NDWI by McFeeters (1996) to remedy this issue. The MNDWI Equation (2.2) is defined as follows:

$$MNDWI = \frac{\rho_{Green} - \rho_{SWIR}}{\rho_{Green} + \rho_{SWIR}} \quad (2.2)$$

where ρ_{Green} is the reflectance in the green band, and ρ_{SWIR} is the reflectance in the near-infrared band.

Xu (2006) found that water bodies have even lower reflectance and higher absorption characteristics in the shortwave infrared (SWIR) band, and built-up features and soil have greater reflectance in the SWIR band. Thus, in the MNDWI image, water features are accurately enhanced and vegetation and built-up features are effectively suppressed, producing negative values for built-up features and vegetation (Xu, 2006; Wang et al., 2013).

Li et al. (2013) found that the MNDWI performs more effectively than the NDWI in mapping water bodies.

To date, the MNDWI is one of the most widely used water index to enhance, delineate and extract water surfaces from vegetation and built-up features (Dues and Gloaguen, 2013; Ning et al., 2015; Liang and Yan, 2017; Ji et al., 2018). The use of the MNDWI in Landsat imagery, Landsat 5 Thematic Mapper (TM) Landsat 7 Enhanced Thematic Mapper Plus (ETM+) and Landsat 8 Operational Land Imager (OLI) to delineate and enhance water features are prevalent in many studies (see Murray et al., 2012; Li et al., 2013; El-Asmar et al., 2013; Rokni et al., 2014; Buma et al., 2018). Other applications include the use of MODIS (Deus and Gloaguen, 2013; Ji et al., 2018) and Synthetic Aperture Radar (SAR) sensors (Brisco, 2015; Cazals et al., 2016).



Chapter 3: Coastal wetland resilience to climate change: modelling inundation responses to rising sea levels

3.1 Introduction

The future of the world's coastal wetlands will be greatly influenced by anthropogenic contributions to climate change and associated sea level rise. These contributions are driven by accelerating anthropogenic concentrations of greenhouse gas emissions which are largely a result of increasing economic activity and population growth (IPCC, 2013). Despite global and regional efforts to reduce greenhouse gas emissions through policies, environmental management plans and advances in technology, anthropogenic influences on the global climate continue (IPCC 1st – 5th Assessment Reports 1990; 1996; 2001; 2007; 2013).

The IPCC 5th Assessment Report (Church et al., 2013) suggests that global mean sea level will rise into and beyond the 21st century, thus increasing the vulnerability of the world's coastal wetlands. Coastal wetlands are highly productive ecosystems, providing indispensable services and resources to society and the environment (Mitch & Gosselink, 2015). It is estimated that by the 2080's up to 22% of the world's coastal wetlands could be lost as a result of sea level rise (Nicholls, 1999). Neumann et al. (2000) documents a number of biophysical losses and degradation of coastal wetlands associated with sea level rise; namely inundation, erosion, total or partial loss and/or displacement of wetland marsh and ecosystems, and salt water intrusion into coastal aquifers and rivers. The cumulative impacts will strongly affect coastal ecosystems, and associated human livelihoods.

Predicting changes to naturally dynamic coastal ecosystems is complicated by the variety of non-linear interactions occurring across time and space between biota and the physical environment. In some environments, certain biological interactions are known to offer resistance and/or resilience to perturbations or gradual change (Martinez et al., 2017). Holling (1973) originally defined resilience as the amount of disturbance that an ecosystem can withstand without changing self-organised processes and structures. Integral to the understanding of resilience of ecosystems is that an ecosystem may exist at multiple stable states.

Ecological resilience may be considered the tolerance of the system to a perturbation before a transition to an alternative stable state (or multiple stable states) (Gunderson, 2000). An example here would be the transition of a salt marsh to a mud flat due to continuous sea level rise. Martinez et al. (2017) suggests that some coastal ecosystems are not merely resilient; they may be resistant in that the system is able to hold a force without any modification.

For coastal wetlands, increasing levels of inundation, salinity and occasional disturbance are primary drivers of change related to sea level rise. In order to maintain process and structure, sediment must accrete vertically at a rate faster or equivalent to that of rising sea levels (Day et al., 1999; Morris et al., 2002; Mitsch and Gosselink, 2015). Sediment accretion rates in coastal wetlands are influenced by sediment yields which may vary due to anthropogenic activities, the construction of dams within catchments (Wang et al., 2016) and/or as a result of natural rainfall variability (Aalto et al., 2003). Sediment accretion may also be restricted by topography and human construction along the coast, (e.g. flood protection barriers) (Titus, 1991; Nicholls 2004; Mitsch and Gosselink 2015), or there may simply be insufficient space for ecosystems to migrate inland as sea level rises (i.e. “coastal squeeze”, Doody, 2013).

Applying models to predict changes in physical environments is essential to aid sustainable and comprehensive planning. However, this is a complex task as processes within physical environments are influenced by many biophysical interactions (Rogers et al., 2012). Grenfell et al. (2016) suggests changes to ecosystems may be understood by studying existing environmental gradients to determine which factors have a large impact on the ecosystem. Reed et al. (2002) suggest that by measuring and quantifying important environmental processes such as sediment accretion and the rate of sea level rise, and using it as a proxy, it is possible to understand and predict the response of coastal wetlands to ongoing sea level rise.

Studies have shown that some coastal wetlands may be resilient to rising sea levels (see Patrick and DeLaune, 1990; Morris et al., 2002; Reed, 2002; Temmerman et al., 2004). In these environments, increasing sediment yields have a positive influence on wetland accretion rates as elevation is sustained above that of rising sea levels. However, in environments where sediments yields are low, coastal wetlands are unable to keep pace with rising sea levels, resulting in wetland loss (see Day et al., 1999; Goor et al., 2003).

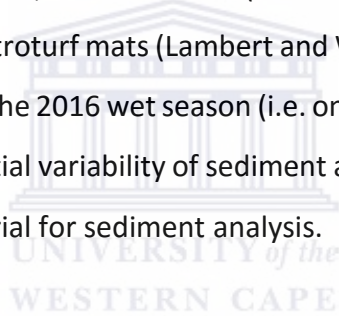
This chapter attempts to model and predict coastal wetland resilience to sea level rise for the Droë River coastal wetland on the Agulhas Plain, South Africa (Figure 3.1). The course of the Droë River wetland is an abandoned channel of the Kars River, which drains the Bredasdorp Mountain and Soetmuisberg. The time when the channel was abandoned and how this occurred are unknown. The old meandering channel is well preserved in the landscape, indicating that the river was laterally active.

3.2 Materials and Methods

3.2.1 Data collection

3.2.1.1 Determining sediment accretion rates

Two methods were used to estimate and measure short and long-term sediment accretion rates within the Droë River wetland; astroturf mats (i.e. artificial grass mats) and radiometric dating (^{210}Pb) (see Figure 3.1). Astroturf mats (Lambert and Walling, 1987) were used to gauge sediment accretion rates during the 2016 wet season (i.e. one year). This method allows direct measurement of the current spatial variability of sediment accretion rates across the wetland and capture the deposited material for sediment analysis.



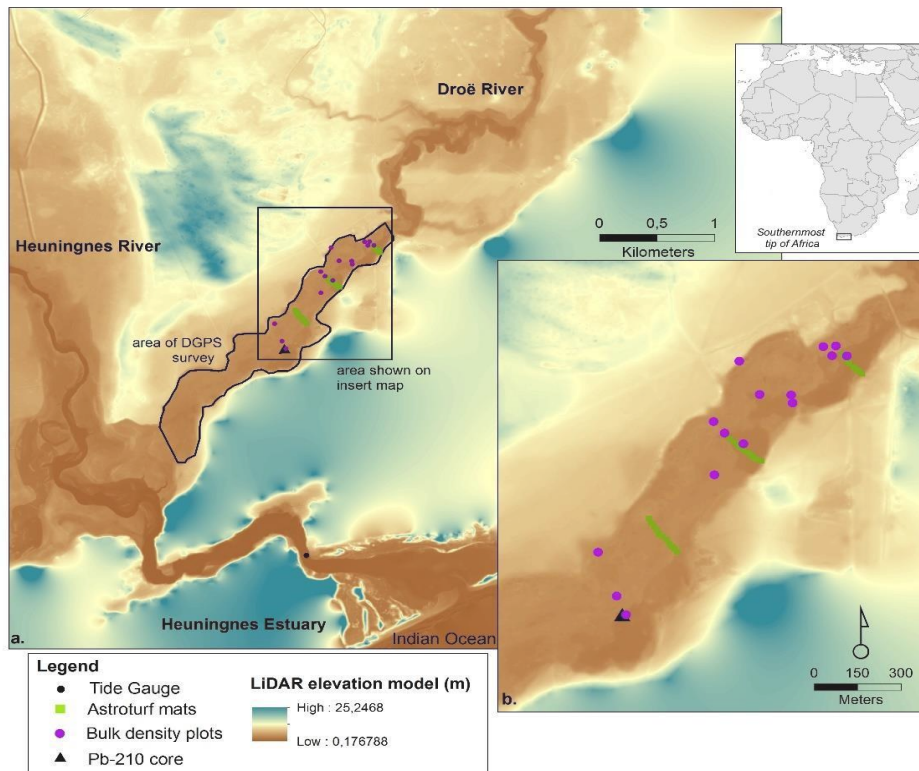


Figure 3.1: Location of the Droë river wetland (i.e. study site) adjacent to the Heuningnes Estuary indicated by the large map (Figure 3.1a). The Droë River is located on an abandoned channel of the Kars River, which now flows into the Heuningnes River toward the west. The inset map of Figure 3.1b indicates the position of the bulk density plots, astroturf mats, the ^{210}Pb sediment core as well as the area of the detailed DGPS survey.

A total of 38 astroturf mats (31 m² in size) were installed across the wetland along three transects (see Figure 3.1), and where GPS positions were recorded. The mats were placed on individual squares of heavy duty plastic sheets. The mats were secured onto the wetland surface using stainless steel nails to prevent them being disturbed by wildlife and or blown away by prevailing winds (see Figure 3.2). During the dry season of February 2017, 27 mats and sheets were carefully removed and placed into labelled and resealable bags. 11 mats were not recovered, because some had been removed while others were submerged under water.



Figure 3.2: Astroturf mats were installed across the Droë River wetland to measure the rate of short-term sediment accretion.

To complete the measurement of sediment accretion, bulk density surface samples were taken using an Eijelkamp bulk density sampling kit. The samples were collected during the dry season of May 2017 across various homogenous sites within the wetland. A total of 15 soil samples were collected at undisturbed sites which were identified according to the dominant vegetation species within the wetland. The soil sampling ring was placed on the topsoil and gently hammered into the ground (Figure 3.3). Once the ring was filled with soil, the soil surrounding the ring was excavated to allow the sample to be gently removed. Each sample was labelled and sealed with core sampler caps to ensure that the sediment was not disturbed.



Figure 3.3: Bulk density samples were collected at various homogenous sites within the wetland. Sampling sites were stratified by vegetation community within the wetland, *Sarcocornia perennis* or *Sarcocornia littorea* (left), salt tolerant samphire's, grass and creeping herbs (middle) and *Phragmites australis* (right).

The sediment which had accumulated on the astroturf mats was rinsed into pre-weighed and labelled beakers to calculate the total sediment mass. Bulk density of the oven dried samples

was calculated. Loss of ignition was used to calculate the percentage of organic content, ~3 g of dry sediment was placed in a muffle furnace for 4h at 450 °C.

The long-term sediment accretion rate was estimated from a sediment core taken during the dry season in February 2017. The wetland core was taken with a stainless steel gouge corer at an undisturbed homogenous site within the wetland. A core length of 140 cm was obtained, and sub-sampled into 2 cm increments. The sub-samples were sent to the University of Exeter (UK) to determine the ^{210}Pb activity. The method for determining ^{210}Pb is outlined by Grenfell et al. (2012) and Aalto and Dietrich (2005). The 'constant rate of supply' dating model (Appleby and Oldfield, 1978) was applied to calculate the rate long-term of sedimentation within the wetland. This model is based on the assumption that the production of "unsupported" ^{210}Pb is constant over time while the rate of accretion is not (Nolte et al., 2013).

3.2.1.2. Topographic survey

To model the current wetland surface, elevation (m) data was collected using Stonex Differential Global Positioning System (DGPS) surveying equipment and software. This system allows for the collection of xyz coordinates at sub-cm accuracy which is corrected in real-time. Accurate operation of a DGPS depends on suitable weather conditions for secure GLONASS and GPS satellite connections, the setup of the base station (i.e. the DGPS receiver) at a fixed location of known xyz coordinates and secure connection to and from the rover (i.e. the DGPS sender). The rover is used to collect the elevation points which are sent to and received by the base station. In real-time, the error range received by the base station is accurately calculated to correct the position measured by the rover (i.e. Real time Kinematics) (see Figure 3.4).

Real-Time Differential GPS

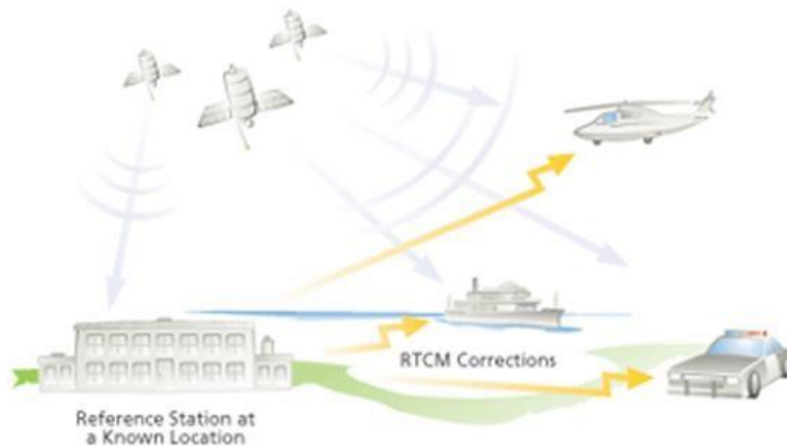


Figure 3.4: How a differential GPS works (ESRI, 2018). The base station receiver is setup precisely at a known position. The location of the receiver is computed based on a number of satellites e.g. GLONASS satellites. The difference in base station position is calculated and corrected in real-time relative to the rover GPS receiver.

For the DGPS survey of the Droë River wetland, the base station was setup at Lammerskop Trigonometric beacon 174 identified on the 3420CA & CC Bredasdorp 1:50 000 Topographic map (South Africa, 2007). Once the setup was complete, the survey was conducted along transects across the wetland (Figure 3.5). Due to the low and gentle gradient of the wetland, few data points were surveyed across flatter areas while most points were surveyed in areas of noticeable and rapid changes in elevation.



Figure 3.5: A detailed DGPS survey was conducted within the wetland. The survey captures the morphology of the wetland, in some areas, the old river course can be seen.

After the DGPS survey was completed, a LiDAR (Light Detecting and Ranging) Digital Terrain Model (DTM) was sourced from the Department of Environmental Affairs and Development Planning (DEA&DP) (Figure 3.6). This is an airborne surveying technique which uses a pulse-laser to detect and measure the height of terrain features and objects in relation to the sensor (Baltensweiler et al., 2017). For the wetland surface elevation model, ground hit points representing bare-earth were extracted from the LiDAR point cloud.

For both elevation datasets (i.e. DGPS and LiDAR), a raster surface elevation model was created in ArcMap 10.3 using the Topo to Raster interpolation tool (1 m resolution). Both methods provide high density and accurate data for the study site. On a local scale, the DGPS survey was more accurate than the LiDAR. This is a result of direct ground surface measurements which were not inhibited by the influence of dense vegetation, a common challenge faced when using LiDAR (Baltensweiler et al., 2017). However, LiDAR provides extensive coverage of the study site, which extends beyond the boundaries of the wetland (Figure 3.6). This is in contrast to the DGPS survey which is limited to the boundaries of the wetland (Figure 3.6). As such, the LiDAR dataset was selected to create a Digital Elevation Model for the wetland.

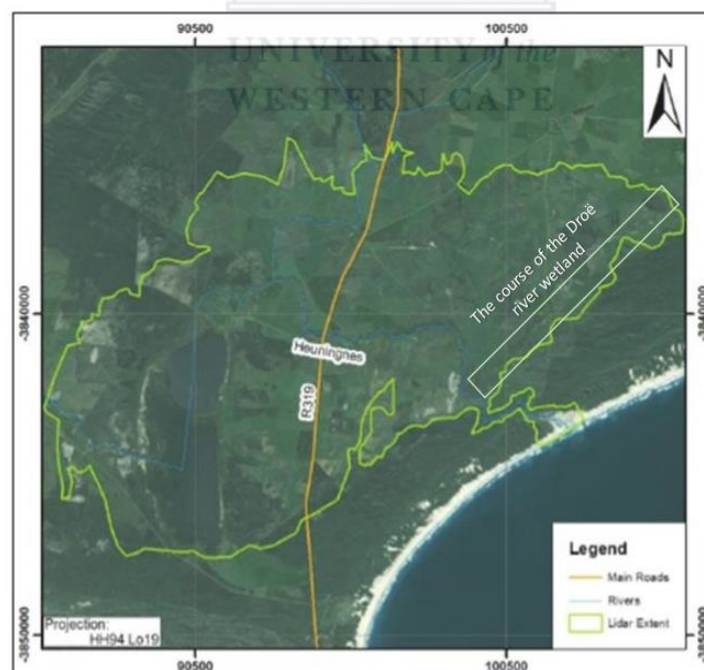


Figure 3.6: Extent of the LiDAR dataset across the Agulhas Plain (Cape Nature, 2017).

3.2.1.3. Sea level rise and tide predictions

Global mean sea level rise predictions were obtained from the Intergovernmental Panel on Climate Change 5th Assessment Report (IPCC 5th AR) (Church et al., 2013). These predictions are based on the Process-Based Model outputs from 21 Coupled Model Intercomparison Project Phase 5 (CMIP5) Atmosphere-Ocean General Circulation Models (AOGCMs). Four Representative Concentration Pathway (RCP) scenarios, RCP 2.6, 4.5, 6.0 and 8.5 were developed. Each projection is based on predicted anthropogenic greenhouse gas emissions and potential mitigations measures (see Figure 3.7). The RCP predictions range between 0.26 m- 0.98 m by 2100, RCP 2.6 is classified as a low emission scenario, RCP 4.5 and 6.0 are considered stabilization and late mitigation scenarios, and RCP 8.5 is classified as an extremely high greenhouse gas emission scenario with no mitigation. Median sea level rise values were used as model inputs, percentiles were not run as the range of scenarios were considered to provide a good range of potential outcomes.

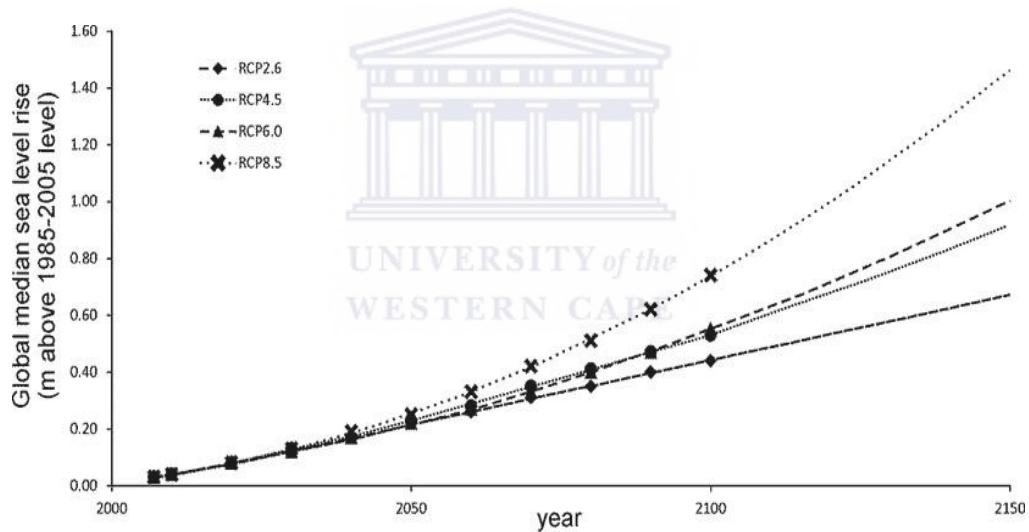


Figure 3.7: IPCC RCP global mean sea level rise projections corrected to Hartebeeshoek 94 datum.

The 2017 Mean High Water Neap (MHWN) and Mean High Water Spring (MHWS) tide estimates were obtained from the Hydrographic Office of the South African Navy (Table 3.1). These tides are published according to Chart Datum heights (m) derived from the Lowest Astronomical Tide of all ports in South Africa and Namibia (Hydrographer South African Navy, 2017). In order to incorporate the sea level rise and tide data with the DGPS and LiDAR datasets, the data were corrected to the Land Levelling Datum (LLD) of South Africa,

Hartebeesthoek94 (the coordinate system and geodetic datum used by the Republic of South Africa is the Gauss Conform Coordinate system which is referenced to the Hartebeesthoek94 datum). LLD, also referred to as Mean Sea Level (MSL) is used as a baseline for all heights in the sea level rise model presented in this study.

Table 3.1: The tide levels below are mean heights for MSL, MHWN, MHWS and HAT tides.

PLACE	MSL	MHWN	MHWS	HAT
Mossel Bay	1.17	1.46	2.10	2.44
<i>Chart Datum Height relative to Land Levelling Datum (1 Jan 2003 onwards)</i>				-0.933

Daily tidal records for the Heuningnes Estuary G5T002 water level station located on the footbridge at De Mond, referenced to the LLD, were obtained from the Department of Water and Sanitation South Africa for 2001 to 2018 (Table 3.2). The river gauge is located in the middle of the De Mond footbridge, which extends across the mouth of the Heuningnes River (Figure 3.1.). This location captures variation in water levels which are associated with both river discharge and storm surges from the ocean. To provide insight into projected flood frequencies and associated water levels (depth and spatial extent) for the Droë River wetland, the recurrence intervals were calculated using $RI = n+1/m$ (Equation 3.1); where n is the number of events and m is the event rank. The 2-, 4- and 8-year flood recurrence interval water levels were estimated for respective sea level rise RCP scenarios.

Table 3.2: The water level station for the Heuningnes River is located downstream, in the De Mond Nature Reserve. It is attached to the footbridge which extend across the river and is operated by the Department of Water and Sanitation.

Station ID	Parameter	Location	Data Period
G5T002 Heuningnes at De Mond	Surface water level (m)	34° 42' 39" S 20° 06' 15" E	13-07-2000 to 14-02-2017

3.2.2 Data analysis

3.2.2.1 Development of sediment accretion and sea level rise model

In order to investigate coastal wetland response to rising sea levels, a simplistic GIS-based empirical model was developed in ArcMap 10.3. Two main processes were modelled over time. Firstly, the projected change in elevation as a result of ongoing sediment accretion within the wetland, and secondly, the effect of rising sea level on frequency of inundation (see Figure 3.8).

Model data inputs

The model starting point is based on the topographic survey conducted as part of this study. The DGPS survey was considered more accurate as the LiDAR did not use ground reference points. However, in order to visualise more extensive changes that could not be physically surveyed, the LiDAR was appended to the DGPS survey. Predicted rising sea level conditions such as mean high water spring, mean high water neap tidal conditions and the recurrence interval of 2-, 4- and 8-year water levels were modelled for respective time steps (25 years of this study).

Model steps and iterations

1. The spatial extent of sediment accretion is determined

The area of active wetland sediment accretion was mapped by considering topography and vegetation. As the accretion rate had been measured in a very particular geomorphic setting, only similar regions were included. The actively meandering stretch of the Heuningnes River was not modelled in terms of sediment accretion.

2. The impact of sediment accretion on wetland elevation is calculated

The model assumes that sediment accretion rates are constant over time and space. The sediment accretion area defined in the previous iteration is used to predict new wetland elevation for the respective year. This output is added onto the wetland surface elevation as determined in Step 1, creating new estimated/predicted wetland surface elevation.

3. Inundation due to IPCC sea level rise predictions are determined

The predicted wetland surface elevation determined in Step 1 and 2 is compared to respective predicted RCP sea level rise scenarios. The output is based on static inundation, and assumes inundation is instantaneous. Dynamic models are considered more accurate than static models, but are computationally expensive, and are thus often applied to large areas at a low resolution (e.g. > 100 m cells, Breilh et al., 2013; Ramirez et al., 2016; Vousdoukas et al., 2016). In this case, a static model was selected to reduce computational requirements considering the high resolution of the elevation data set (1 m) which was necessary to capture rapid changes in elevation over a small distance. This was considered acceptable as Breilh et al. (2013) showed that static model predictions were improved when wetlands were within 5 km of the landward boundary, in this case the wetland is less than 5 km from the tidal gauge. For each time step, areas inundated by neap and spring tides and at the 2, 4 and 8-year recurrence intervals were extracted.

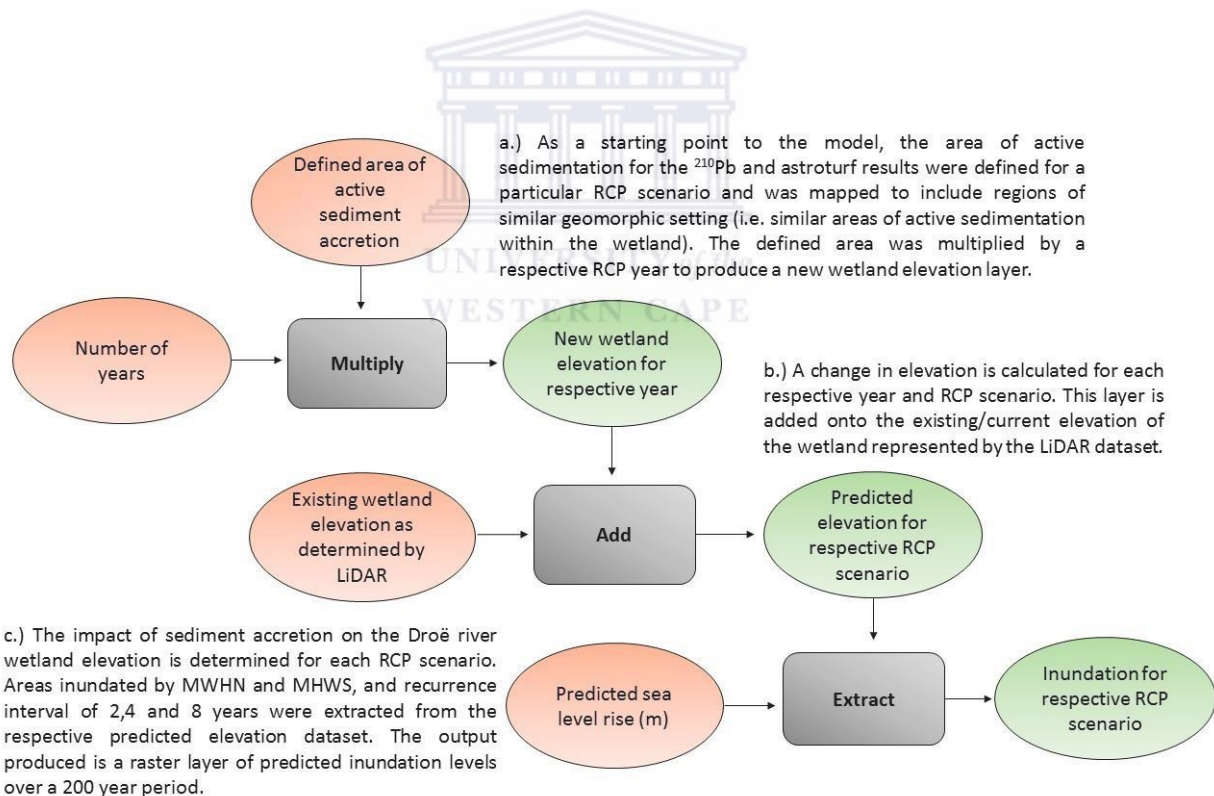


Figure 3.8: Sediment accretion and sea level rise model iteration workflow summary.

3.3 Results

3.3.1 Sediment accretion rates

Sediment accretion rates were estimated using two methods (Figure 3.9). ^{210}Pb activity was measured on a 140 cm core taken within the wetland, the resultant long term average rate of accretion was $3.99\text{mm}\cdot\text{a}^{-1}$. In contrast, the mean rate of accretion measured using the amount of sediment collected on the recovered astroturf mats (corrected for bulk density and organic content) after a single season was $0.75\text{mm}\cdot\text{a}^{-1}$. There was considerable variation within measured rates on the astroturf mats, with a minimum value of 0.006 and a maximum value of $3.864\text{mm}\cdot\text{a}^{-1}$. Bioturbation and post-depositional disturbance were considered to be a major factor as the wetland was used by a flock of Lesser flamingos (*Phoeniconaias minor*) and was also occasionally grazed by sheep and horses. The effect of relative elevation and landscape setting was considered but no relationship was found.

A visual inspection of the rate of ^{210}Pb sediment accretion curve suggests that the rate is slowing, a view which conforms to the geomorphic evolution of the system. The sediment accretion rate was likely higher immediately following abandonment, but would have slowed as less flood waters moved down the drainage line. The time when the channel and floodplain was abandoned is not known, but predates the first aerial photography of the area (ca. 1939). It is likely that the $3.99\text{mm}\cdot\text{a}^{-1}$ as measured from the ^{210}Pb core indicates an upper maximum sediment accretion rate and that the real rate is slightly lower. The accretion rate of the wetland is not coupled to sea level, which has been gradually rising for the last century. Instead, radiometric dating suggests that variation in accretion rates is linked to fluvially derived sediment rather than marine sources.

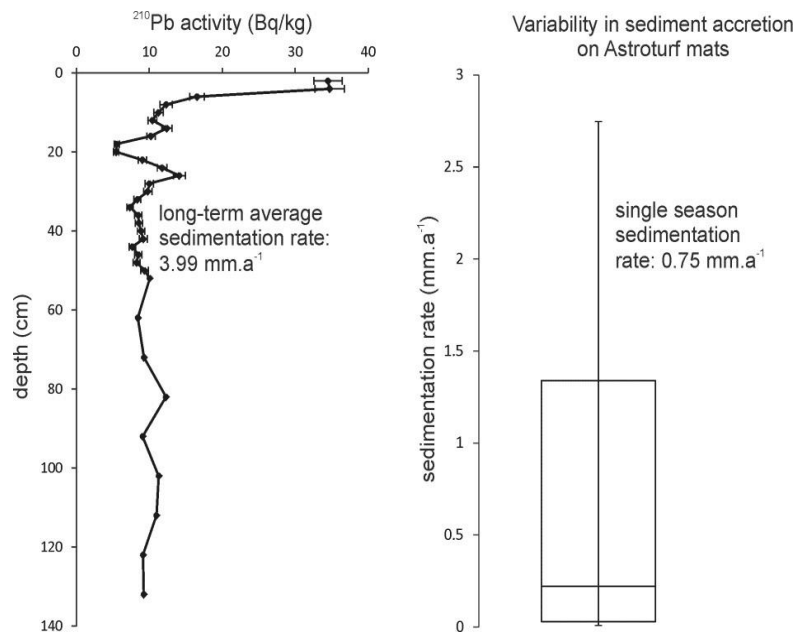


Figure 3.9: The Pb^{210} activity profile of the wetland core (left) and variability in sediment accretion rates as calculated from sediment deposited on recovered astro turf mats.

3.3.2 Sediment accretion rates and sea level rise outputs

The sediment accretion rates gauged from the ^{210}Pb core and astro turf mats provide a variation of accretion rates, with a maximum 3.99 mm.a^{-1} (^{210}Pb accretion rate) and minimum 0.75 mm.a^{-1} (astro turf accretion rate) range. The accretion results were used to produce high and low estimate scenarios for modelled changes associated with IPCC rising sea estimates for respective RCP scenario's and associated neap and spring tides, and the 2-, 4- and 8-year recurrence interval over a 200 year period (Figures 3.10-3.19). Results for all 4.5 and 6.0 RCP scenario are notably similar with slight changes associated with inundation depth. These are stabilization scenarios in which total radiative forcing is stabilized after the year 2100.

Inundation associated with the MWHN and MHWS tides increase across all high accretion rate scenarios, but not in areas where sediment accretion has been modelled at 3.99 mm.a^{-1} (Figure 3.10). These model simulations suggest that the sediment accretion rates are locally faster than the rate of rising sea levels under all RCP MWHN and MHWS scenarios (Figure 3.10). In contrast, results for the low accretion rate scenarios were similar for the most part, partial increase in inundation associated with MHWS tides is seen within the wetland modelled area for respective RCP scenarios (Figure 3.11). These model simulations suggest

that in 125 years for RCP 8.5 and 150 years for RCP 4.5 and 6.0, sediment accretion is unable to keep up with the rate of sea level rise (Figure 3.11).

When the combined effect of river inputs and tides are considered using recurrence interval data from the De Mond water level gauge, the impact of rising sea level on inundation levels is markedly different (Figures 3.12-3.19). Despite sediment accretion rates being relatively high in comparison to IPCC RCP sea level estimates, model simulations indicate that the frequency and depth of inundation will increase when water levels associated with river inputs and tides are considered for both low and high accretion rate scenarios.



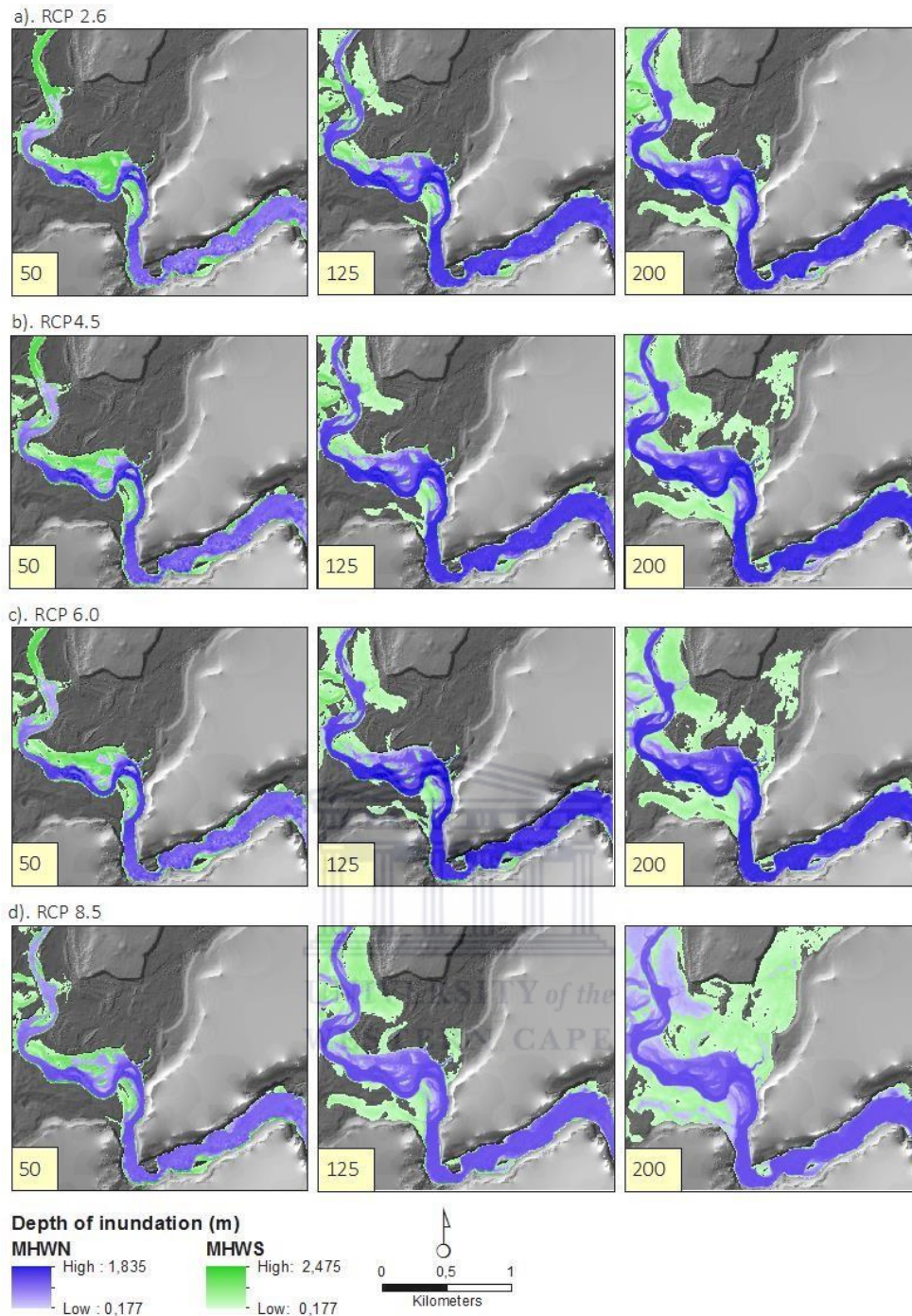


Figure 3.10: Low accretion rate scenario for Inundation levels associated with the astro turf accretion rate: Mean High Water Neap (MHWN) and Mean High Water Spring (MHWS) tide model predictions for respective Representative Concentration Pathway (RCP) scenarios, a). RCP 2.6 (low emission scenario) b). RCP4.5 (intermediate emission scenario) c). RCP 6.0 (intermediate emission scenario) and d). RCP 8.5 (high emission scenario).

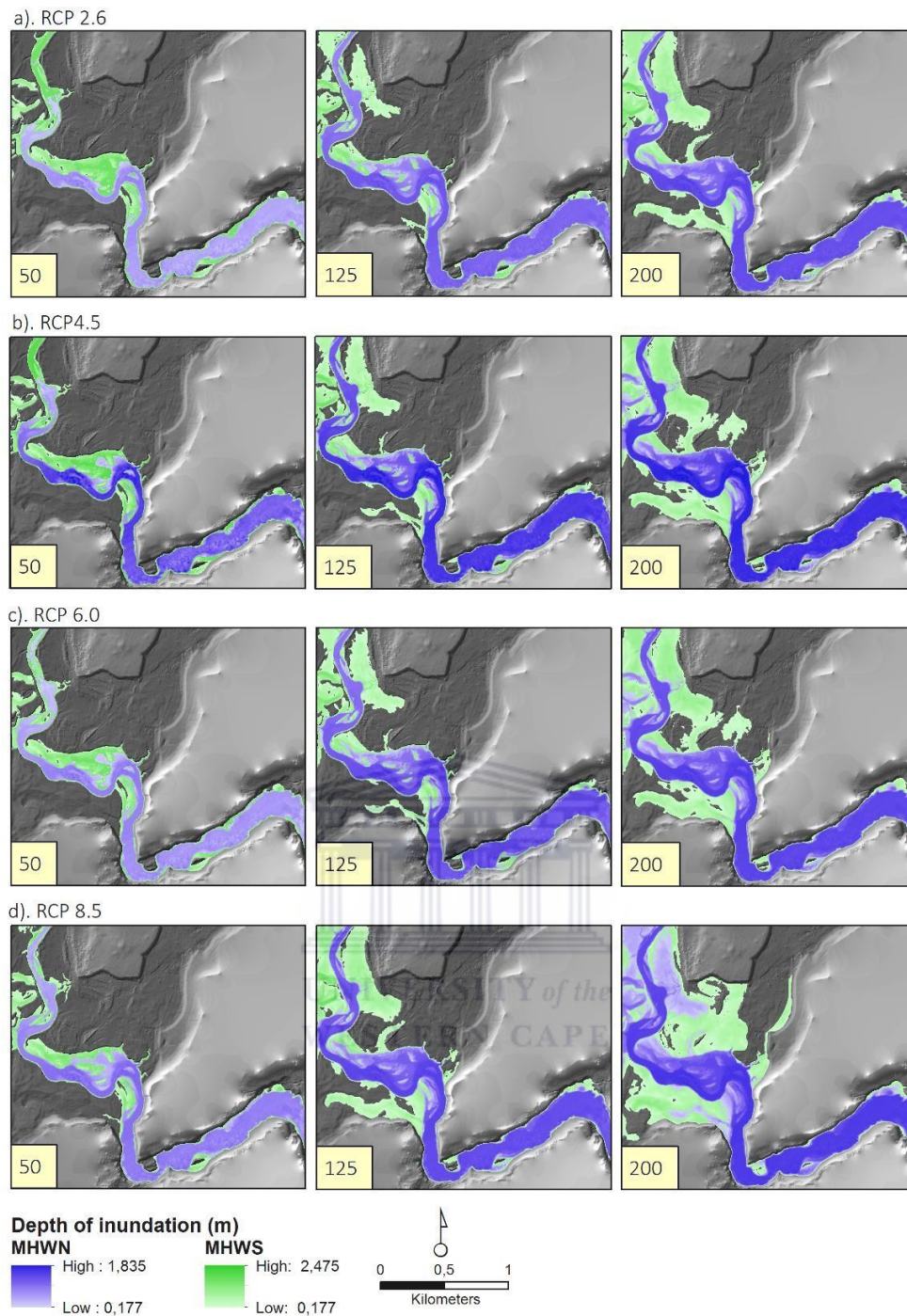


Figure 3.11: High accretion rate scenario for Inundation levels associated with the Pb^{210} accretion rate: Mean High Water Neap (MHWN) and Mean High Water Spring (MHWS) tide model predictions for respective Representative Concentration Pathway (RCP) scenarios, a). RCP 2.6 (low emission scenario) b). RCP4.5 (intermediate emission scenario) c). RCP 6.0 (intermediate emission scenario) and d). RCP 8.5 (high emission scenario).

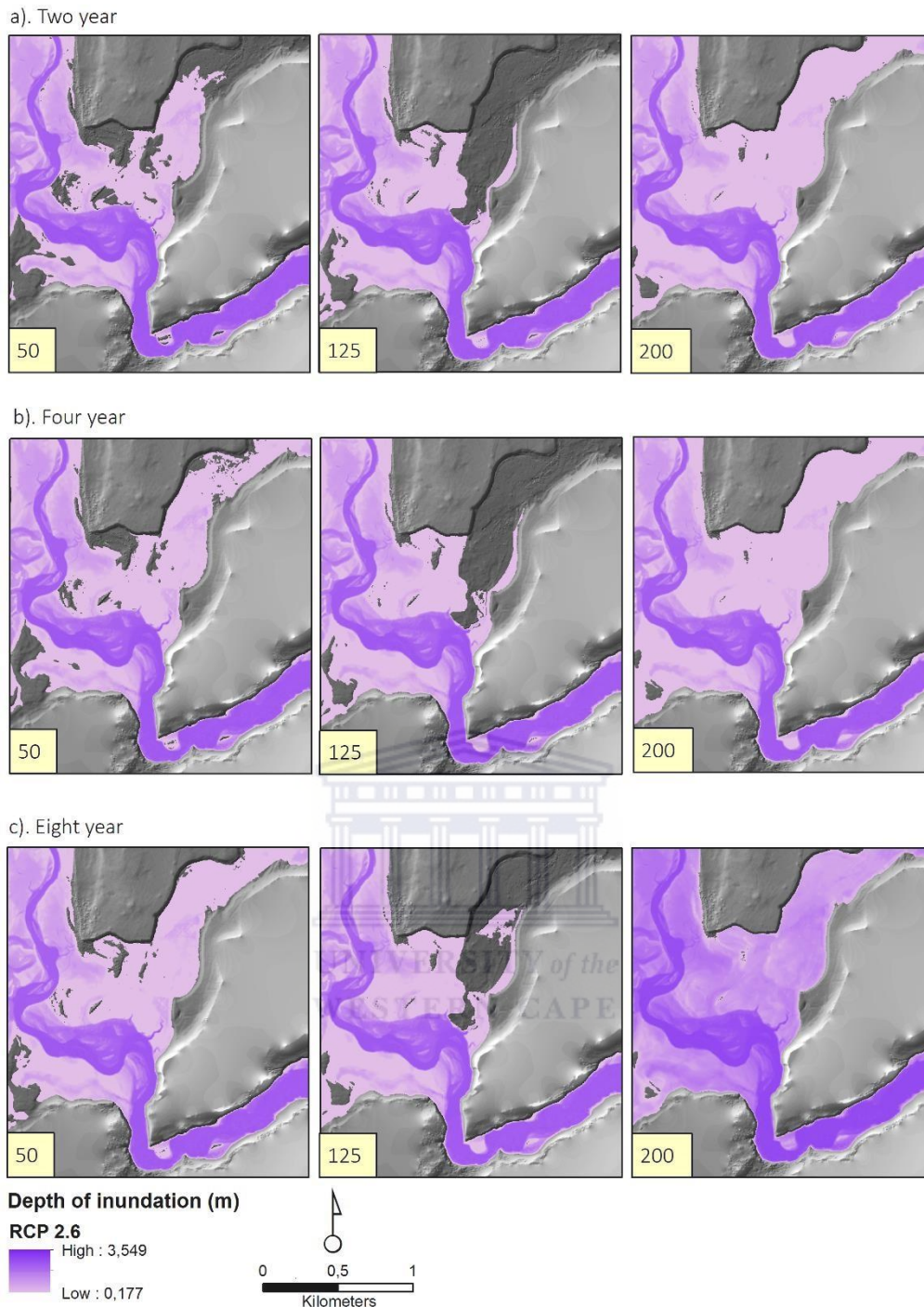


Figure 3.12: Low accretion rate scenario comparing water levels at different recurrence interval model for the astroturf accretion rate: predictions for RCP 2.6 (low emission scenario), a). 1 in 2 years b). 1 in 4 years and c). 1 in 8 years.

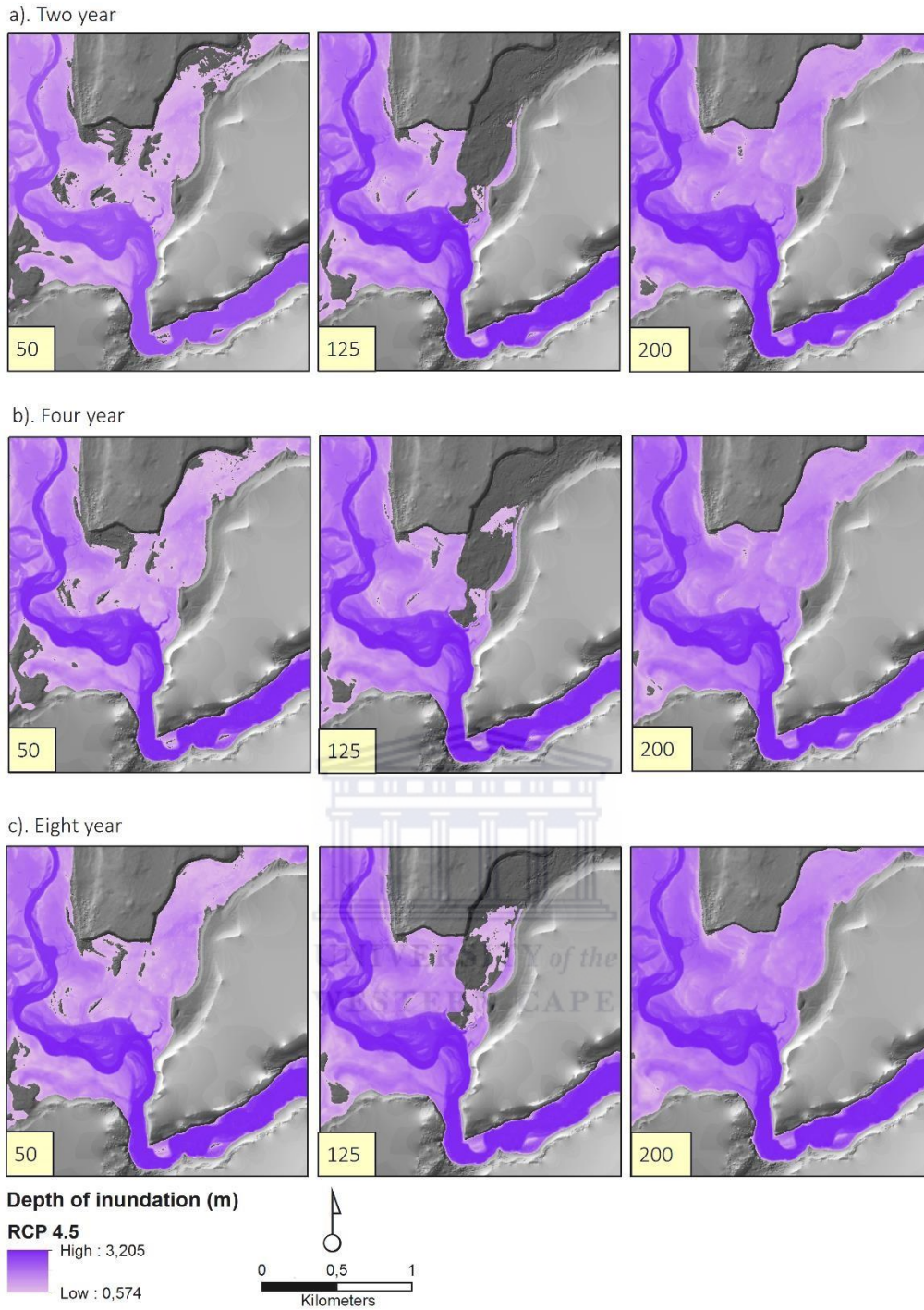


Figure 3.13: Low accretion rate scenario comparing water levels at different recurrence interval model for the astroturf accretion rate: predictions for RCP 4.5 (intermediate emission scenario), a). 1 in 2 years b). 1 in 4 years and c). 1 in 8 years.

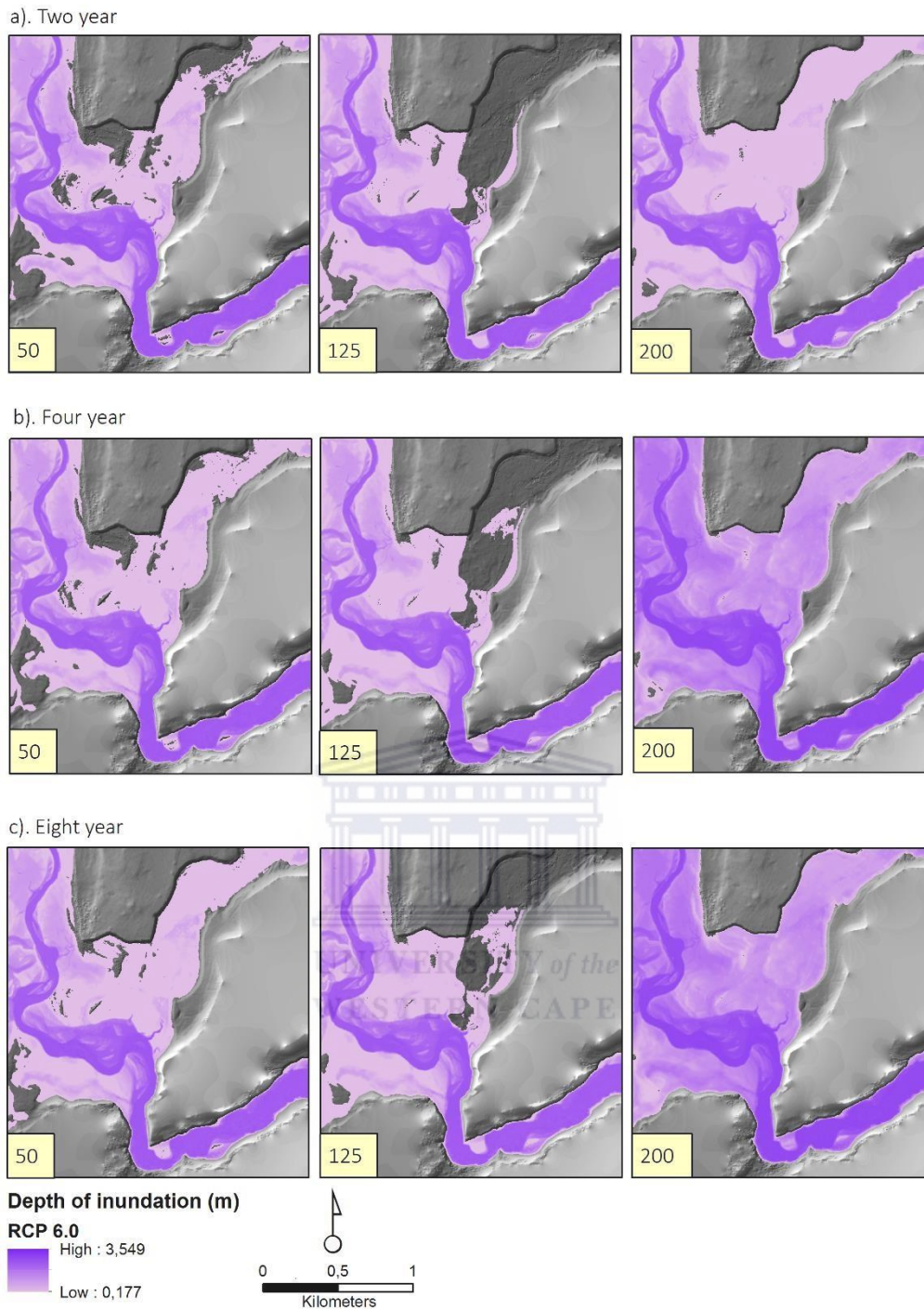


Figure 3.14: Low accretion rate scenario comparing water levels at different recurrence interval model for the astroturf accretion rate: predictions for RCP 6.0 (intermediate emission scenario), a). 1 in 2 years b). 1 in 4 years and c). 1 in 8 years.

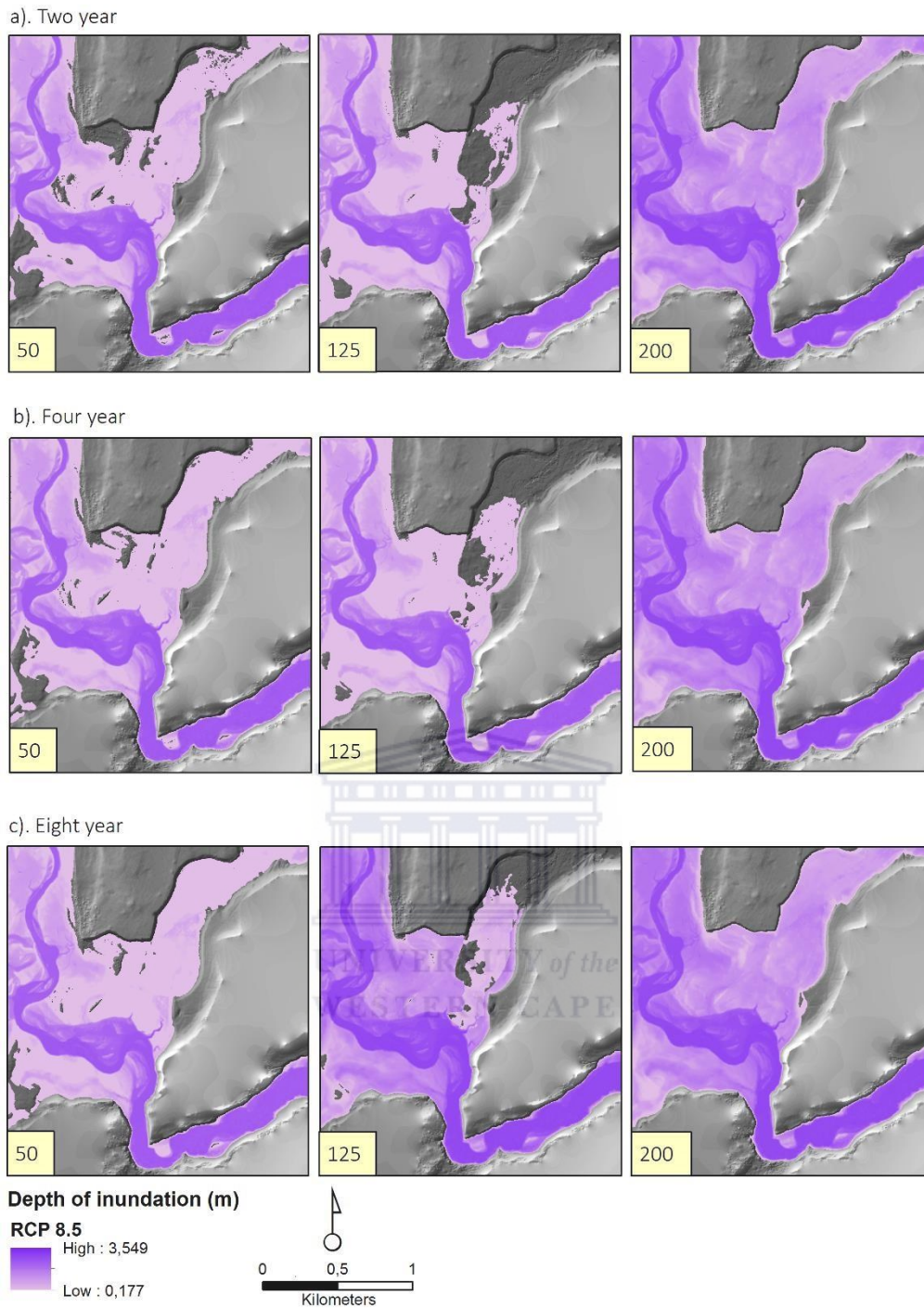


Figure 3.15: Low accretion rate scenario comparing water levels at different interval model for the astroturf accretion rate: predictions for RCP 8.5 (high emission scenario), a). 1 in 2 years b). 1 in 4 years and c). 1 in 8 years.

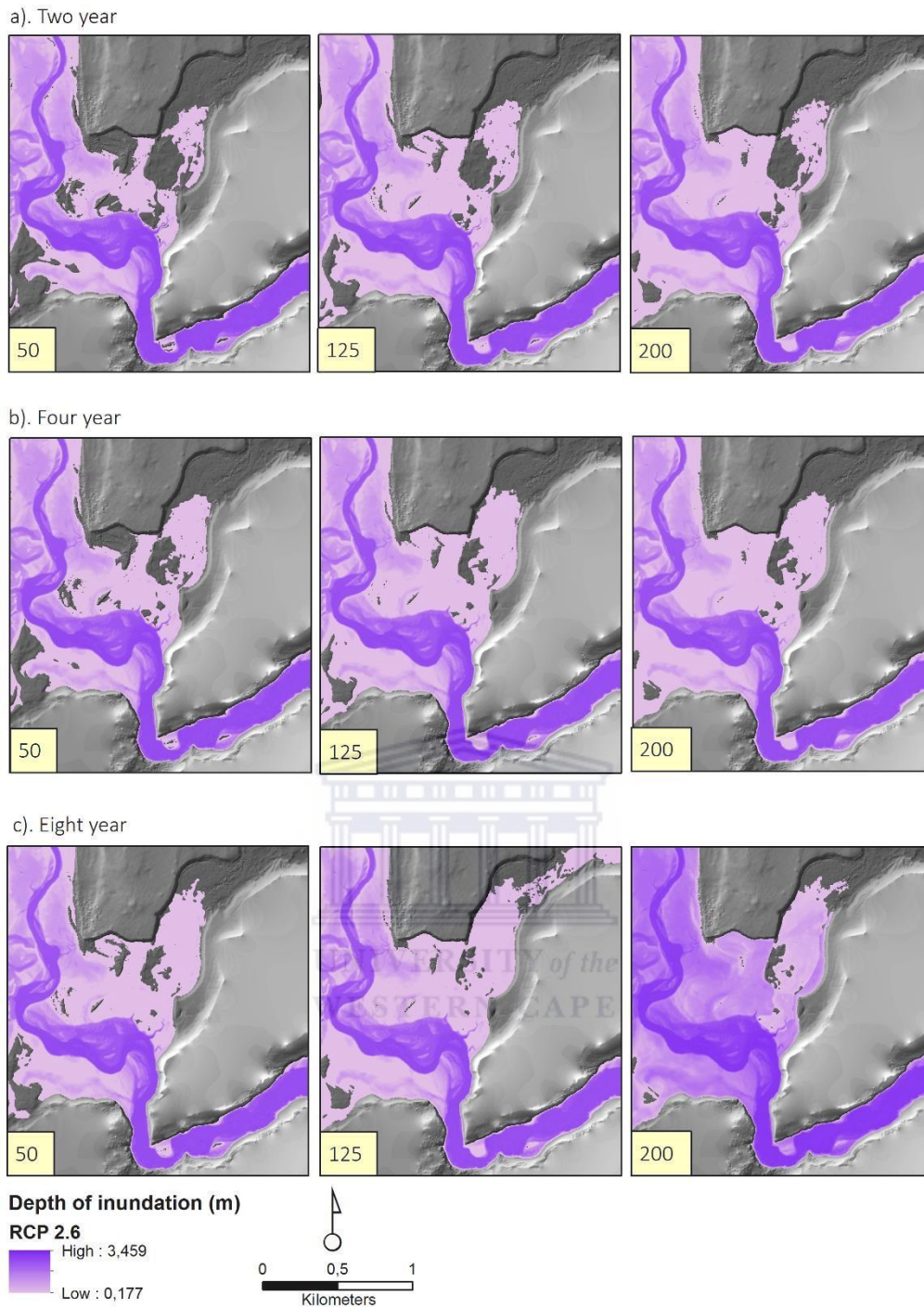


Figure 3.16: High emission scenario comparing water levels at different recurrence intervals based on the Pb^{210} accretion rate. Predictions for RCP 2.6 (low emission scenario), a). 1 in 2 years b). 1 in 4 years and c). 1 in 8 years.

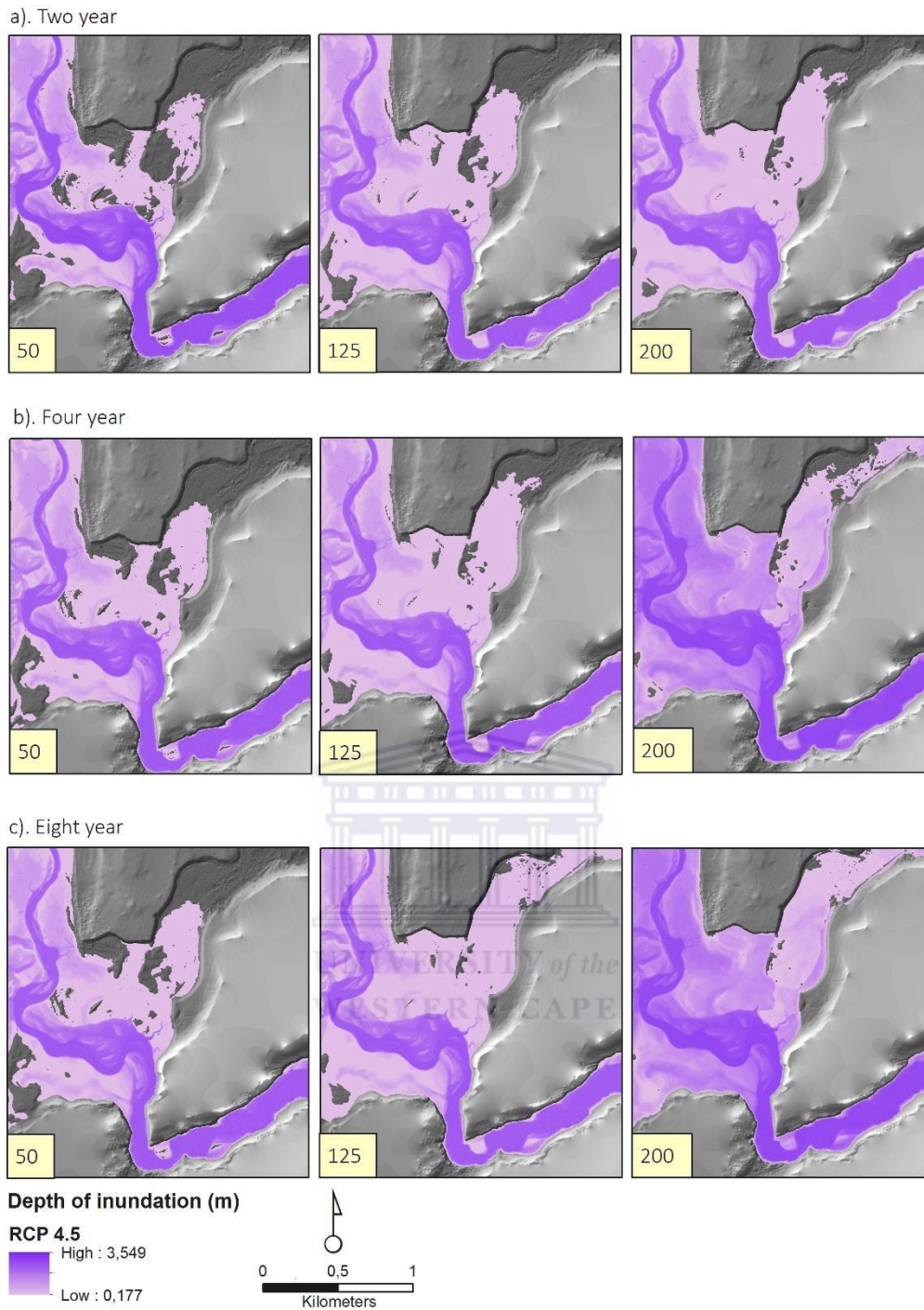


Figure 3.17: High accretion rate scenario comparing water levels at different water level recurrence interval model for the ^{210}Pb accretion rate: predictions for RCP 4.5 (intermediate emission scenario), a). 1 in 2 years b). 1 in 4 years and c). 1 in 8 years.

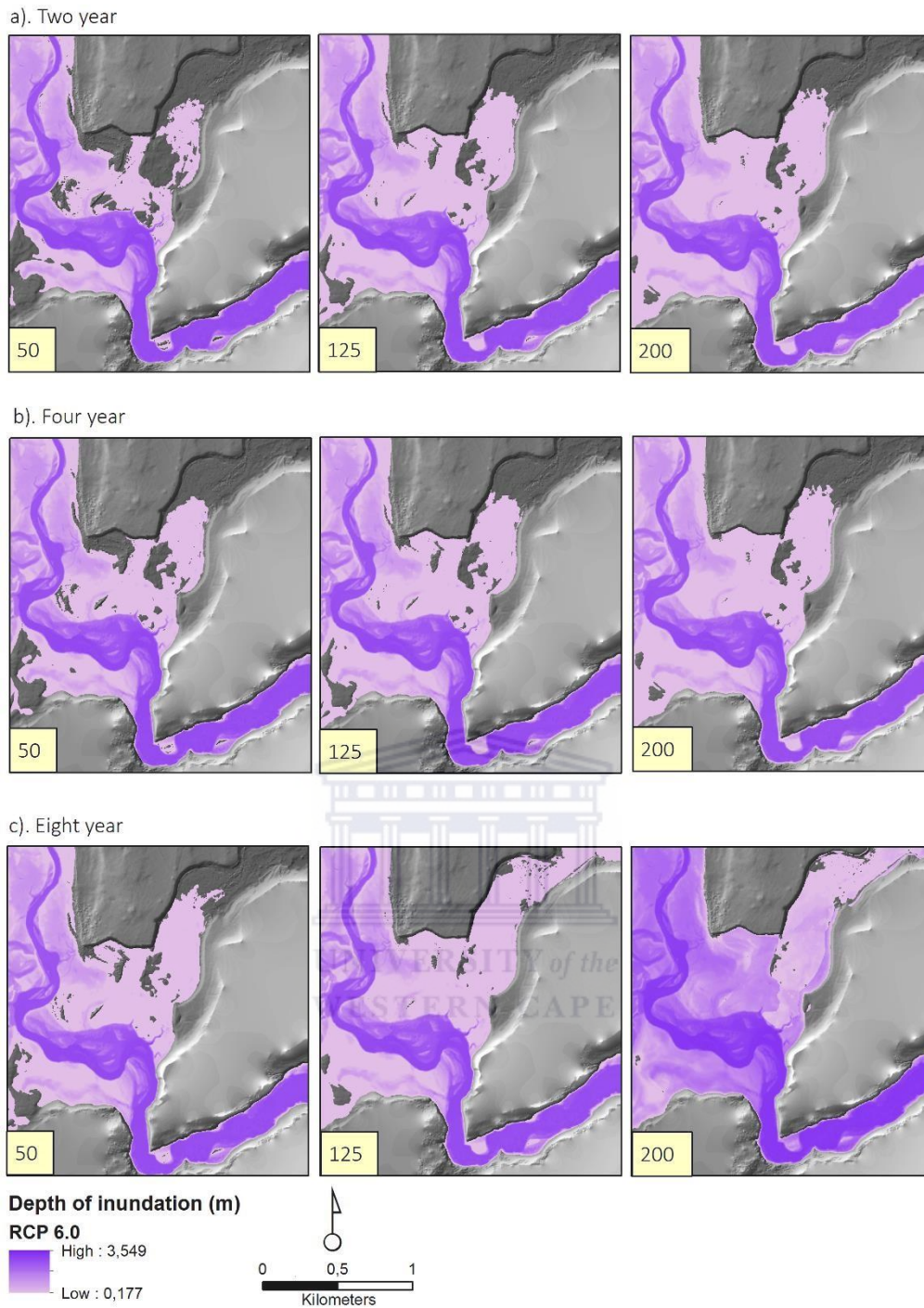


Figure 3.18: High accretion rate scenario comparing water levels at water level recurrence interval model for the ^{210}Pb accretion rate: predictions for RCP 6.0 (intermediate emission scenario), a). 1 in 2 years b). 1 in 4 years and c). 1 in 8 years.

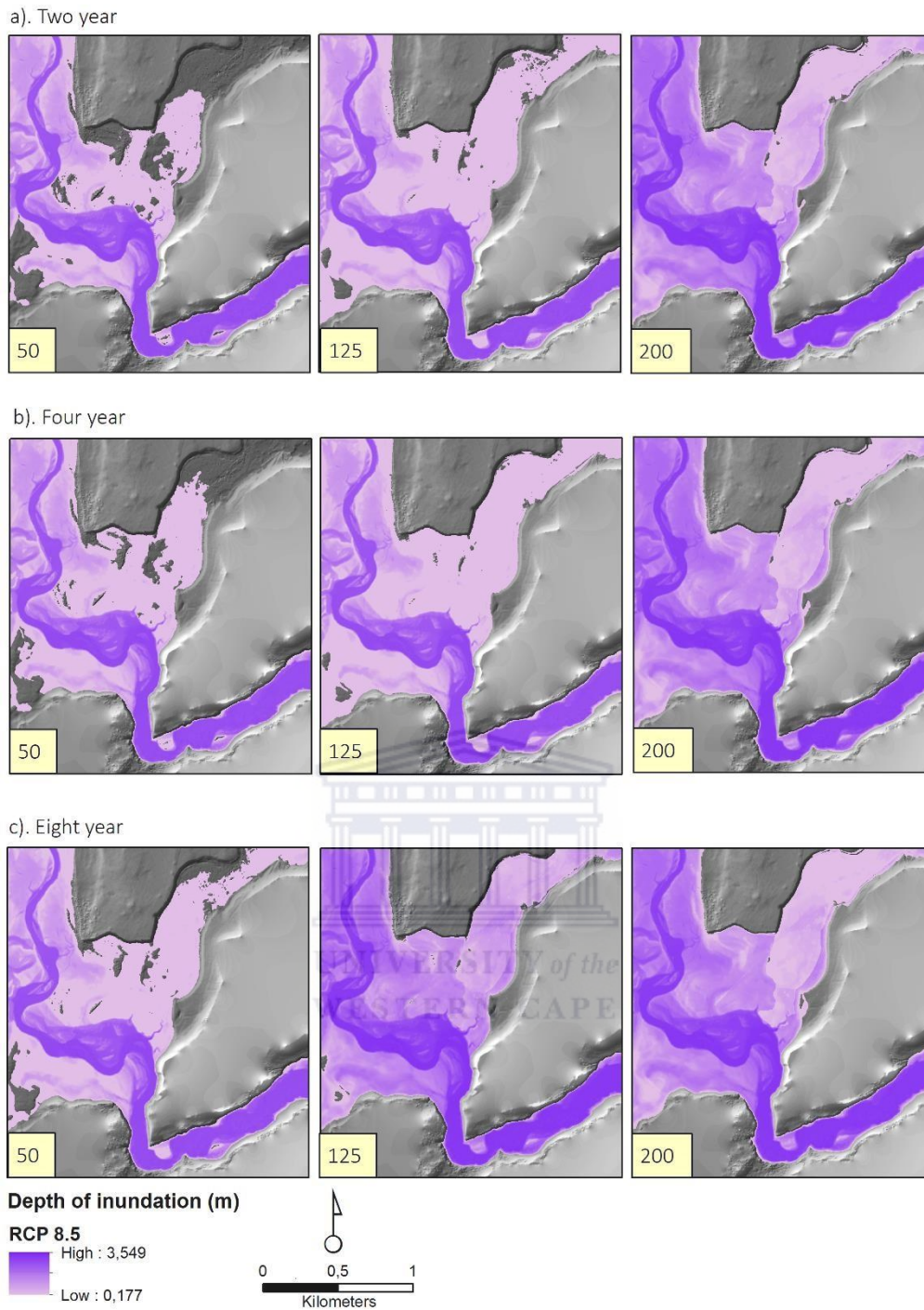


Figure 3.19: High accretion rate scenario comparing water levels at different water level recurrence interval model for the ^{210}Pb accretion rate: predictions for RCP 8.5 (high emission scenario), a). 1 in 2 years b). 1 in 4 years and c). 1 in 8 years.

Rising sea levels associated with flood events (i.e. 1 in 2, 4 and 8 years) show an incremental increase in inundation for the next 200 years under all high and low accretion rate RCP scenarios (Figures 3.12-3.19). These simulations indicate that over time flood water levels increase in depth and frequency across the wetland area under current conditions. The low and high accretion rate scenarios suggests that for an event that occurs every 2-, 4- and 8-years, inundation occurs adjacent to the Heuningnes Estuary and extends across the modelled portion of the wetland area. However, there are conspicuous variations in the nature of these flood events.

Model simulations suggest that under low accretion rate scenarios (i.e. current conditions), immediate inundation is evident in 25 years for respective recurrence intervals across all RCP scenarios (Figures 3.12 – 3.15). Inundation increases incrementally for an event that occurs every 2 years for the 2.6 RCP (Figure 3.12a). In 50 years, widespread flooding of the modelled area extends up to ~1 km into the wetland (Figure 3.12). Thereafter, flooding increases, resulting in widespread flooding in 200 years for the 2.6, 4.5, 6.0 and 8.5 RCP scenarios (Figure 3.12-3.15). The results are similar for an event that occurs every 4 years with an indication of slightly more inundation in 125 years, inundation increases to a maximum depth of ~2 m for the 2.6, 4.5, 6.0 and 8.5 RCP scenarios (Figure 3.12b – 3.15b). Extensive large-scale flooding is seen for a 1 in 8 year event across all RCP scenarios, with the entire wetland inundated in 200 years. In scenario 8.5, the depth of inundation increases to ~3 m in 200 years (Figure 3.15c).

Model simulations for the high accretion rate scenarios indicate that an event that occurs every 2 years typically results in inundation close to the estuary, with only small downstream portions of the modelled drainage line being flooded (Figures 3.16a – 3.19a). Flooding increases incrementally in 125 years for the 2.6, 4.5 and 6.0 RCP scenarios (Figures 3.16 – 3.19). In contrast, in RCP 8.5, a 1 in 2 year event would result in largescale flooding of the entire drainage line in 100 years (Figure 3.19a). Results for the 1 in 4 year event are similar, but flooding is slightly more extensive for RCP 2.6, 4.5 and 6.0 scenarios in 125 years than for a 1 in 2 year event (Figures 3.16b – 3.19b). In the RCP 8.5 scenario, flooding during the 1 in 4 year event is extensive, with the entire modelled wetland flooded within 75 years (Figure 3.19b). Currently, an event that occurs every 8 years results in flooding that is generally

confined to the Heuningnes floodplain and lower reaches of the modelled wetland for RCP scenario 2.6 and 4.5 (Figures 3.16c – 3.17c). In RCP scenario 6.0, depressions all the way up the modelled wetland are linked by flood water the entire system is flooded to an average depth of 2.6m (Figure 3.18c). Similarly, in scenario 8.5, the depth of inundation increases to ~3 m (Figure 3.19c).

3.4 Discussion

3.4.1 Coastal wetland resilience: sediment accretion versus sea level rise

Sediment is contributed to coastal wetlands by perennial rivers, ocean tides and storm surges. In the Droë River wetland, none of these sediment sources is constant as the wetland is located in the valley of an abandoned river channel that occasionally receives floodwater from a downstream river course. Despite the absence of a river within the valley, the long-term rate of sediment accretion is relatively high at 3.99 mm.a^{-1} . There are multiple potential sediment sources such as wind-blown sand from coastal dunes, marine sediment delivered by extremely high tides, and lastly, terrestrial sediment from the Heuningnes River and Nuwejaars fluvial network during extreme floods.

A wetland's ability to maintain elevation and survive under rising sea levels depends on the rate of sediment deposition (Mitsch and Gosselink, 2015), prompting some authors to assert that accretion rates are the driving force behind coastal wetland resilience to sea level rise (Schuerch et al., 2012; Belliard et al., 2016). In the Droë River wetland, the short-term sediment accretion rates rate is largely faster than the projected rate of sea level rise up for the next 125 years in all MNHWN and MHWS RCP scenarios (Figure 3.10). However, the 200 year simulations suggest otherwise, here, inundation extends onto the area where sediment accretion has been modelled. This suggests the rate of sea level has exceeded the rate of sediment accretion at 200 years. This indicates that at 200 years, the Droë River wetland is unable to maintain elevation and will therefore not be able to provide resilience to mean sea level. This however, the results for the long-term sediment accretion rate is faster than the projected rate of sea level rise in all MHWN and MHWS RCP scenarios (Figure 3.11). This

suggest that the Droë River wetland has the capacity to maintain elevation for the next 200 years, providing ecosystem resilience to mean sea level rise.

The consideration of water level data that combines the impact of variation in river flows with tides provides a deeper understanding. While accretion rates may be sufficient to offer resilience to changes in mean sea level, MHWN and MHWS, the wetland is vulnerable to slight increases in water level associated with a combination of tides and river flow (i.e. river floods, see Figures 3.16 - 3.19). In these scenarios, increases in inundation of the Droë River wetland occurred at all recurrence intervals modelled. Furthermore, the model outputs suggest that flooding of the Heuningnes River provides connectivity between the wetland and the estuary.

The wetland is rarely flooded by increases in mean sea level alone, but requires heightened water levels in the Heuningnes River to be flooded. The results are similar for water levels associated with the astroturf accretion rate (Figures 3.12 - 3.15).

Some authors have indicated that in some coastal wetlands, there is a feedback between inundation and accretion rate (e.g. Friedrichs and Perry 2001; Temmerman et al., 2004). During flood events, sediment transported by the river and/or tides is deposited on the wetland. As a result, an increase in sea level can result in an increase in accretion rate provided sediment concentrations are sufficiently high. Depending on the balance of sediment supply and elevation, it is possible that an initial increase in frequency of inundation can result in an increase in accretion rate that results in maintenance of the wetland elevation, and therefore wetland resilience. In a scenario where sediment accretion remains lower than the rate of rising sea level, elevation is not maintained and the wetland becomes vulnerable to flooding.

The Droë River wetland's current exposure to seasonal floods may be a predisposing factor in facilitating its resilience to rising sea levels. The deposition of suspended sediment associated with seasonal floods provide a surplus concentration of sediment to the wetland, enabling sediment accretion after a flooding event (see Friedrichs and Perry, 2001). Modelling results indicate that the depth of inundation and frequency of such flood events may increase. Climate change studies predictions an increase in extreme sea level and a marginal increase in local wave height, indicating that these model results may well be conservative estimates

(Vousdoukas et al., 2018). However, this increase may favour an increase in the sediment accretion rate, as it is likely to provide additional sediment to the wetland.

3.4.2 Coastal wetlands in balance: the impact of flow variability

The maintenance of elevation is dependent on the rate of sea level rise relative to sediment accretion within the wetland; this balance is what underlies wetland resilience (Figure 3.20a). However, the relationship is dynamic rather than simplistic in that changes in the frequency of inundation, as occurs when sea levels rise, also causes a change to sediment supply and therefore accretion rate (e.g. Temmerman et al., 2004). Some wetlands may therefore be able to dynamically respond to an increase in sea level by increasing the rate of sediment accretion.

The modelling outputs suggest that for the Droë River wetland, the current sediment accretion rate exceeds potential sea level rise in all high simulation scenarios, resulting in minor changes to frequency of inundation when only the effect of tides were considered. However, this understanding changes significantly when water levels affected by river flows and tides are modelled. In coastal wetlands characterised by variable climates, wet and dry phases may have a major impact on wetland resilience. A wet phase is a series of years where rainfall is above the mean, resulting in the wetland being flooded for an extended period of time. In contrast, a dry phase is when rainfall is below the mean. In extreme dry phases, the wetland may not be flooded at all during the year.

The effect of flow variability on wetland resilience is conceptualised in Figure 3.20. Wetland resilience is a balance between sediment accretion and sea level rise. If sea level rise accelerates, provided sediment accretion accelerates at a similar pace, the wetland maintains elevation and processes remain unchanged. The wetland is resilient (Figure 3.20a).

However, resilience (or balance) may also be maintained through feedbacks or cycles of climatic phases. During a wet climatic phase, seasonal river flows are higher and longer, increasing the frequency and depth of wetland inundation. In combination with a slow increase in sea level, flooding can be extensive. This results in an increase in sediment supply to the wetland. In Figure 3.20b, sediment supply is conceptualised as a ball that moves and can adjust the balance between sea level rise and sediment accretion rate. As sediment supply increases, sediment accretion rates are enhanced. This increases the elevation of the wetland

and reduces the impact of sea level rise. The system is momentarily out of balance as the sediment accretion rate is higher than the rate of sea level rise. However, as the elevation of the wetland is increased, it is subjected to fewer flood events which reduce sediment supply and accretion on the wetland. The system therefore rebalances through a feedback between sediment supply and inundation frequency.

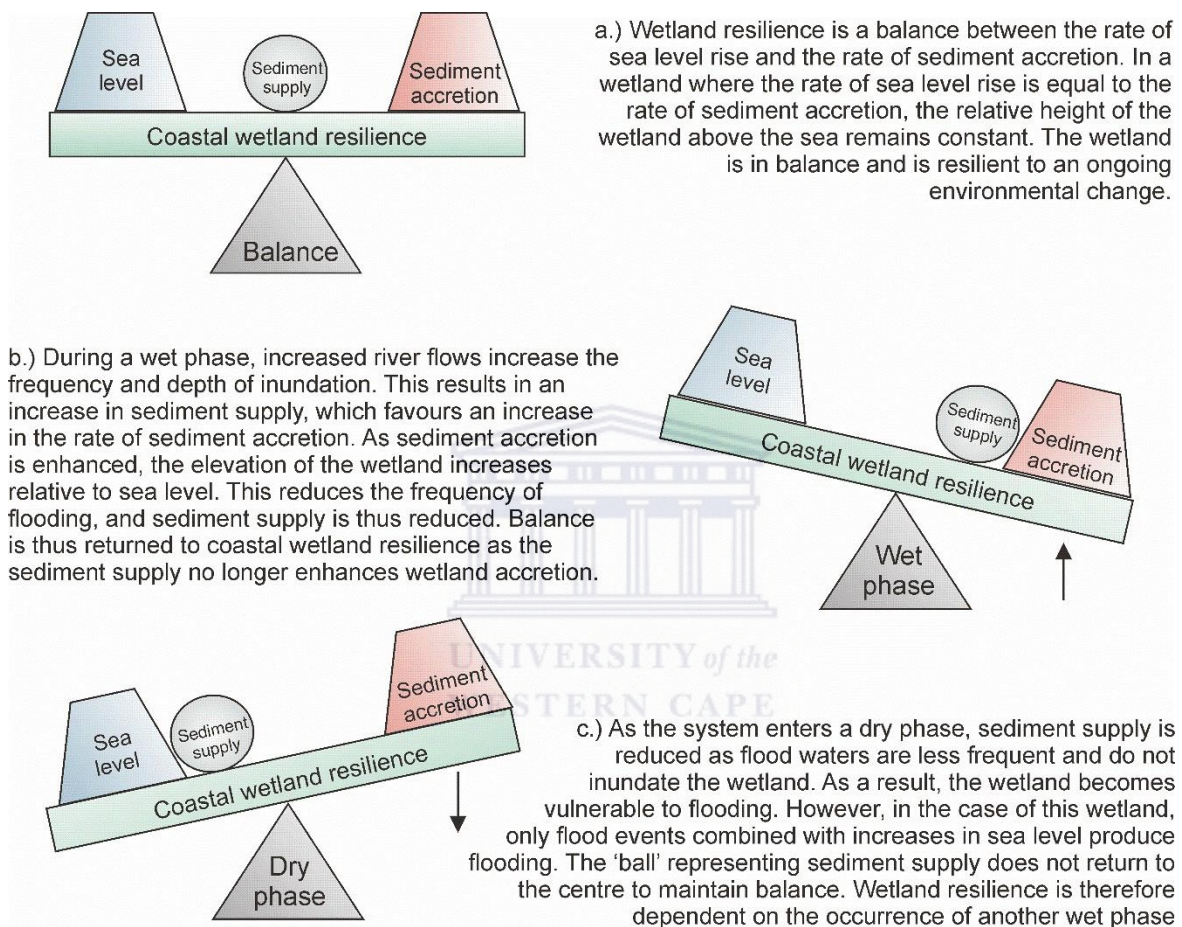


Figure 3.20: Conceptual model of coastal wetland resilience and the feedbacks between flow variability, sea level rise and wetland accretion rates.

During a dry phase, the wetland experiences fewer periods of inundation as the river is less frequently flooded. This reduces the rate of sediment accretion on the wetland. In theory, a reduction in sediment accretion rate should lead to an increase in frequency of inundation if the rate of sea level rise remains constant (Figure 3.20c). However, modelling results indicate that for the Droë River wetland, this effect is minimal (Figure 3.10), with inundation of the

modelled wetland negligible for spring flood tides as sea level rises. In this wetland, inundation only occurs when the river floods, regardless of sea level rise. During the dry phase, the counter feedback between accretion rate and frequency of inundation does not operate, the sediment accretion rate is merely reduced. When the wet phase begins, flooding would initially be more severe, reducing over time as the accretion rate increased, resulting in increased elevation. Long-term wetland resilience is therefore dependent on the occurrence of wet phases of seasonal flooding that bring sediment to the wetland.



Chapter 4: Inland wetlands on a hydrological continuum: variations in hydrological inputs determined using a remote sensing approach

4.1 Introduction

The hydrological characteristics of wetland ecosystems are generally defined by the input (e.g. precipitation, groundwater discharge, surface/channelized inflow and subsurface inflows) and output (e.g. evapotranspiration, groundwater recharge, and surface/ channelized outflow) components of the water budget (Mitsch and Gosselink, 2015). Integral to these components is understanding the characteristics of the catchment and local landscape, as these processes are intricately linked to climate, geomorphology and human activities (Ollis et al., 2013; Mitsch and Gosselink, 2015). Several regional classification systems have therefore been developed in an attempt to principally conceptualise the diversity of wetlands globally and in southern Africa (Ollis et al., 2013; Tooth and McCarthy, 2007).

In South Africa, wetlands are usually classified according to a hydrogeomorphic type as this theoretically provides information about ecosystem service provision. The hydrogeomorphic classification attempts to classify wetlands according to their dominant water source and typical geomorphology (Ollis et al., 2013; Ellery et al., 2009). This classification system describes how water enters and flows through a wetland, taking into account the topographical position of wetlands in the landscape. The hydrogeomorphic classification system suggests that wetlands belonging to the same classification unit share similar characteristics regarding the path of water to the wetland and the way in which water flows through and out of the wetland.

The hydrological pathways of water are known to influence the areal extent of water surface area which is considered to be an essential resource for the biophysical environment (Deus and Gloaguen, 2013). Wetlands are largely known for their sensitivity to changes in external environmental conditions such as global and regional climate fluctuations (e.g. droughts and floods). However, according to Tooth et al. (2007), these ecosystems are inherently dynamic and may therefore respond and adapt to these changes in the absence of human influence. Nevertheless, current and future threats to wetlands hydrological regime are driven by land

use change (e.g. the conversion of wetlands to agricultural lands) and climatic variability with exacerbated rainfall cycles of droughts and floods (Wei, et al., 2013; Deus and Gloaguen, 2013).

In southern Africa, rainfall variability has increased, with a particular shift towards increased and widespread drought cycles (Fauchereau et al., 2003). This is plausible as rainfall patterns are projected to decrease over southern Africa under enhanced greenhouse gas emissions (Engelbrecht et al., 2015). As such, slight variations in annual and seasonal rainfall patterns are likely to influence the hydrological processes within a catchment thus affecting the productivity of wetland ecosystems by directly altering their functioning and structure.

Understanding how wetlands respond to changes in hydrological processes as a result of exacerbated rainfall patterns is essential for effective wetland management, rehabilitation and conservation (Baker and Maltby, 2009). The water surface area in wetlands is intricately influenced by these interactions and may therefore reflect how different wetlands function hydrologically through the application of remote sensing. Advances in the spatial, temporal and spectral resolution of remote sensing technology provide a unique platform for the investigation of historical and present wetland hydrological patterns and variations in surface waters (see Ning et al., 2015; Dona et al., 2016; Ji et al., 2018). In this chapter, the relationship between rainfall and wetland water surface area was investigated to understand wetland water budgets and to establish historical ranges of variability in wetland water surface area.

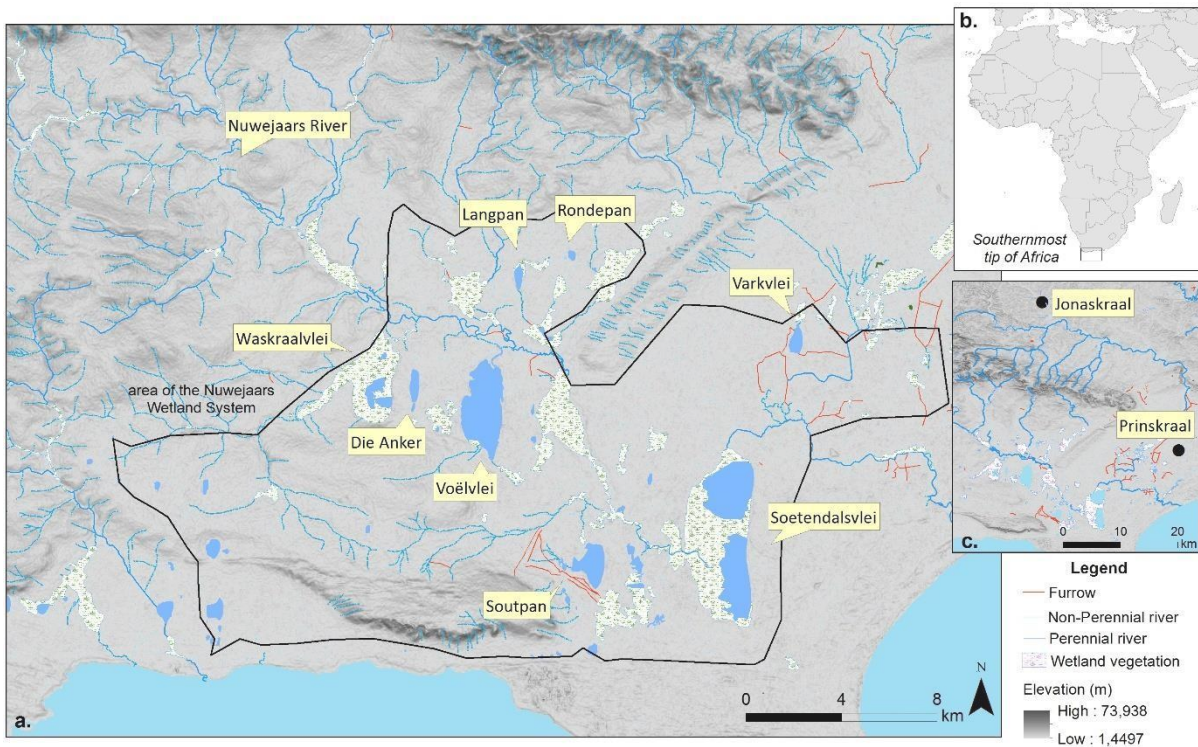


Figure 4.1: The location of Nuwejaars wetland system (map a), near the southernmost tip of Africa (insert map b). These wetlands are characterized by large areas of open surface water, some are interlinked to the Nuwejaars River system and other are isolated endorheic pans/depression. Insert map c indicates the locations of local (Prinskraal) and catchment (Jonaskraal) rainfall stations relative to the wetlands.

UNIVERSITY of the
WESTERN CAPE

4.2 Materials and Methods

4.2.1 Study site

The study site are the wetlands with large water surface areas on the Agulhas coastal plain (Figure 4.1). Here, some wetland ecosystems are linked to the Nuwejaars River system and others are endorheic pans/depressions with an outflow stream (see Table 4.1). Wetlands such as Soetendalsvlei are directly linked to the Nuwejaars River system; a tributary flows through Waskraalvlei and feeds into the Nuwejaars River; and Voëlvlei has a unique outlet channel which typically flows into the Nuwejaars River. However, most of the time during extreme rainfall, the outlet channel is an inflow channel from the Nuwejaars River which then feeds into Voëlvlei. Endorheic pans such as Soutpan; Langpan; Rondepan; Die Anker and Varkvlei are located across the plain (see Figure 4.1). These pans are typically circular and oval in shape,

relatively shallow, and some are characterized by vegetation growth on the edges (i.e. Rondepan) and small stream channels flowing into or out of the pan.

Table 4.1: Hydrogeomorphic characteristics of the Nuwejaars wetland ecosystems. The relative size of the Hydrogeomorphic catchment type has been delineated based on a Google Earth and topographical map interpretation, and field verification. The following categories were determined: < 10 km² (small), 10 – 100 km² (intermediate) and > 100km² (large).

Wetland name	Hydrogeomorphic type	Relative catchment size	Management
Die Anker	Endorheic depression - not connected by a drainage network or small channel.	Small	Nuwejaars Wetland Special Management Area (SMA)
Waskraalvlei	Lake depression fed by the confluence of Uintjieskuil and Plaaskloof river, after which it flows into the Nuwejaars River.	Intermediate	
Varkvlei	Depression linked to a furrow extending from Poort river (a non-perennial river).	Small	
Rondepan	Depression - not connected by a drainage network or small channel.	Small	
Voëlvlei	Lake depression fed by a non-perennial stream and outflows into the Nuwejaars River. However, during extreme rainfall and floods, the Nuwejaars River flows into Voëlvlei via the outlet channel.	Intermediate	
Soutpan	Saline depression linked to a non-perennial river channel.	Small	Agulhas National Park
Langpan	Depression linked to a non-perennial river channel and has channel outflow.	Small	Nuwejaars Wetland SMA
Soetendalsvlei	Lacustrine depression linked to the main drainage network of the Nuwejaars River, the outflow confluence with the Kars River to form the Heuningnes River.	Large	The Nuwejaars Wetland SMA Agulhas National Park and Cape Nature

4.2.2 Data collection

4.2.2.1 Satellite image acquisition

Multispectral imagery from Landsat 5 TM and Landsat 8 OLI were used to detect spatial and temporal changes in wetland surface water extent on the Agulhas Coastal Plain. Landsat Surface Reflectance images were acquired through the United States Geological Survey (USGS) EarthExplorer Landsat Collection 1 (level 2 on-demand) at WRS-2 Path 174, Row 84 (<https://earthexplorer.usgs.gov/>) (Figure 4.1). A total of 63 Surface Reflectance images were selected for the analysis, resulting in a full record for the period 1989 – 2017. A number of images within Landsat Collection 1 were rendered as unusable as extensive cloud cover masked the study site. Satellite imagery from Landsat 7 ETM+ were excluded from this study as a result of the permanent failure and effects of the Scan Line Corrector (SLC) (Zanter, 2018). The suitability of Landsat satellites and associated sensors is predominantly attributed to the length of its historical data collection (since 1972); the availability of the datasets which are cost free; the spatial, spectral and temporal resolutions (Table 4.2); the surface reflectance products and latest Tier Collections. The latter advancements provide “application-ready” and sophisticated quality data for its global users across three tiers (Zanter, 2017). These data products are particularly useful when working with large datasets, as they allow for immediate application of spectral indices which require images to be corrected for reflectance, and time-efficient for users, alleviating the application of image pre-processing (e.g. Top of Atmosphere Correction).

Table 4.2: Landsat 5 TM and Landsat 8 OLI specifications.

Satellite	Band	Description	Wavelength (μm)	Spatial resolution (m)	Return period
Landsat 5 TM	1	Blue	0.45 - 0.52	30m	16 days
	2	Green	0.52 - 0.60	30m	
	3	Red	0.63 - 0.69	30m	
	4	Near infra-red	0.76 - 0.90	30m	
	5	Short wave infra-red 1	1.55 - 1.75	30m	
	6	Thermal infra-red	10.40 - 12.50	120m	
	7	Short wave-infra-red 2	2.08 - 2.35	30m	
Landsat 8 OLI	1	Coastal aerosol	0.43 - 0.45	30m	
	2	Blue	0.45 - 0.51	30m	
	3	Green	0.53 - 0.59	30m	
	4	Red	0.64 - 0.67	30m	
	5	Near-infrared	0.85 - 0.88	30m	
	6	Shortwave infrared 1	1.57 - 1.65	30m	
	7	Shortwave infrared 2	2.11 - 2.29	30m	
	8	Panchromatic	0.50 - 0.68	15m	
	9	Cirrus	1.36 - 1.38	30m	

4.2.2.2 Precipitation record

Daily precipitation records for the study site were obtained from the Agricultural Research Council (ARC) to characterize local (i.e. Prinskraal stations) and catchment rainfall (i.e. Jonaskraal) (Table 4.3). Two neighbouring rainfall stations were used to characterize the precipitation record for Prinskraal (i.e. station no. 20062 and 30764) and Jonaskraal (i.e. station no. 20060 and 30983) respectively (Table 4.3 and Figure 4.1). These stations were selected primarily based on the length of the rainfall record, i.e. 46 years. A long-term dataset is essential to determine an accurate representation of rainfall that is not influenced by year-to-year variability. ARC has a series of weather stations located on the Agulhas Plain, the oldest station for this region dates back to 1904, however, most of these stations do not have a uninterrupted historical record or are not operating at present.

Table 4.3: Specifications of ARC rainfall stations.

Station number	Station name	Start and end date	Coordinates	Altitude (m)
20062	Prinskraal	01-01-1973 to 09-30-2006	-34,6333 S; 20,11667 E	15
30764	Bredasdorp: Prinskraal	01-08-2006 to 20-08-2018	-34,6274 S; 20,11616 E	12
20060	Jonaskraal	01-04-1973 to 30-06-2014	-34,39454 S; 19,90167 E	106
30983	Jonaskraal	01-10-2013 to 20-08-2018	-34,39456 S; 19,90171 E	99

4.2.3 Data analysis

4.2.3.1 Determining wetland water surface area

In order to examine the inter-annual variations in wetland water surface area, a three-pronged remote sensing approach was adopted in ArcMap 10.3 (Figure 4.2). Firstly, the Modified Normalized Difference Water Index (MNDWI) was applied to detect and enhance changes in wetland water surfaces (Xu, 2006). This spectral water index method has been designed to effectively mask vegetation, soil and built-up features while enhancing open water surface features (Li et al., 2013; Rokni et al., 2014). Secondly, a threshold value of > 0 was applied to respective MNDWI processed images. Lastly, the water surface areas were calculated.

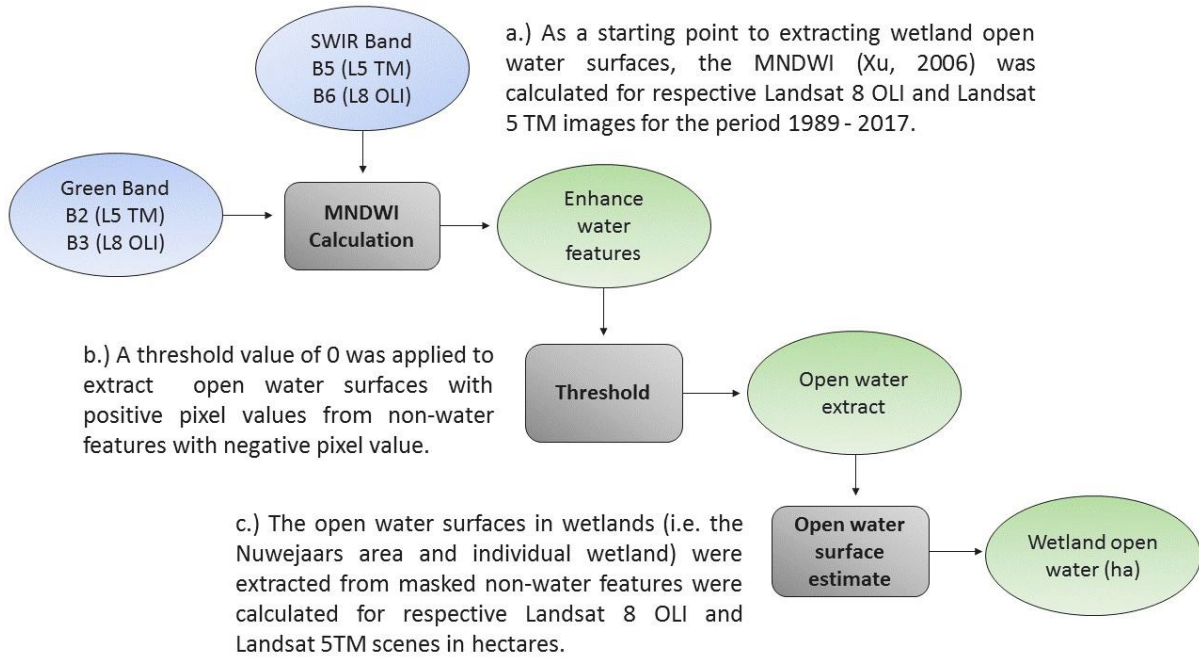


Figure 4.2: MNDWI iteration summary for Landsat 5 TM and Landsat 8 OLI for the period 1989 – 2017.

MNDWI Water Surface Area steps and iterations

1. The computation of Xu (2006) MNDWI for the period 1989 - 2017

Xu (2006) MNDWI was applied to respective Landsat 8 OLI and Landsat 5 TM images to enhance water features and suppress non-water features (see Table 4.4). The MNDWI measure the reflectance of water by using the green and shortwave infrared bands. As a result, water features are characterized by positive pixel values while non-water features are characterized by negative pixel values. The MNDWI has been applied successfully in many studies and is considered to be highly accurate compared to other water indices such as the NDWI (see Li et al., 2013; El-Asmar et al., 2013; Acharya et al., 2016; Buma et al., 2018).

Table 4.4: The MNDWI equation for Landsat 5 TM and Landsat 8 OLI.

MNDWI Index	Landsat sensor	Equation
$\text{MNDWI} = \frac{\rho_{\text{Green}} - \rho_{\text{SWIR}}}{\rho_{\text{Green}} + \rho_{\text{SWIR}}}$	Landsat 5 TM	$\text{MNDWI} = (\text{band2} - \text{band5}) / (\text{band2} + \text{band5})$
	Landsat 8 OLI	$\text{MNDWI} = (\text{band3} - \text{band6}) / (\text{band3} + \text{band6})$

2. Extraction of wetland open water surface area

The MNDWI threshold is based on the spectral signatures assigned to each feature, separating water features from non-water features. Adjusting the threshold can be applied to increase the overall accuracy of the delineation of water in respective images using the Otsu method (Ji et al., 2009). This method adopts the rule of maximum class between variance and assumes pixels can be classified into two classes, ranging distinctively between water and non-water classes (Ji et al., 2009). According to Ji et al. (2009), when applying a threshold to discriminate between water and land, the Otsu method decreases the possibility of mixed pixels. However, since the Otsu method is applied to respective images, the threshold values are not constant and therefore do not allow for accurate comparisons between images. In this case, a default threshold value of > 0 was applied to effectively extract water features from respective Landsat 8 OLI and 5 TM images satellite images.

3. Wetland open water surface area is determined

The surface area extracted for respective Landsat images in step 1 and 2 represents wetland open water surface. The open water surface area were calculated in hectares for the Nuwejaars wetland area and individual wetlands. The following Equation (4.1) was applied:

$$\text{Surface Area Estimate} = \frac{\text{number of pixels recorded} \times \text{pixel size (m}^2\text{)}}{\text{area (ha)}} \quad (4.1)$$

where the number of water pixels recorded are the pixels (or cells) extracted by the MNDWI threshold for each image; pixel size is 900 m²; and area (hectares).

4.2.3.2 Statistical analysis of rainfall and wetland water surface area

The inter-annual variations for rainfall and surface water extent were examined using a number of statistical analysis. For the local (Prinskraal) and catchment (Jonaskraal) rainfall records, annual rainfall, mean monthly rainfall and inter-annual variability (Coefficient of Variation) were calculated. The Coefficient of Variation (CV %) is a statistical indication of inter-annual (year-to-year) variations (Dettinger and Diaz, 2000). A high CV (%) indicates more variability (i.e. extreme variability in wetland water surface area fluctuations) and a low CV

(%) indicates less variability (i.e. constant water surfaces and minimal fluctuations) on a year-to-year basis (Dettinger and Diaz, 2000).

The Coefficient of Variation was calculated to examine inter-annual variability of wetland water surface area for the Nuwejaars Wetland Area and selected wetlands, namely, Die Anker, Waskraalvlei, Varkvlei, Rondepan, Voëlvlei, Soutpan, Langpan, and Soetendalsvlei. The CV for the Nuwejaars wetland system and respective wetlands were derived from the surface water extracted from Landsat 5 TM and 8 OLI for the period 1989 – 2017.

Wetland hydrological inputs and the proportion of the variation in water surface area were examined using a Pearson Correlation analysis (a measurement of linear correlation between two variables, i.e. rainfall and water surface area). The statistical significance of wetland water surface area and rainfall was determined using a two-tailed test. The r^2 value (measures the strength of the relationship between two variables) provides an indication of the usefulness and strength of the relationship.

4.3 Results

4.3.1 Rainfall variability of two rainfall stations

The mean annual precipitation at Prinskraal is 428 mm/yr and the mean monthly precipitation is 33.5 mm/month (Figure 4.3). Precipitation is seasonal, peaking in the autumn month of April, receiving 50.5 mm/month of rainfall, and the driest month is in December in early-summer, receiving 21.5 mm/month of rainfall (Figure 4.3). The inter-annual variability of precipitation is fairly high, with a coefficient of variation of 27%. The driest year for this record is 1974, that received 295 mm/yr, and the wettest year is 2013, receiving an annual rainfall of 721 mm/yr. The record for 2010 has missing values for January to December and is therefore not complete.



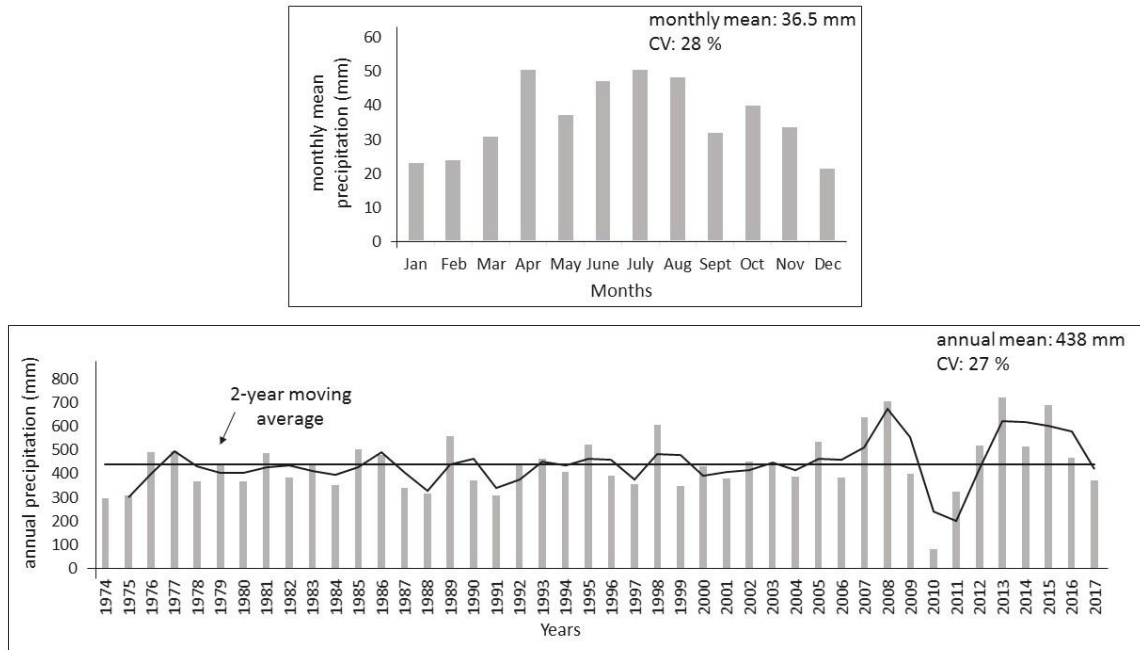


Figure 4.3: Precipitation record presented for Prinskraal, indicating monthly mean precipitation, annual precipitation, seasonality and inter-annual variability.

The annual mean precipitation at Jonaskraal is 402 mm/yr and the mean monthly precipitation is 33.5 mm/month (Figure 4.4). Precipitation is seasonal, peaking in the winter month of July, receiving 51.3 mm/month of rainfall, and the driest month is in mid-summer of February, receiving 21.5 mm/month of rainfall (Figure 4.4). The inter-annual variability of precipitation is fairly low, with a coefficient of variation of 20 %. The driest year for this record is 1974, receiving an annual rainfall of 271 mm/yr, and the wettest year for this record is 2014, receiving an annual rainfall of 602 mm/yr.

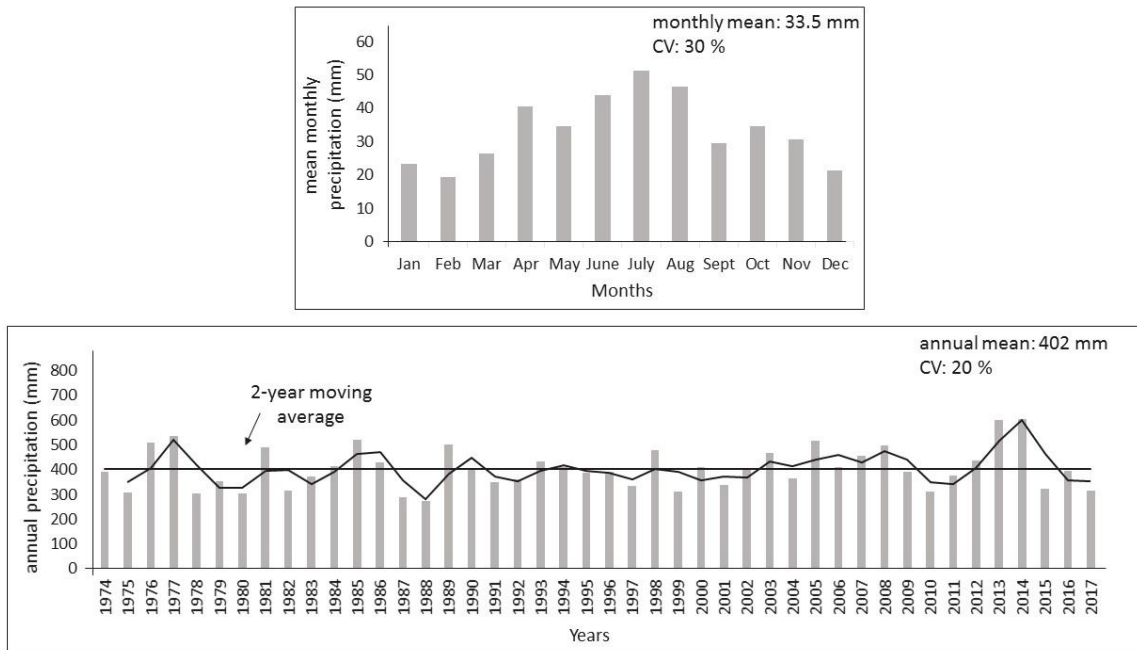


Figure 4.4: Precipitation record presented for Jonaskraal, indicating monthly mean precipitation, annual precipitation, seasonality and inter-annual variability.

The long-term records for both statistics indicates a precipitation pattern from 1974 onward, during which there were regular dry phases of 2-3 years, followed by an extreme wet year (Figures 4.3 and 4.4). From 2007 onward, there was an anomalously high rainfall, followed by an unprecedented 3 year drought. This was followed by a few extremely high rainfall years, followed by a drought again in 2017. These dry phases potentially indicate the influence of El Niño related droughts, which are clearly observable for known drought periods recorded, these include 1978/1980, 1982/1983, 1989/1990, 1991/1992, 1994/1995, 1997/1998, 2003/2004, 2007/2008, 2009/2010 and 2015/2016 (Tyson and Preston-Whyte, 2000, Bahta et al., 2016; Baudion et al., 2017).

4.3.2 Variability in wetland water surface

The CV (%) was used to determine the variability (of wetland water surface area for the Nuwejaars Wetland System and respective wetlands within the Nuwejaars Wetland System (Table 4.4 and Figures 4.5 – 4.12). The Nuwejaars Wetland System as a whole has a CV of 33 %, suggesting a relatively low degree of variability. In contrast, the CV for respective wetland systems presents more detail of the variability of wetland water surface area. The CV

range between 92 % for Waskraalvlei (high variability) to 21 % for Soetendalsvlei (low variability). This range of variability suggests that the water surface area in some wetlands can double or halve in size seasonally or from year to year.

Table 4.5: Coefficient of Variation (%) in wetland water surface area (ha).

Wetland name	mean	min	max	St. dev	CV (%)
Nuwejaars wetland system	1768	997	3475	577	33
Waskraalvlei	61	10	234	56	92
Die Anker	19	0	45	17	89
Varkvlei	24	0	48	17	71
Rondepan	6	0	10	4	62
Voëlvlei	300	168	532	103	34
Soutpan	131	4	169	34	26
Langpan	21	0	28	5	23
Soetendalsvlei	962	658	1563	204	21

The variations in wetland water surface area for the Nuwejaars Wetland System and respective wetland systems are illustrated in Figure 4.5 – 4.13 for the period 1989 - 2017. These MNDWI results provide a clear indication of the spatial and temporal distribution of wetland water surface area for the Nuwejaars Wetland System and respective wetlands (Figure 4.5 – 4.13).

The Nuwejaars wetland system

The average surface water area for the Nuwejaars Wetland System is 1768 ha, with a maximum of 3475 ha. The results indicate that all the wetlands are inundated and the course of the Nuwejaars river is visible (e.g. 3 August 1989). In June 2004, the water surface area reached its minimum extent of 997 ha, with some wetlands drying up completely and no longer visible.

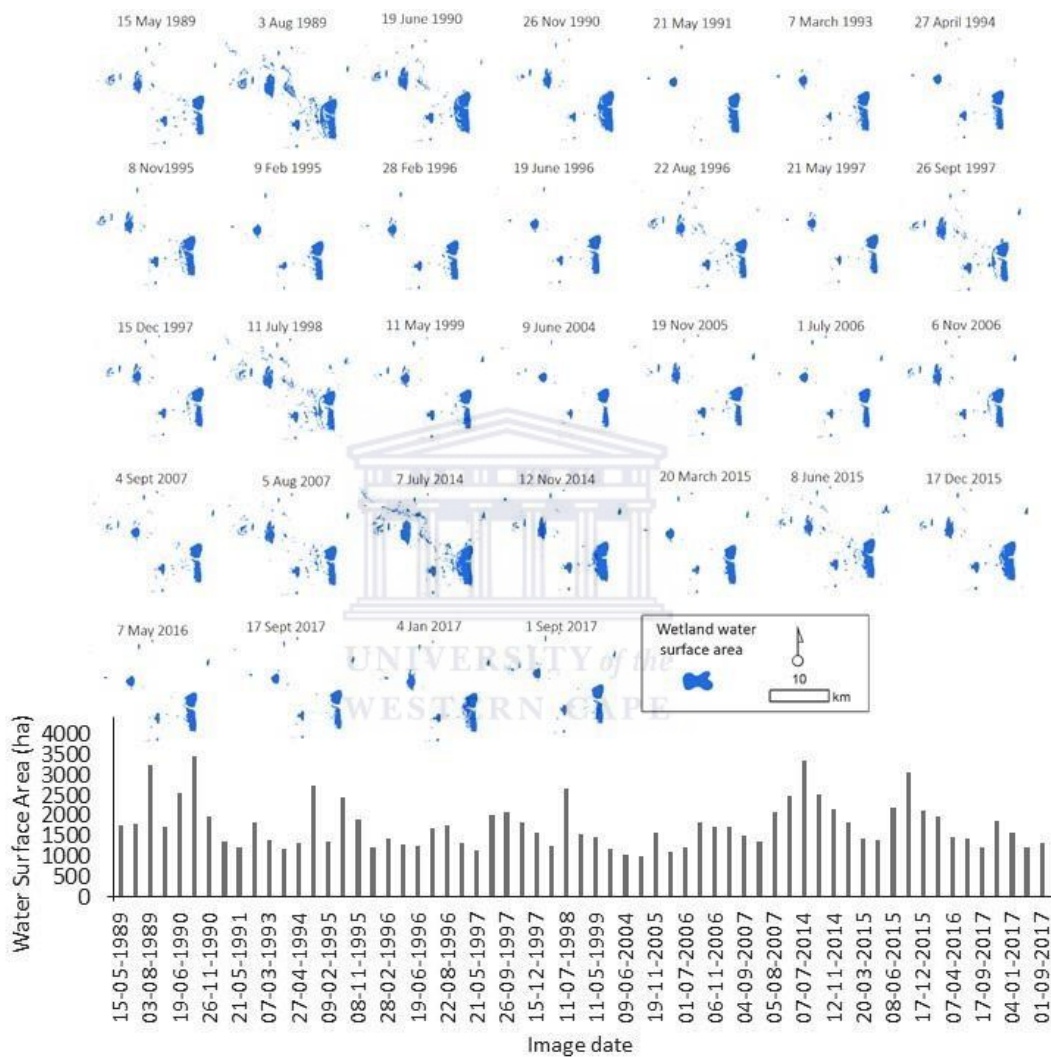


Figure 4.5: Variations in wetland water surface area for the Nuwejaars Wetland System (period 1989 -2017).

Waskraalvlei

In Waskraalvlei, the variability of water surface area is extremely high (Figure 4.6). Waskraalvlei usually covers an average of 61 ha, with a maximum area of 234 ha as indicated by 3 August 1989 image. There is one tiny pool that indicates minimum capacity which usually covers ~10 ha (21 May 1991). The patches of water indicated throughout the images are not well connected. This is as a result of extensive reed growth and saltmarsh vegetation within Waskraalvlei, particularly within the middle and northern portion of the wetland. During a high rainfall season, these areas are inundated by water (e.g. 3 August 1989).

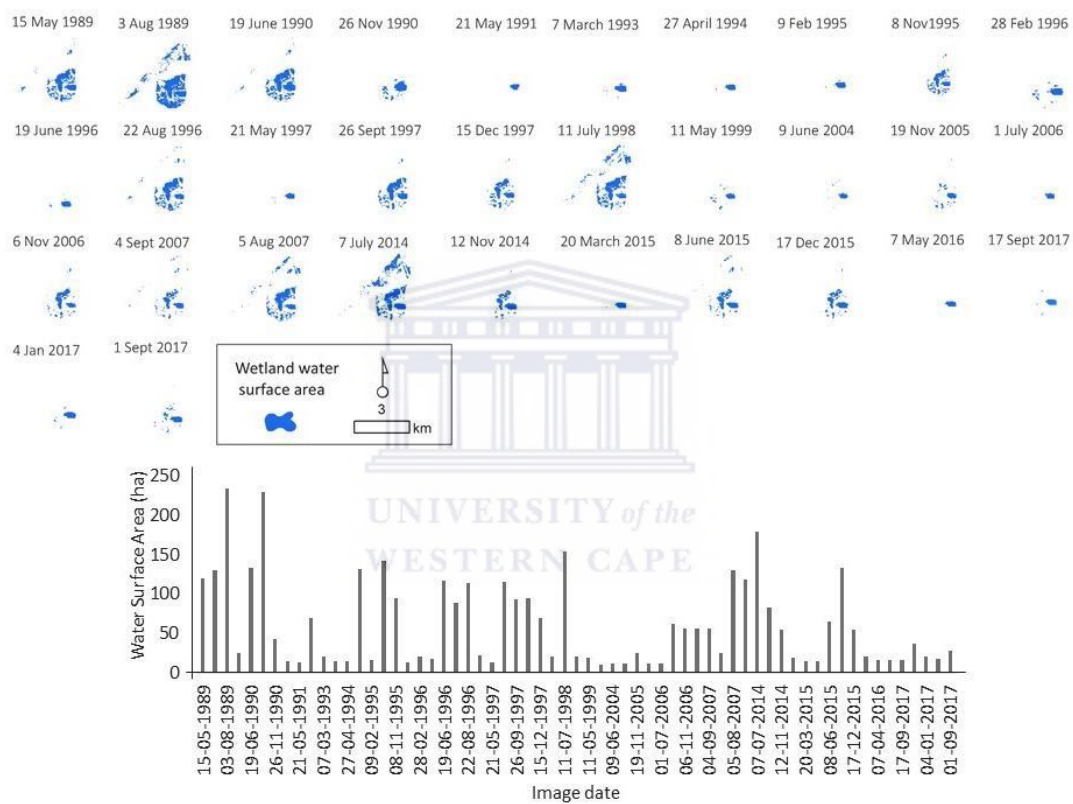


Figure 4.6: Variations in wetland water surface area for Waskraalvlei (period 1989 -2017).

Die Anker

The long-term record indicates the year-to-year variability of surface water for Die Anker (Figure 4.7). Die Anker has an average water surface area of 19 ha, and appears to have a capacity as it usually fills up to 45 ha (see image date: 11 July 1998), or dries completely (see image date: 21 May 1991). This is well matched to the precipitation record and period of known droughts.

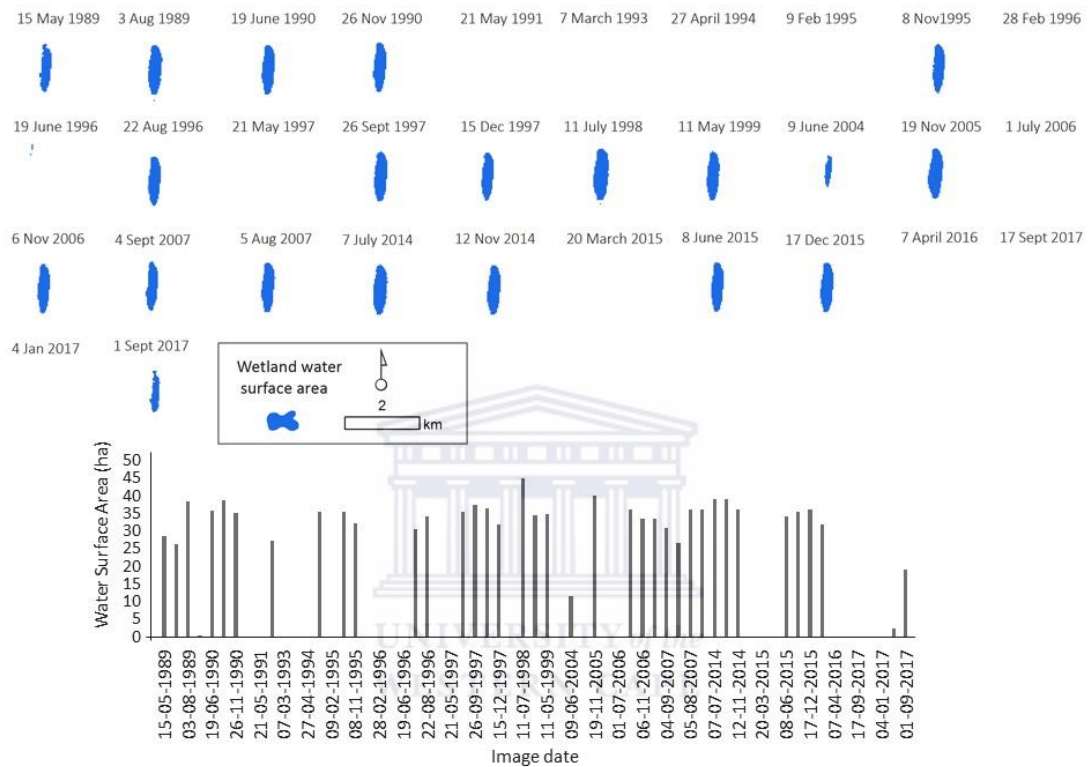


Figure 4.7: Variations in wetland water surface area for Die Anker (period 1989 -2017).

Varkvlei

The variability of water surface area in Varkvlei is high as indicated by the CV value of 71 % (Table 4.5). The average water surface for Varkvlei is 24 ha, with a maximum area of up to 48 ha (26 July 2015), and in some cases dries up completely (26 November 1990). The wetland appears to be full from 2005 onwards, this corresponds with the precipitation record, when the region experienced an anomalously high rainfall (see Figure 4.3 and 4.4). It may also be an indication of anthropogenic influence. Furrows have been made to link the Kars River with Varkvlei, indicating an augmented supply of water from the Kars River and/or potential borehole water.

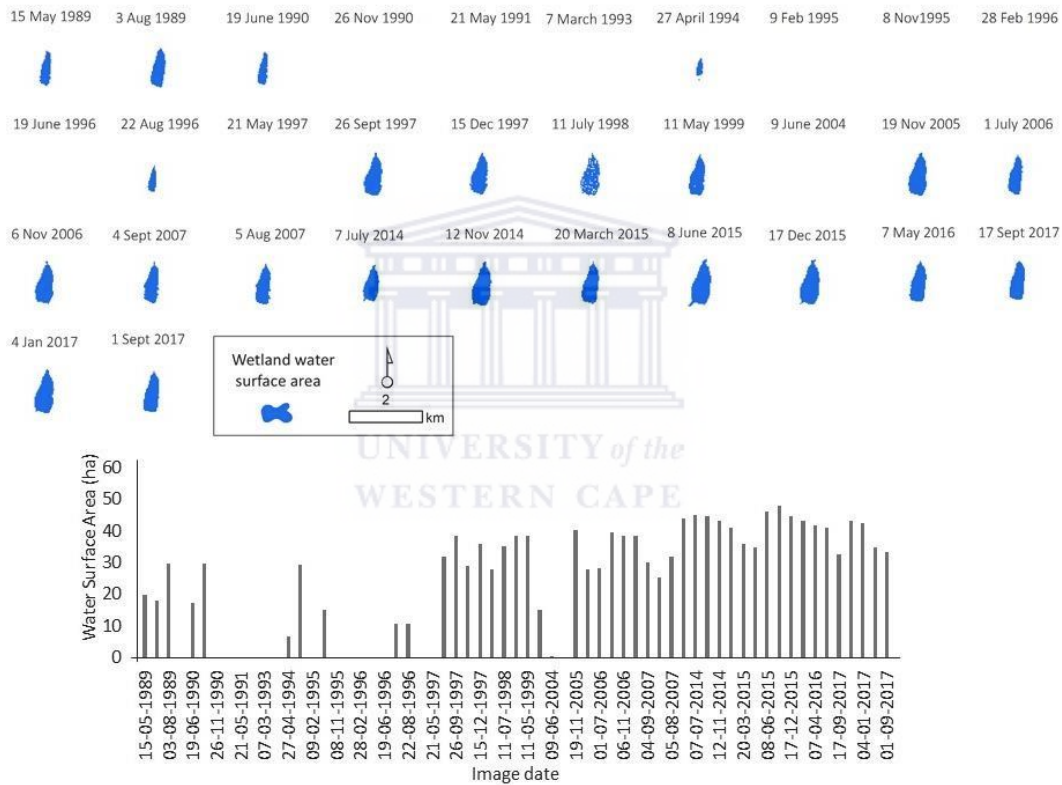


Figure 4.8: Variations in wetland water surface area for Varkvlei (period 1989 -2017).

Rondepan

In Rondepan, the variability in water surface area is high as indicated by a CV of 62 % (Table 4.5). Rondepan has an average water surface area of 6 ha, and usually covers an area of 10 ha (29 June 2017), otherwise it dries out completely. The variability in surface water seems to be matches the precipitation record from 2005 onwards (see Figure 4.3 and 4.4).

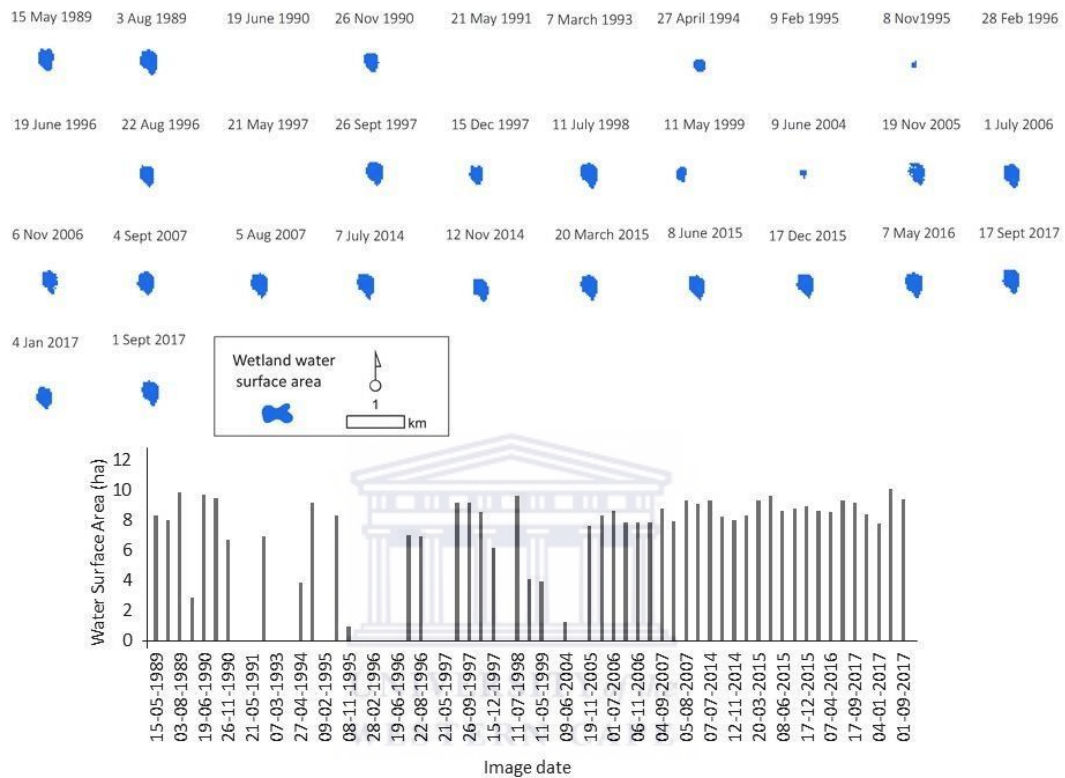


Figure 4.9: Variations in wetland water surface area for Rondepan (period 1989 -2017).

Voëlvlei

The long-term record for Voëlvlei indicates a low year-to-year variability in water surface area, with a CV of 34 % (Table 4.5). The average water surface area for Voëlvlei is 300 ha, with a maximum extent of 532ha 21 July 1990. This is depicted by the 7 July 2014 image which has a surface area of 525 ha and a minimum area of 168 ha (21 May 1991). Voëlvlei is characterized by extensive reed growth around the northern and southern section of the wetland, which is inundated during extreme rainfall. In some images, vegetation appears to disconnect portions of the surface water from the main waterbody, which seems to be permanently inundated.

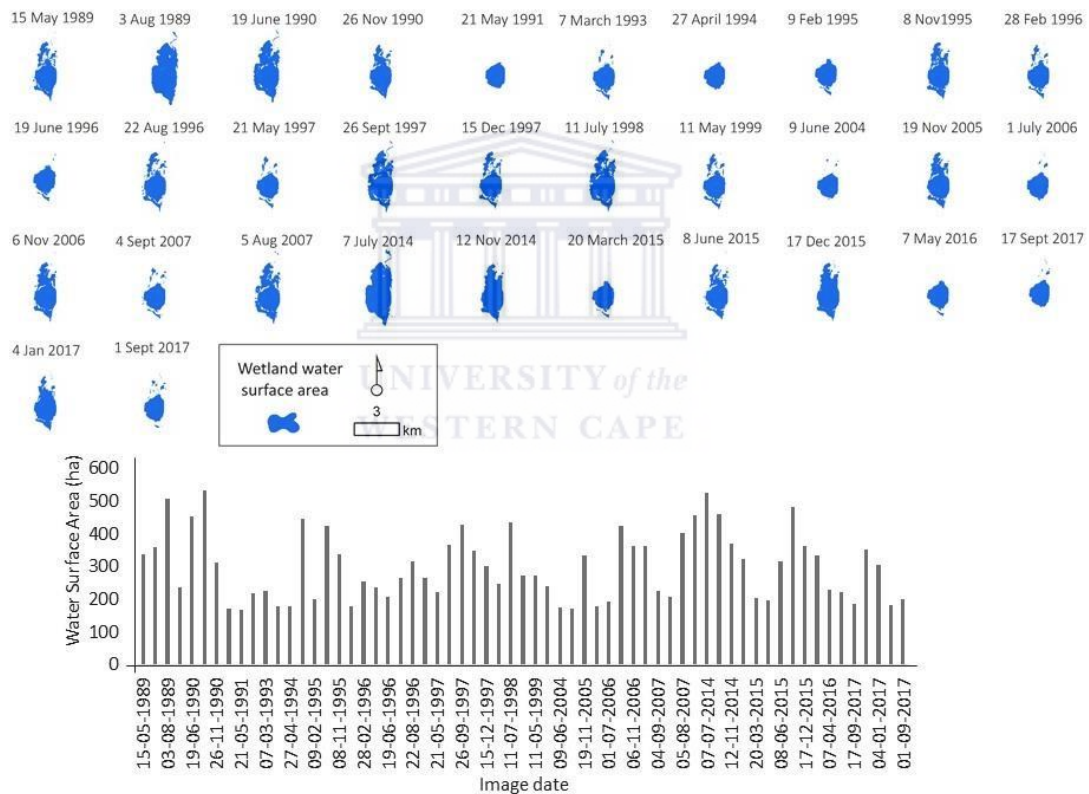


Figure 4.10: Variations in wetland water surface area for Voëlvlei (period 1989 -2017).

Soutpan

The surface area for Soutpan is relatively constant, with a fairly low inter-annual variability of 26 % (Table 4.5). Soutpan has an average surface area of 131 ha, and fills up to a maximum area of 169 ha (3 August 1989) and at times dries up, reaching a minimum of 4ha (21 May 1991). Soutpan is permanently inundated despite dry phases indicated in the precipitation record (see Figure 4.3 and 4.4).

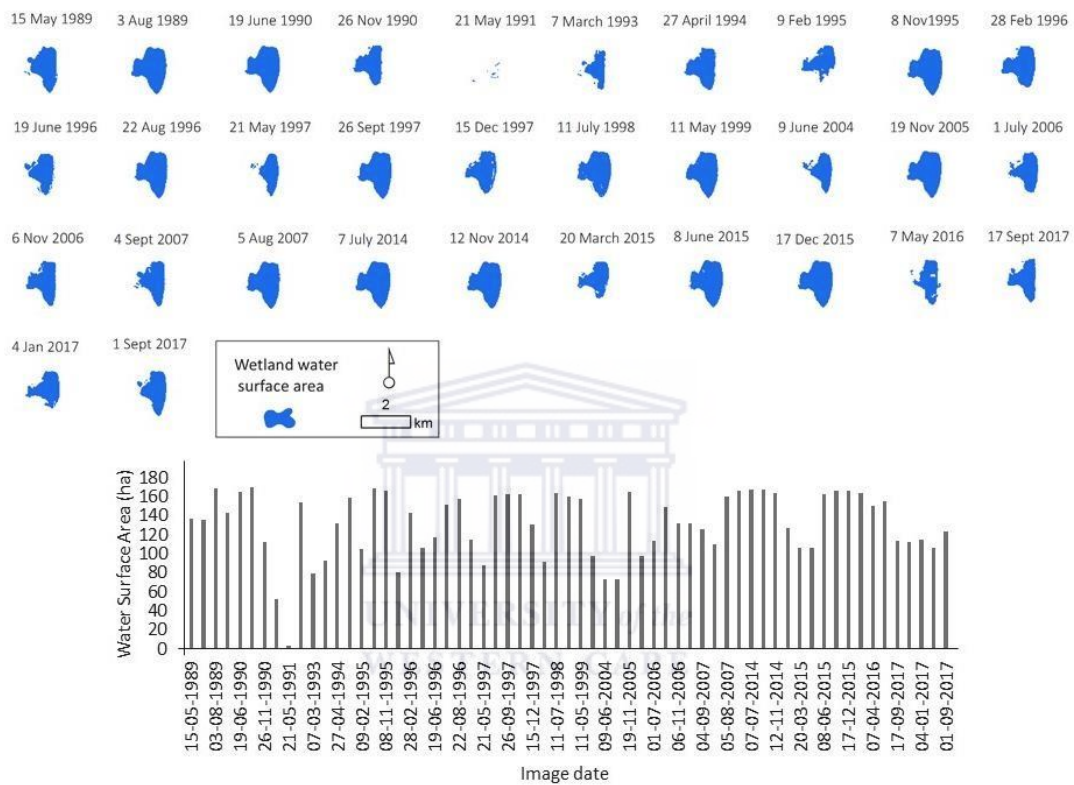


Figure 4.11: Variations in wetland water surface area for Soutpan (period 1989 -2017).

Langpan

In Langpan, the variability in water surface area is indicated by a CV of 23 %. The average surface water area is 21 ha, with a maximum areal extent of 28 ha (7 July 2014) and anomalously dries out completely (7 March 1993). Langpan appears to have a constant surface water regardless of the dry phases indicated in the precipitation record (Figure 4.3 and 4.4).

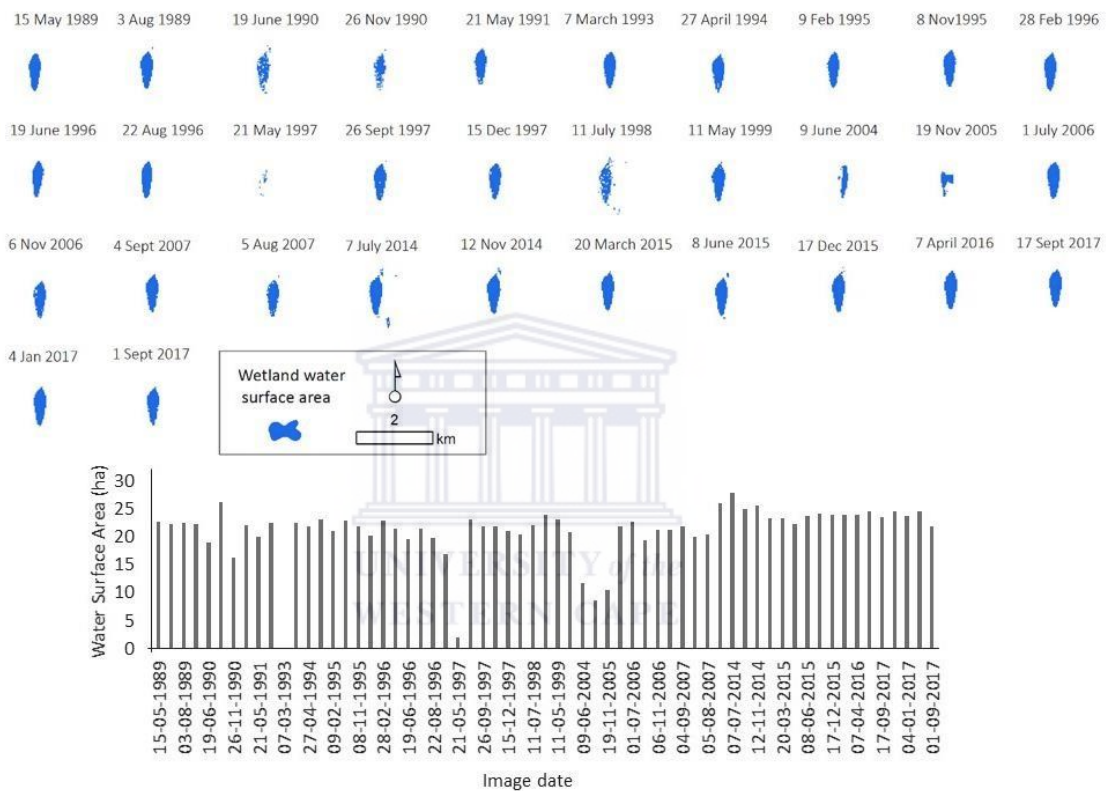


Figure 4.12: Variations in wetland water surface area for Langpan (period 1989 -2017).

Soetendalsvlei

The results indicate that Soetendalsvlei has an average water surface area of 962 ha, and has a maximum extent of 1563 ha (21 July 1990, indicated by the 19 June 1990 image with a surface area of 1352 ha) and a minimum extent of 658ha (9 June 2004). The maximum and minimum areas coincide with high and low rainfall respectively (Figure 4.3 and 4.4). Soetendalsvlei is characterized by widespread reed growth which is visible on the western part of the vlei. The reeds extend across the vlei which at times separate the vlei into two waterbodies. During years with high rainfall, Soetendalsvlei is inundated and forms one waterbody.

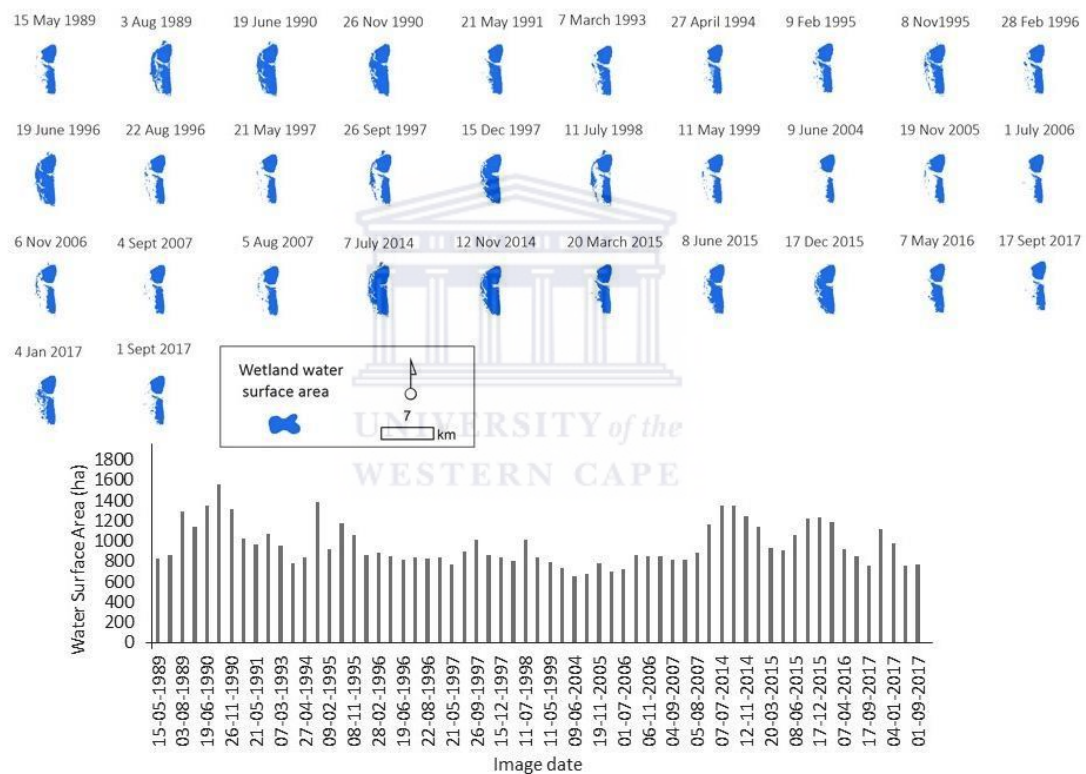


Figure 4.13: Variations in wetland water surface area for Soetendalsvlei (period 1989 -2017).

4.3.3 Wetland water surface area and rainfall correlations

A correlation analysis for wetland water surface area and rainfall estimates were used to investigate wetland response to local and catchment rainfall. The results presented in Table 4.6, compare the water surface area for specific images to total rainfall (local and catchment) for the preceding two years. In order to examine the temporal variation in wetland response (i.e. water surface inundation) to rainfall, water surface area was compared to rainfall in the image month, with the sum of rainfall in the preceding 3, 6, 9, 12 and 24 months. The correlations may also be interpreted in terms of water inputs. As such, wetlands with a high correlation between water surface area and rainfall for preceding 1 to 3 months are likely responding to direct rainfall, channelized inflow, overland flow and throughflow; 6 to 9 months are likely responding to interflow and base flow; and wetlands with high correlations over longer time periods (12 to 24 months) have larger base flow and groundwater contributions.

Table 4.6: Correlations between wetland water surface area for the Nuwejaars Wetland System and respective wetlands, and rainfall (local and catchment) for 1 to 24 months preceding image date. Significant correlations (2-tailed test) are in italics (0.01 confidence) and bold (0.05 confidence).

Sum of rainfall for preceding months	Local Rainfall Correlation (Prinskraal)						Catchment Rainfall Correlation (Jonaskraal)					
	1	3	6	9	12	24	1	3	6	9	12	24
Nuwejaars Wetland System	<i>0.368</i>	<i>0.548</i>	<i>0.554</i>	<i>0.422</i>	<i>0.398</i>	<i>0.356</i>	<i>0.399</i>	<i>0.573</i>	<i>0.568</i>	<i>0.455</i>	<i>0.414</i>	<i>0.408</i>
Waskraalvlei	<i>0.459</i>	<i>0.557</i>	<i>0.456</i>	<i>0.256</i>	0.215	0.013	<i>0.518</i>	<i>0.658</i>	<i>0.496</i>	<i>0.338</i>	<i>0.272</i>	0.099
Die Anker	<i>0.423</i>	<i>0.568</i>	<i>0.511</i>	<i>0.350</i>	0.226	0.079	<i>0.342</i>	<i>0.537</i>	<i>0.526</i>	<i>0.329</i>	0.187	0.174
Varkvlei	<i>0.250</i>	<i>0.391</i>	<i>0.481</i>	<i>0.421</i>	<i>0.380</i>	<i>0.581</i>	0.119	0.238	<i>0.393</i>	<i>0.322</i>	0.223	<i>0.533</i>
Rondepan	<i>0.402</i>	<i>0.466</i>	<i>0.443</i>	<i>0.330</i>	0.318	<i>0.428</i>	<i>0.306</i>	<i>0.372</i>	<i>0.324</i>	0.171	0.123	<i>0.369</i>
Voëlvlei	<i>0.316</i>	<i>0.551</i>	<i>0.620</i>	<i>0.473</i>	<i>0.405</i>	<i>0.289</i>	<i>0.371</i>	<i>0.634</i>	<i>0.715</i>	<i>0.591</i>	<i>0.469</i>	<i>0.404</i>
Soutpan	<i>0.396</i>	<i>0.516</i>	<i>0.545</i>	<i>0.562</i>	<i>0.532</i>	<i>0.300</i>	<i>0.290</i>	<i>0.389</i>	<i>0.423</i>	<i>0.347</i>	0.202	<i>0.259</i>
Langpan	0.121	<i>0.248</i>	<i>0.279</i>	0.188	<i>0.232</i>	<i>0.445</i>	0.188	<i>0.285</i>	<i>0.283</i>	0.175	0.138	<i>0.345</i>
Soetendalsvlei	0.117	<i>0.291</i>	<i>0.411</i>	<i>0.376</i>	<i>0.382</i>	<i>0.457</i>	0.218	<i>0.352</i>	<i>0.459</i>	<i>0.427</i>	<i>0.416</i>	<i>0.446</i>

The correlation results demonstrates how different each system is, and explains which hydrological input are more or less significant (i.e. the high and low significant value). When the r^2 value is converted to a percentage, it indicates what percent of variation in water surface area can be explained by variations in rainfall for the preceding months (see Figure 4.14). So, the amount of rainfall received within either 1, 3, 6, 9, 12 and 24 months may explain either a large or small proportion of the variance in water surface area (i.e. to what degree rainfall explains the variation in water surface area).

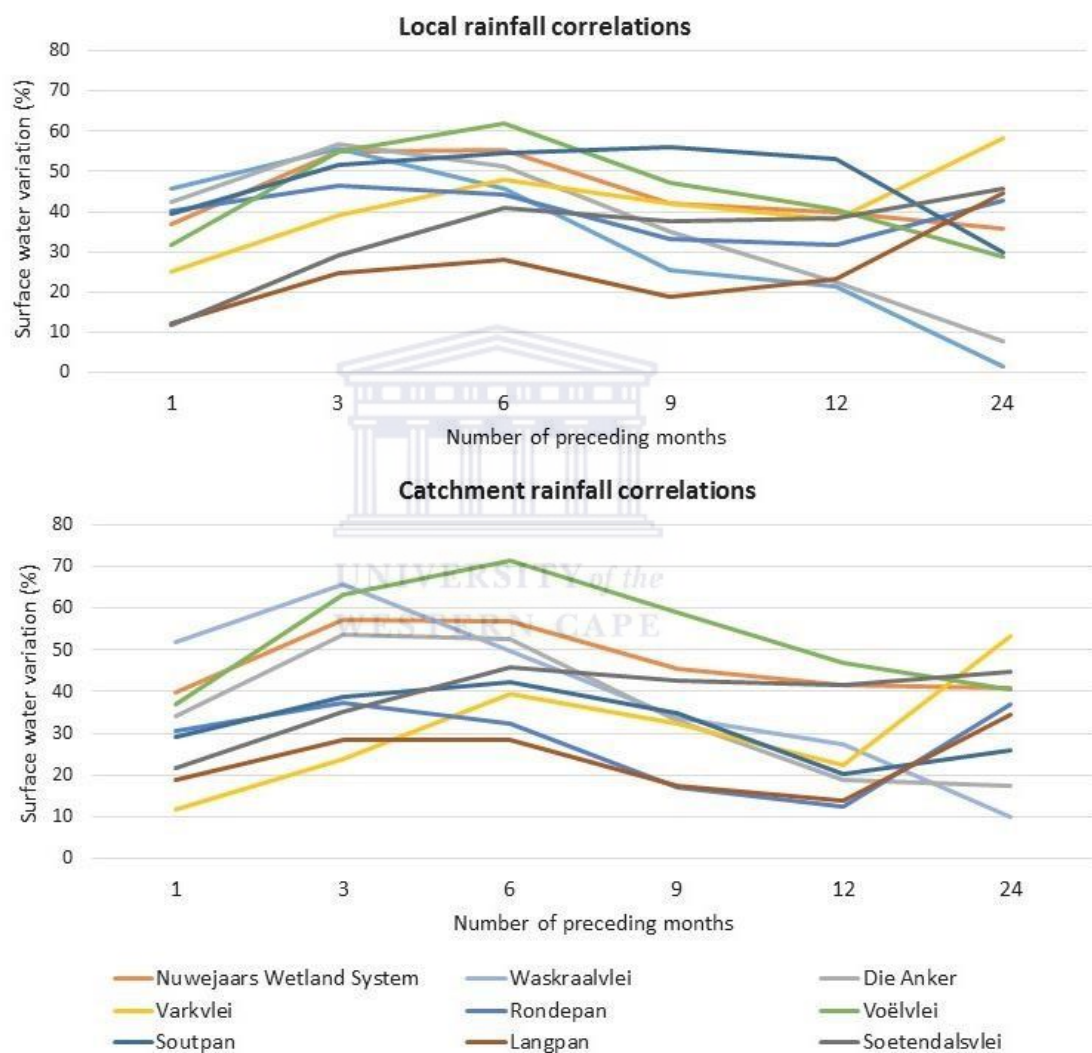


Figure 4.14: Percentage of variation in wetland water surface area for the preceding 1 – 24 months.

The Nuwejaars Wetland System

The Nuwejaars wetland system as indicated in Figure 4.1, includes a variety of wetland types, some which are connected to the river through an inflow or outflow channel, while others are isolated depressions. The relationship between wetland water surface area, and rainfall (local and catchment) were found to be positively correlated for the Nuwejaars wetland system, with a significance of 99 % ($p = 0.01$ significance) (see Table 4.6). This suggest that the wetland system as a whole responds to direct (i.e. 1 to 3 months); intermediate (i.e. 6 to 9 months); and long-term (i.e. 12 to 24 months) local and catchment rainfall.

The significant correlations between wetland water surface area and local rainfall is in the preceding 1 to 24 months. The highest significant correlation is indicated in the preceding 6 months ($p = 0.01$, $r^2 = 0.554$) signifying that interflow accounts for 55.5 % of the variation in surface water. The lowest significant correlation is indicated for the preceding 24 months ($p = 0.01$, $r^2 = 0.356$) with a groundwater contribution of 35.6 %.

When compared to rainfall in the catchment at Jonaskraal, a similar picture emerges, although the r^2 values are higher for every time period compared. The highest significant correlation was in the preceding 3 months ($p = 0.01$, $r^2 = 0.573$) and the lowest significant correlation was indicated for the preceding 1 month ($p = 0.01$, $r^2 = 0.399$). This indicates that the largest contribution to water surface area is interflow (56.8 %). A smaller response, although still statically significant with a 39.9 % contribution from direct precipitation, overland flow and channelized inflow.

Waskraalvlei

Waskraalvlei is a lake depression fed by the Uintjieskuil and Plaaskloof non-perennial rivers of which the outflow feeds into the main channel of the Nuwejaars River. Waskraalvlei is vulnerable to sporadic changes in wetland water surface area, its local catchment is intermediate in size and is characterized by extensive wetland vegetation growth. The significant relationship between wetland water surface area and local rainfall at Prinskraal is in the preceding 1 to 9 months, with the highest significant correlation in the preceding 3 months ($p = 0.01$, $r^2 = 0.557$). This suggests that throughflow explains 55.7 % of the variations in wetland water surface area. The r^2 values are similar for the preceding 1 (p

= 0.01, $r^2 = 0.459$) and 6 ($p = 0.01$, $r^2 = 0.456$) months, explaining 45 % of the surface water area, which is influenced by precipitation, channelized inflow, and throughflow, and minimal input from base flow at 9 months ($p = 0.05$, $r^2 = 0.256$).

However, when compared with catchment rainfall, the results are similar but slightly higher, and includes the preceding 12 months. Groundwater seems to be less significant as an input, with r^2 values tapering off after 3 months and further scaling down to the lowest significant correlation at 12 months ($p = 0.05$, $r^2 = 0.272$). The highest significant correlation is indicated for the preceding 3 months ($p = 0.01$, $r^2 = 0.658$), which is similar to the response to local rainfall, explaining 65.8% of the variation.

Die Anker

Die Anker, a depression that is not linked to a drainage network and has a small catchment, is vulnerable to erratic water surface areas. The significant correlations for local rainfall are similar to Waskraalvlei as indicated for the preceding 1 to 9 months. The highest significant correlation is in the preceding 3 months ($p = 0.01$, $r^2 = 0.568$), thus responding to throughflow which explains 56.8% of the variation in wetland water surface area. The lowest significant correlation is indicated in the preceding 9 months ($p = 0.01$, $r^2 = 0.350$), indicating limited contributions from base flow.

When compared with catchment rainfall, the correlation results are similar for the time periods (i.e. significance for the preceding 1 to 12 months), but in this case, it is somewhat lower. The correlation peaks in the preceding 3 months ($p = 0.01$, $r^2 = 0.537$) suggesting a significant contribution by throughflow, and interflow in the preceding 6 months ($p = 0.01$, $r^2 = 0.526$). The r^2 values for drops significantly in the preceding 1 ($p = 0.01$, $r^2 = 0.342$), and 9 ($p = 0.01$, $r^2 = 0.329$) months. This indicates that Die Anker does not respond immediately to local catchment rainfall and run-off, instead, there is a delayed response to soil throughflow. There is no significant relationship with long-term (12 to 24 months) local and catchment rainfall, indicating a negligible groundwater contribution.

Varkvlei

Varkvlei is a small depression wetland fed by a stream. The water surface area in this system is influenced by agricultural activities as indicated by furrows which divert water from the

Kars River to the vlei (Figure 4.1). This may therefore affect the responses to local and catchment rainfall. The significant correlations for local rainfall range between the preceding 1 to 24 months, with the lowest contributions from direct rainfall, overland flow and channelized inflow ($p = 0.5$, $r^2 = 0.25$). Contributions from groundwater is the highest at 58 % for the preceding 24 months ($p = 0.01$, $r^2 = 0.581$).

Similarly, contributions from catchment rainfall at Jonaskraal is highest at 24 months ($p = 0.01$, $r^2 = 0.533$). The correlations indicate no short-term responses to catchment rainfall, however, the correlations are positive suggesting minor inputs from direct rainfall, overland flow throughflow. Interestingly, the responses to groundwater from both local and catchment rainfall are the highest for all correlation results presented in this study. The long-term responses may be influenced by large contributions from the Kars River which is draining a large catchment. The water input contributes may therefore be furrows from the Kars into Varkvlei, rather than from groundwater discharge.

Rondepan

Rondepan is a small depression wetland located adjacent to Langpan. The results at Prinskraal indicate statistical significance in the preceding 1 to 9 and 24 months. As such, the response are associated with direct rainfall and overland flow in the preceding month ($p = 0.01$, $r^2 = 0.402$). This is followed by a peak in the r^2 value for in the preceding 3 months ($p = 0.01$, $r^2 = 0.466$) suggesting a significant input from throughflow. The r^2 value decline at 9 months ($p = 0.01$, $r^2 = 0.330$) indicating limited contributions from base flow. Nevertheless, a delayed response from groundwater is indicated in the preceding 24 months ($p = 0.01$, $r^2 = 0.428$), explaining 42.8 % of the variation in surface water area.

In comparison to local rainfall, a similar picture exists in response to Jonaskraal. However, the r^2 values are much lower in comparison. The peak r^2 value is in the preceding 3 months ($p = 0.01$, $r^2 = 0.372$) (i.e. throughflow) and the in this case, the lowest r^2 value in the preceding 6 months ($p = 0.01$, $r^2 = 0.324$) suggesting partial interflow input. Groundwater input is statistically significant at 24 months ($p = 0.01$, $r^2 = 0.369$), explaining 36.9 % of the variation in wetland water surface area.

Voëlvlei

Voëlvlei is a coastal lake depression characterized by an intermediate catchment size and a fairly stable water surface area. It is fed by a non-perennial river flowing from the north facing slopes of Soetanyberg and feeds into the Nuwejaars River. However, this outlet channel also serves as a reverse inlet channel from the Nuwejaars River during extreme rainfall and floods. The responses to local rainfall is statistically significant for the preceding 1 to 24 months. Thus, the responses are associated with precipitation, overland flow and channelized inflow, throughflow, interflow, base flow and groundwater inputs. The r^2 value peaks in the preceding 6 months ($p = 0.01$, $r^2 = 0.620$) (i.e. interflow) and decrease significantly in the preceding 12 months ($p = 0.05$, $r^2 = 0.289$) (i.e. limited groundwater contribution).

The correlation results are similar when compared to catchment rainfall, with considerably higher r^2 values for the preceding months. However, in this case, lowest r^2 value is in the preceding 1 month ($p = 0.01$, $r^2 = 0.371$), precipitation, overland flow and channelized inflow are fairly low contributing input factors. In contrast, the peak r^2 value is indicated by interflow in the preceding 6 months ($p = 0.01$, $r^2 = 0.715$), explaining 71.5 % of the variation in water surface area.

Soutpan

Soutpan is a hypersaline depression with a relatively small local catchment and is characterized by non-variable water surface area. Soutpan is fed by a non-perennial stream and has no outflow channel. The response to rainfall at Prinskraal is in the preceding 1 to 24 months, with the highest significant correlation for the preceding 9 months ($p = 0.01$, $r^2 = 0.562$), indicating a sufficient base flow input. Contributions from groundwater is significant at 12 months ($p = 0.01$, $r^2 = 0.532$) but declines to the lowest significant value in the preceding 24 months ($p = 0.01$, $r^2 = 0.300$) and explains 30% of the variation in water surface area.

When compared to catchment rainfall, the correlation result are similar but significantly lower. Interflow is indicated as the dominant water input in the preceding 6 months ($p = 0.01$, $r^2 = 0.423$) and the lowest significant correlation is indicated for the preceding 24 months ($p = 0.01$, $r^2 = 0.259$). Contributions from groundwater declines significant in comparison to the other inputs for the preceding 1, 3, 9 and 12 months.

Langpan

Langpan is located adjacent to Rondepan, its surface water is influenced by a small non-perennial river of which the outflow channel flows into a wetland that connected to the Nuwejaars River. The r^2 value is significant for the preceding 3 to 6 and 12 to 24 months, indicating no or little response to direct local rainfall and base flow. The r^2 value increases through the preceding 3 to 6 months and explains approximately 26 % of the variation in surface water respectively. The r^2 value decreases in the preceding 12 months ($p = 0.05$, $r^2 = 0.232$) to the lowest significant correlation and then peaks significantly at 24 months ($p = 0.01$, $r^2 = 0.445$) indicating a large contribution from groundwater. The results are similar for the wetlands response to catchment rainfall, however, the lowest contributions are indicated by throughflow ($p = 0.05$, $r^2 = 0.285$) and interflow ($p = 0.05$, $r^2 = 0.283$).

Soetendalsvlei

Soetendalsvlei is fed by the main channel of the Nuwejaars River, it has a relatively large catchment size and a non-variable water surface area. The correlations results indicates that Soetendalsvlei responds to local rainfall at Prinskraal and catchment rainfall at Jonaskraal in the preceding 3 to 24 months (as indicated by the significant correlations). For local rainfall, the highest significant correlations is in the preceding 24 months ($p = 0.01$, $r^2 = 0.457$) indicating a strong contribution from groundwater. Surprisingly, relationship for the preceding 1 month is not significant, suggesting that direct local rainfall is an input, but it is not as important as the other inputs. Throughflow is an essential input ($p = 0.05$, $r^2 = 0.291$), although the lowest correlation for local rainfall contributing 29 % to water surface area

The correlation results are similar in response to catchment rainfall at Jonaskraal. Direct rainfall has a positive correlation, and throughflow in the preceding 3 months is lowest response ($p = 0.01$, $r^2 = 0.358$). However, it is slightly higher contributing at 35 % to surface water area. Intermediate responses from interflow ($p = 0.01$, $r^2 = 0.459$) and base flow ($p = 0.01$, $r^2 = 0.427$) are slightly higher than the responses to local rainfall, and contributions from groundwater ($p = 0.01$, $r^2 = 0.446$) are slightly slower.

4.4 Discussion

4.4.1 Understanding the variability of wetland water surface area

The hydrogeomorphological characteristics of wetland systems are often considered as the driving force behind the occurrence and distribution of wetlands (Mitsch and Gosselink, 2015; Riddell et al., 2012). In dryland regions, where the rate of evaporation exceeds that of precipitation, the prevalence of wetlands are largely as a result of factors which promote positive surface water balances (Riddell et al., 2012; Tooth and McCarthy, 2007). These include precipitation, river inflow and subsurface flows, groundwater discharge and local geomorphology (Tooth and McCarthy, 2007). The surface water area in wetlands are influenced by these factors, however, it varies significantly across the landscape as wetlands system are unique in terms of their functional capacity, hydrologic and physical characterises (Cole et al., 1997).

For the respective wetlands of the Nuwejaars River system, the CV for Waskraalvlei is 92 % and Die Anker is 89 %, this is extremely high in comparison to the CV for Voëlvlei which is 34 %, Soutpan at 26 % and Soetendalsvlei at 21 % (Table 4.5). These extremes suggests that wetland surface water is either highly seasonal and extremely variable (i.e. the amount of water in the wetland is not very reliable, or predictable and is highly vulnerable to drying up) or fairly constant and less variable (i.e. the amount of water constant and reliable, indicating that these systems will have open water throughout the year, every year). However, the Nuwejaars wetland system, when considered as a whole, has a CV of 33 %. This indicates that although some wetlands are vulnerable to drying up, there will always be some open water within the Nuwejaars wetland system. The Nuwejaars wetland system therefore provides more resilience to changes in surface water area and rainfall, than individual wetlands.

Some authors suggests that the permanent and seasonal characteristics displayed in the water surface area of wetlands are influenced by hydrological inputs and outputs (Baker and Maltby, 2009; Mitsch and Gosselink, 2015; Ellery et al., 2016), the physical characteristics of the wetland and potentially an aquifer (Anibas et al., 2012). The consideration of the relationship between wetland water surface area and rainfall time-scales provide an understanding into these extreme (i.e. high and low) variations, particularly for respective wetlands (Table 4.6). The results suggest that the variability in surface water can be explained by variations in water inputs, whereby wetlands with a high CV respond mainly to direct precipitation, channelized input, overland flow

and throughflow (i.e. preceding 1-3 month); and possibly interflow and base flow (i.e. preceding 6-9 months). Whereas wetlands with a low CV respond not only to short-term inputs, but to long-term inputs such as groundwater discharge sourced from an aquifer (i.e. 12-24 months).

While some wetlands are restricted to surface water inputs, others display possible connections to groundwater (Mitsch and Gosselink, 2015). This is arguably the case for some wetlands of the Nuwejaars wetland system as these wetlands are located on the Agulhas Coastal Plain (Carr et al., 2006). However, Novitzki (1982) suggests that not all wetland systems are linked to groundwater. The variations of surface water in some wetlands are extremely dynamic, and may therefore not only be related to water inputs, but variations in water outputs, such as evapotranspiration and outflow channel (Mitsch and Gosselink, 2015); and the physical characteristics of the wetland are equally important (Cole et al., 1997; Novitzki, 1982).

As a result, small wetlands such as Die Anker (endorheic depression) and Waskraalvlei (lake depression with a slightly larger catchment), are extremely variable, respond to immediate (1-3 months) and intermediate (6-9 months) perturbations (Table 4.5). These wetlands therefore experience a high proportion of water input from direct precipitation, channelized stream flow, overland flow, throughflow and possibly base flow (particularly from catchment rainfall). Considering outflows, evapotranspiration may be extremely high and the basin of these wetlands shallow. In contrast to relatively larger wetland systems such as Soetendalsvlei (lacustrine depression) and Voëlvlei (lake depression with an intermediate catchment size), are less variable, respond to intermediate (6-9 months) and long-term (12-24 months) perturbations (Table 4.5). The results suggests that these wetlands receive a high proportion of water inputs from interflow, throughflow, base flow and groundwater contribution. However, when considering factors such as basin depth and water outputs, these wetlands may be deeper and therefore able to hold water for longer, and evapotranspiration is possibly low.

The variability of wetland water surface area for the Nuwejaars Wetland System and its respective wetlands can be placed on a continuum, ranging between an extremely high to low CV (Figure 4.15). The continuum illustrates the hydrologic behaviour of these respective wetlands systems, indicating that although some wetlands are vulnerable to drying up, there will always be some open water within the Nuwejaars wetland system. Particularly in wetlands which are either connected to

groundwater or are fed by larger catchments with some base flow components or are shallow with low evapotranspiration rates.

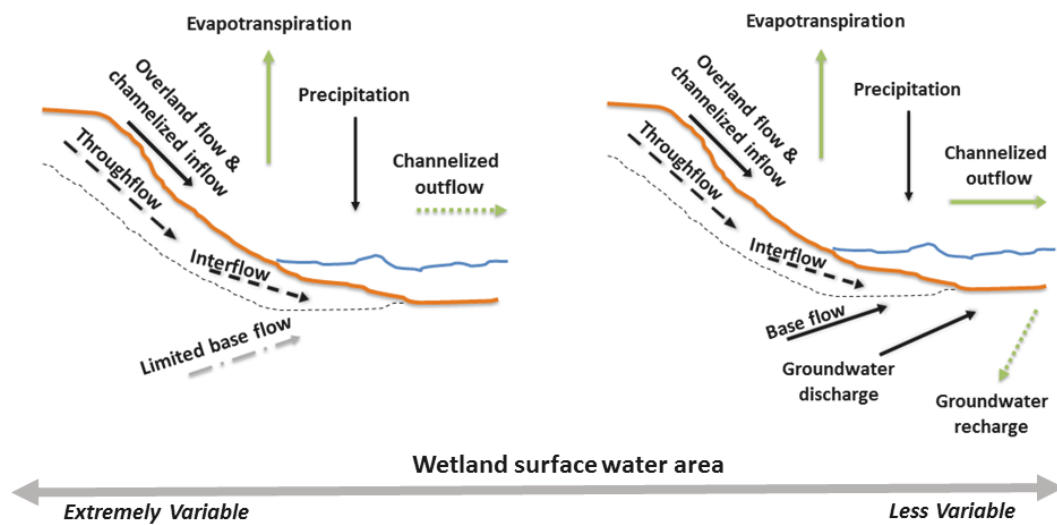


Figure 4.15: The continuum of wetlands on the Agulhas coastal plain and their associated wetland hydrological inputs and outputs.

4.4.2 Implications for wetland management and rehabilitation

Wetland ecosystems globally and in South Africa are under constant threat despite their importance to human livelihoods and ecosystems services (Mitsch and Gosselink, 2015). To address these threats and to maintain the integrity and structure of wetland ecosystems, a number of strategies have been implemented through short- and long-term management and rehabilitation plans. Some plans are often exhaustive and the implementation expensive. A 'passive' approach to wetland management through the introduction and reintroduction of ecosystem engineers to river and wetland environments have therefore become of interest to many decision-makers (Law et al., 2017).

As such, wetland managers and conservationist who are focused on enhancing the hydrologic conditions of wetlands ecosystems have introduced ecosystem engineers such as hippopotamus (*Hippopotamus amphibious*) and wildebeest (*Equus burchelli*) (Moore, 2006). These animals modify and improve the hydrologic conditions of freshwater ecosystems, which is considered to be an essential wetland management practice (Mitsch and Gosselink, 2015),

through creating channels for flood waters, moving and mixing soil, creating habitats, redirecting the flow of water, etc. (Gereta and Wolanski, 1998). However, introducing these animals to wetland environments, especially highly variable wetlands such as on the Agulhas Plain, is extremely challenging as they are accustomed to particular habitats. Hippos are territorial animals that inhabit permanent water bodies such as rivers, lakes and wetland ecosystems, and they require sufficient grazing grass (Lewison, 2007). Crocodiles inhabit freshwater, salty and swampy waters (Ashton, 2010) and wildebeest inhabit grassy plains and bushlands (Davis-Mostet, 2016).

In the case of the Nuwejaars wetland system, introducing ecosystem engineers such as the hippopotamus, crocodile and wildebeest may be challenging for wetland managers and conservationists. This is as a result of the range of wetlands in this regions, which lie on a continuum, from permanent to highly variable wetlands (Table 4.5). The results demonstrate the importance of rainfall in maintaining wetland surface waters, indicating that even during periods of low rainfall, the water surfaces in some wetlands will be maintained, while others may partially or completely dry up.

Wetlands such as Soetendalsvlei and Voëlvlei are less variable and resilient (i.e. not vulnerable to drying up) during dry periods. They have a permanent and predictable water surface area, with sufficient vegetation and grazing grounds to hosts hippopotamus, crocodiles and wildebeests during dry and wet periods. In comparison to Waskraalvlei which has sufficient vegetation and grazing grounds, is highly variable, with an unpredictable surface waters and is extremely vulnerable to drying up during periods of low rainfall. Waskraalvlei is therefore potentially unsuitable to host hippopotamus and wildebeest. However, Waskraalvlei could possibly host wildebeest, as the surface waters in the pan on the southern portion of Waskraalvlei seems to be permanent despite dry periods.

In addition to hosting terrestrial animals at specific wetlands, wetland birds are particularly fond of the Agulhas Plain (Kraaji, 2008). The variability in wetland surface waters and associated fluctuating water levels create habitats (temporary and/or permanent) for a variety of wetland birds (Keddy, 2000). As a result of the variability of wetlands on the continuum, wetlands which are extremely variable such as Waskraalvlei are likely to provide temporary habitats for birds, while becoming unfavourable during dry periods. In contrast,

habitat conditions in Voëlvlei and Soetendalsvlei will be maintained since these wetlands are less variable and are characterized by permanent water surface area. These conditions may become more favourable during dry periods as the water level decreases exposing submerged vegetation, thus creating favourable conditions for birds which prefer low water levels. This suggests that wetlands which are less variable are likely to become more diverse, particularly during dry periods.

4.4.3 A potential monitoring tool

Management and rehabilitation interventions strategies for wetland ecosystems are generally expensive, extremely challenging and the outcomes are often uncertain (Euliss et al., 2008). The need to conduct baseline assessment has become a priority for wetland managers and conservationists because these assessments provide a platform from which informed decisions can be made to facilitate effective and feasible interventions (Euliss et al., 2008). As such, the results presented in Table 4.5 suggest that the methods of this chapter could possibly aid and inform conservation efforts particularly where emphasis is placed on improving the hydrologic conditions of wetlands by introducing large animal's (e.g. ecosystem engineers).

Firstly, the application of remote sensing data coupled with rainfall analysis can be used to develop an understanding of the hydrological characteristics (i.e. water surface variability and water inputs) of wetland ecosystems. With this understanding, generalizations about the wetland water surface resilience based on the hydrogeomorphic type of the wetland.

Secondly, we can build a picture of the historical functioning of a wetland, which can be used to determine if there has been a change (e.g. maybe a wetland never dries up, but more recently it has), and what are the factors driving these changes. Finally, essential to wetland functioning is vegetation productivity, the Normalized Difference Vegetation Index (NDVI), can be used in wetlands which are not characterized by open water surfaces (e.g. Lumbierres et al., 2017). Estimates of vegetation productivity is complex, particularly in regions characterized by strong seasonal climates (Lumbierres et al., 2017). Generally, vegetation productivity is sensitive to variations in precipitation and temperature (Mitsch and Gosselink, 2015). Under the influence of climate change and climatic variability, growth cycles are

irregular, with temporal shifts in the start, end and duration of the growth season (Lumbierres et al., 2017). An accurate assessment of vegetation productivity therefore requires a time series analysis consisting of consecutive growth seasons to estimate the responses of wetland vegetation to temperature and precipitation.



Chapter 5: Discussion and conclusion

5.1 Wetlands in dry climates: the influence of wet cycles

Southern Africa is a highly variable region, prone to the occurrences of droughts and floods (Engelbrecht et al., 2015). As a result of increased anthropogenic activities and associated climate change, exacerbated drought and flood cycles are expected to influence many regions across the globe (Hartmann et al., 2013). Southern Africa in particular is projected to become drier under enhanced anthropogenic forcing, this means that annual and seasonal rainfall will decrease across this region, predominantly over the south-western Cape (i.e. the Agulhas plain region) (Engelbrecht et al., 2015).

The influence of El Niño oscillations are evident in the rainfall data, resulting in regular spells of about three years being drier than average, followed by one year wetter than average. The influence of ENSO in the winter rainfall region has recently been confirmed in the study by Philippon et al. (2012), predominantly evident from the 1976/1977 climatic shift. They suggest that ENSO in this region may have a strong decadal component which seems to be restricted to the recent decade's post 1976 (Philippon et al., 2012).

The rainfall records at Prinskraal (local) and Jonaskraal (catchment) are similar. This is likely due to the strength and intensity of the rainfall system as it moves across the south-western Cape coast region. Nevertheless, the rainfall records indicate that the whole of the Agulhas region is influenced by the same weather systems; that is the South Atlantic Anticyclone in summer, resulting in mainly dry conditions (Reason et al., 2003). In winter, rainfall arrives predominantly from cold fronts and partly from cut-off lows (Reason et al., 2003). These weather systems dominate the supply of rainfall to the wetlands of the Agulhas Plain.

Muhammed and Savenije (2014) suggest that wetlands in dry regions may be more resilient to changes in rainfall given their adaptive nature to marginal climates. This may be correct to some degree, however, integral to the functioning of wetlands on the Agulhas Plain are wet cycles. This study suggests that wet cycles, which are generally short and intense, act as a buffer to wetlands during prolonged dry periods. Coastal wetlands, such as the Droë river wetland, rely on flood waters during wet phases for sufficient sediment loads to enable

accretion and build resilience against rising sea level. Similarly, the maintenance of wetland water surface area is dependent rainfall during wet years to recharge groundwater.

5.2 Wetland management in variable landscapes: local versus catchment management

Maintaining and increasing ecosystem resilience in environmental management has become a rigorous task fundamental to the conservation and sustainability of natural ecosystems (Klien et al., 2003; Côté and Darling, 2010). However, for wetland ecosystems, this is a challenging task which is attributed to the dynamic nature of wetlands which are often considered as standalone ecosystems, although in South Africa, most wetlands are linked to drainage lines and therefore catchments (Ellery et al., 2016). Furthermore, it is arguably also influenced by the general confusion of ecosystem management, which according to Yaffee (1999), has multiple meanings and is therefore perceived in different ways by different people and conservation authorities.

Thus, the capacity and motivation to manage these ecosystems differ among various stakeholders (i.e. conservation and management authorities, government stakeholders and landowners), prompting decision makers to manage wetlands according to their mandate and expectations (Kotze et al., 2009). As a result, the management of wetlands has commonly been geared towards site specific wetlands and the mandate of the management authority (Mensik and Paveglio, 2004). Though this approach may be relevant and beneficial for some wetlands, it can be conflicting in other systems.

By understanding the variability of wetlands on a temporal and spatial scale, and the environmental perturbations which influence wetland functioning and processes, we are able to identify how ecosystems can be optimally managed (Euliss et al., 2008). Ecosystem management with a catchment perspective is therefore essential to managing wetlands in a highly variable landscape. In this regard, it would be feasible to introduce large ecosystem engineers such as hippos to highly variable wetlands provided that they are able to move to more suitable habitats which are wetlands that are less variable. This may not be inclusive of to human interest but it will be prospective for wetland ecosystem functioning as a whole.

Furthermore, considering wetlands not only with a landscape perspective, but also with a catchment perspective is necessary. Wetland hydrology is linked to and influenced by

catchment land use, e.g. water abstraction, forestry, alien invasives, or increased run-off from bare ground. These ecosystems can be impacted upon, and be irrevocably altered by actions far removed from them. Catchment risks should therefore be managed on a landscape scale.

5.3 Conclusion

In this study, the maintenance of wetland functioning and resilience to sea level rise and rainfall variability are largely influenced by wet climatic phases. Two main objectives were investigated, firstly, the long-term accretion rate exceeded sea level rise in all RCP scenarios, resulting in very little difference in terms of flooding at spring or neap tides. However, the inclusion of water levels associated with river floods indicated the potential for massive changes in inundation extent and frequency with sea level rise. Furthermore, results suggest that it may be overly simplistic to consider wetland resilience as a relative comparison of the rate of sea level rise and sediment accretion. Feedbacks between inundation, sediment supply and therefore sediment accretion rate require further analysis and morphological modelling in order to further unpack likely changes.

Secondly, the wetlands on the Agulhas Plain can be placed on a continuum of highly variable and less variable wetlands, as indicated by their surface water area variation. Essential to the variability are short- and long-term water inputs. The results indicate that wetlands which respond to short-term inputs such as direct rainfall, overland flow, and channelized inflow and throughflow, are highly variable. In contrast to wetlands which have less variable surface waters, are responding predominantly mainly to base flow and groundwater discharge.

5.3.1 Recommendations

For further analysis, the relationship between wetland vegetation communities and salinity intrusion relative to global and or regional mean sea level rise estimates could be investigated and incorporated into the model. This will provide insight into the potential change on an ecosystem level. With regards to investigating surface water using remote sensing techniques, this data could be coupled with bathymetric data (using a DGPS or Sonar system) to

investigate the influence of changing water levels on habitat conditions for large ecosystem engineers.



References

- Aalto, R., Maurice-Bourgoin, L., Dunne, T., Montgomery, D., Nittrouer, C., Guyot, J., 2003. Episodic sediment accumulation on Amazonian flood plains influenced by El Niño/Southern Oscillation. *Nature*, 425(6957), pp.493-497.
- Aalto, R., Dietrich, W., 2005. Sediment accumulation determined with ²¹⁰Pb geochronology for Strickland River flood plains, Papua New Guinea. *Walling DE, Horowitz (eds) Sediment Budgets, 1*, pp.303-309.
- Acharya, T.D., Yang, I.T., Subedi, A., Lee, D.H., 2016. Change detection of Lakes in Pokhara, Nepal using Landsat Data. *In Multidisciplinary Digital Publishing Institute Proceedings, 1 (2)*, pp.17.
- Ankrah, J., 2018. Climate change impacts and coastal livelihoods; an analysis of fishers of coastal Winneba, Ghana. *Ocean & Coastal Management*, 161, pp.141-146.
- Anibas, C., Verbeiren, B., Buis, K., Chormański, J., De Doncker, L., Okruszko, T., Meire, P., Batelaan, O., 2011. A hierarchical approach on groundwater-surface water interaction in wetlands along the upper Biebrza River, Poland. *Hydrology and Earth System Sciences Discussions*, 8(5), pp.9537-9585.
- Appleby, G., Oldfield, F., 1978. The calculation of lead-210 dates assuming a constant rate of supply of unsupported Pb-210 to the sediment. *Catena*, 5(1), pp.1-8. doi:10.1016/S03418162(78)80002-2.
- Ashton, P.J., 2010. The demise of the Nile crocodile (*Crocodylus niloticus*) as a keystone species for aquatic ecosystem conservation in South Africa: The case of the Olifants River. *Aquatic Conservation: Marine and Freshwater Ecosystems*, 20(5), pp.489-493.
- Bahta, Y.T., Jordaan, A., Muyambo, F., 2016. Communal farmers' perception of drought in South Africa: Policy implication for drought risk reduction. *International Journal of Disaster Risk Reduction*, 20, pp.39-50.

- Baltensweiler, A., Walthert, L., Ginzler, C., Sutter, F., Purves, R.S., Hanewinkel, M., 2017. Terrestrial laser scanning improves digital elevation models and topsoil pH modelling in regions with complex topography and dense vegetation. *Environmental Modelling and Software*, 95, pp.13-21.
- Barker, T., Maltby, E., 2009. 'Chapter 5: Introduction- The Dynamics of Wetlands'. Ed. Maltby, E., Barker, T. *The wetlands handbook*. Oxford: Wiley-Blackwell, pp 116-209.
- Baudoin, M.A., Vogel, C., Nortje, K., Naik, M., 2017. Living with drought in South Africa: Lessons learnt from the recent El Niño drought period. *International Journal of Disaster Risk Reduction*, 23, pp.128-137.
- Belliard, J.P., Di Marco, N., Carniello, L., Toffolon, M., 2016. Sediment and vegetation spatial dynamics facing sea-level rise in microtidal salt marshes: Insights from an ecogeomorphic model. *Advances in water resources*, 93, pp.249-264.
- Biggs, E., Gupta, N., Saikia, S., Duncan, J., 2018. The tea landscape of Assam: Multistakeholder insights into sustainable livelihoods under a changing climate. *Environmental Science and Policy*, 82, pp.9-18.
- Breilh, J.F., Chaumillon, E., Bertin, X., Gravelle, M., 2013. Assessment of static flood modeling techniques: application to contrasting marshes flooded during Xynthia (western France). *Natural Hazards and Earth System Sciences*, 13(6), pp.1595-1612.
- Brisco, B., 2015. Mapping and monitoring surface water and wetlands with synthetic aperture radar. *Remote Sensing of Wetlands: Applications and Advances*, pp.119-136.
- Buma, W., Lee, S.I., Seo, J., 2018. Recent surface water extent of Lake Chad from multispectral sensors and GRACE. *Sensors*, 18(7), p.2082.
- Candela, L., von Igel, W., Javier Elorza, F., Aronica, G., 2009. Impact assessment of combined climate and management scenarios on groundwater resources and associated wetland (Majorca, Spain). *Journal of Hydrology*, 376(3-4), pp.510-527.
- Cape Nature., 2017. Heuningnes Estuary Hydrodynamic Modelling, Flood Line Delineation and Mouth Management Recommendations. Report No. PE 243. SMEC Holdings Limited.

- Carr, A., Thomas, D., Bateman, M., 2006. Climatic and sea level controls on Late Quaternary eolian activity on the Agulhas Plain, South Africa. *Quaternary Research*, 65(02), pp.252-263.
- Cazals, C., Rapinel, S., Frison, P.L., Bonis, A., Mercier, G., Mallet, C., Corgne, S., Rudant, J.P., 2016. Mapping and characterization of hydrological dynamics in a coastal marsh using high temporal resolution Sentinel-1A images. *Remote Sensing*, 8(7), p.570.
- Campbell, J., Wynne, R., 2013. *Introduction to Remote Sensing*. 5th ed. New York and London: The Guilford Press.
- Cole, C., Brooks, R., Wardrop, D., 1997. Wetland hydrology as a function of hydrogeomorphic (HGM) subclass. *Wetlands*, 17(4), pp.456-467.
- Church, J.A., Clark, P.U., Cazenave, A., Gregory, J.M., Jevrejeva, S., Levermann, A., Merrifield, M.A., Milne, G.A., Nerem, R.S., Nunn, P.D., Payne, A.J., Pfeffer, W.T., Stammer, D., Unnikrishnan A.S., 2013. Sea Level Change. In: *Climate Change 2013: The Physical Science Basis. Contribution of Working Group I to the Fifth Assessment Report of the Intergovernmental Panel on Climate Change* [Stocker, T.F., Qin, D., Plattner, G.-K., Tignor, M., Allen, S.K., Boschung, J., Nauels, A., Xia, Y., Bex, V., Midgley, P.M., (eds.)]. Cambridge University Press, Cambridge, United Kingdom and New York, NY, USA, pp.1137–1216. doi:10.1017/CBO9781107415324.026.
- Côté, I.M., Darling, E.S., 2010. Rethinking ecosystem resilience in the face of climate change. *PLoS biology*, 8(7), p.e1000438.
- Dai, A., Trenberth, K.E., Karl, T.R., 1998. Global variations in droughts and wet spells: 1900–1995. *Geophysical Research Letters*, 25(17), pp.3367-3370.
- Day Jr, J.W., Rybczyk, J., Scarton, F., Rismondo, A., Are, D., Cecconi, G., 1999. Soil accretionary dynamics, sea-level rise and the survival of wetlands in Venice Lagoon: A field and modelling approach. *Estuarine, Coastal and Shelf Science*, 49(5), pp. 607-628.
- Davies-Mostert, H., 2016. *Connochaetes gnou* – Black Wildebeest. Wildlife Endangered Trust. Available online: [https://www.ewt.org.za/reddata/pdf/Artiodactyla%20\(36%20assessments\)/2016%20Mammal%20Red%20List%20Connochaetes%20gnou%20LC.pdf](https://www.ewt.org.za/reddata/pdf/Artiodactyla%20(36%20assessments)/2016%20Mammal%20Red%20List%20Connochaetes%20gnou%20LC.pdf)

Dettinger, M.D., Diaz, H.F., 2000. Global characteristics of stream flow seasonality and variability. *Journal of Hydrometeorology*, 1, pp.289–310.

Deus, D., Gloaguen, R., 2013. Remote sensing analysis of lake dynamics in semi-arid regions: implication for water resource management. Lake Manyara, East African Rift, Northern Tanzania. *Water*, 5(2), pp.698-727.

Doña, C., Chang, N.B., Caselles, V., Sánchez, J.M., Pérez-Planells, L., Bisquert, M.D.M., GarcíaSantos, V., Imen, S., Camacho, A., 2016. Monitoring hydrological patterns of temporary lakes using remote sensing and machine learning models: Case study of la Mancha Húmeda Biosphere Reserve in central Spain. *Remote Sensing*, 8(8), pp.618.

Doody, J., 2013. Coastal squeeze and managed realignment in southeast England, does it tell us anything about the future?. *Ocean & Coastal Management*. 79, pp.34-41.

Dieppois, B., Rouault, M., New, M., 2015. The impact of ENSO on Southern African rainfall in CMIP5 ocean atmosphere coupled climate models. *Climate dynamics*, 45(9-10), pp.2425-2442.

Ding, Q., Chen, X., Hilborn, R., Chen, Y., 2017. Vulnerability to impacts of climate change on marine fisheries and food security. *Marine Policy*, 83, pp.55-61

Drexler, J., Ewel, K., 2001. Effect of the 1997-1998 ENSO-Related Drought on Hydrology and Salinity in a Micronesian Wetland Complex. *Estuaries*, 24(3), p.347.

Du, Z., Bin, L., Ling, F., Li, W., Tian, W., Wang, H., Gui, Y., Sun, B., Zhang, X., 2012. Estimating surface water area changes using time-series Landsat data in the Qingjiang River Basin, China. *Journal of Applied Remote Sensing*, 6(1), p.063609.

El-Asmar, H., Hereher, M., El Kafrawy, S., 2013. Surface area change detection of the Burullus Lagoon, North of the Nile Delta, Egypt, using water indices: A remote sensing approach. *The Egyptian Journal of Remote Sensing and Space Science*, 16(1), pp.119-123.

Euliss, N., Smith, L., Wilcox, D., Browne, B., 2008. Linking ecosystem processes with wetland management goals: Charting a course for a sustainable future. *Wetlands*, 28(3), pp.553-562.

Ellery, W., Grenfell, M., Grenfell, S., Kotze, D., McCarthy, D., Tooth, S., Grundling, P-L., Beckedahl, le Maitre, D., Ramsay, L., 2009. Wet Origins: Controls on the distribution and dynamics of wetlands in South Africa. Water Research Commission Research Report No. TT334/09. Water Research Commission, Pretoria.

Ellery, W.N., Grenfell, S.E., Grenfell, M.C., Powell, R., Kotze, D., Marren, P., Knight, J., 2016. Wetlands in southern Africa. In: Knight, J., Grab, S. (Eds.), Quaternary Environmental Change in Southern Africa: Physical and Human Dimensions. Cambridge University Press, Cambridge, UK, pp. 188–202.

Engelbrecht, F., Ndarana, T., Landman, W., van der Merwe, J., Ngwana, I., Muthige, M., 2015. Radiate Forcing of Southern African Climate Variability and Change. Water Research Commission Report No. 2163/1/15. Water Research Commission, Pretoria.

ESRI., 2018. *1-Differential GPS Explained*. [online] Esri.com. Available at: <http://www.esri.com/news/arcuser/0103/differential1of2.html> [Accessed 5 Feb. 2018].

Fauchereau, N., Trzaska, S., Rouault, M., Richard, Y., 2003. Rainfall variability and changes in southern Africa during the 20th century in the global warming context. *Natural Hazards*, 29(2), pp.139-154.

Friedrichs, C.T., Perry, J.E., 2001. Tidal salt marsh morphodynamics: A synthesis. *Journal of Coastal Research*, pp.7-37.

Gesch, D., 2009. Analysis of Lidar elevation data for improved identification and delineation of lands vulnerable to sea-level rise. *Journal of Coastal Research*, 10053, pp.49-58.

Grenfell, S.E., Rowntree, K.M., Grenfell, M.C., 2012. Morphodynamics of a gully and floodout system in the Sneeuwberg Mountains of the semi-arid Karoo, South Africa: Implications for local landscape connectivity. *Catena*, 89(1), pp.8-21.

Grenfell, S., Callaway, R., Grenfell, M., Bertelli, C., Mendzil, A., Tew, I., 2016. Will a rising sea sink some estuarine wetland ecosystems?. *Science of Total Environment*, 554-555, pp. 276-292.

Gereta, E., Wolanski, E., 1998. Wildlife–water quality interactions in the Serengeti National Park, Tanzania. *African Journal of Ecology*, 36(1), pp.1-14.

Gunderson, L.H., 2000. Ecological resilience – in theory and application. *Annual Review of Ecology and Systematics*, 31, pp.425-439.

Guo, M., Li, J., Sheng, C., Xu, J., Wu, L., 2017. A Review of Wetland Remote Sensing. *Sensors*, 17(4), pp.777.

Hartmann, D.L., Klein Tank, A.M.G., Rusticucci, M., Alexander, L.V., Bronnimann, S., Charabi, Y., Dentener, F.J., Dlugokencky, E.J., Easterling, D.R., Kaplan, A., Soden, B.J., Thorne, P.W., Wild, M., Zhai, P.M., 2013: Observations: Atmosphere and Surface. In: *Climate Change 2013: The Physical Science Basis. Contribution of Working Group I to the Fifth Assessment Report of the Intergovernmental Panel on Climate Change* [Stocker, T.F., Qin, D., Plattner, G.K., Tignor, M., Allen, S.K., Boschung, J., Nauels, A., Xia, Y., Bex, V., Midgley, P.M., (eds.)]. Cambridge University Press, Cambridge, United Kingdom and New York, NY, USA, pp.1137–1216. doi:10.1017/CBO9781107415324.026.

Havril, T., Tóth, Á., Molson, J., Galsa, A., Mádl-Szőnyi, J., 2018. Impacts of predicted climate change on groundwater flow systems: can wetlands disappear due to recharge reduction?. *Journal of Hydrology*, 563, pp.1169-1180.

Holling, C.S., 1973. Resilience and stability of ecological systems. *Annual Review of Ecology and Systematics*, 4, pp.1-23.

House, A., Thompson, J., Acreman, M., 2016. Projecting impacts of climate change on hydrological conditions and biotic responses in a chalk valley riparian wetland. *Journal of Hydrology*, 534, pp.178-192.

IPCC., 1990. *Climate Change 1990: The IPCC Scientific Assessment. Contributions of Working Group 1 to the First Assessment Report of the Intergovernmental Panel on Climate Change* [Houghton J.T., Jenkins, G.J., Ephraums, J.J (eds.)]. Cambridge University Press, Cambridge, Great Britain, New York, NY, USA and Melbourne, Australia, pp 1-410.

IPCC., 1996. *Climate Change 1995: The Science of Climate Change: Contributions of Working Group 1 to the Second Assessment Report of the Intergovernmental Panel on Climate Change* [Houghton, J.T., Meira Filho, L.G, Callander, B.A., Harris., Kattenberg, A., Maskell K. (eds.)]. Cambridge University Press, Cambridge, United Kingdom and New York, NY, USA, PP. 1-572.

IPCC., 2001: Climate Change 2001: The Scientific Basis. Contribution of Working Group I to the Third Assessment Report of the Intergovernmental Panel on Climate Change [Houghton, J.T., Ding, Y., Griggs, D.J., Noguer, M., van der Linden, P.J., Dai, X., Maskell, K., Johnson, C.A. (eds.)]. Cambridge University Press, Cambridge, United Kingdom and New York, NY, USA, pp.1-881.

IPCC., 2007: Climate Change 2007: The Physical Science Basis. Contribution of Working Group I to the Fourth Assessment Report of the Intergovernmental Panel on Climate Change [Solomon, S., Qin, D., Manning, M., Chen, Z., Marquis, M., Averyt, K.B., Tignor, M., Miller H.L. (eds.)]. Cambridge University Press, Cambridge, United Kingdom and New York, NY, USA, pp. 1-996.

IPCC., 2013: Climate Change 2013: The Physical Science Basis. Contribution of Working Group I to the Fifth Assessment Report of the Intergovernmental Panel on Climate Change [Stocker, T.F., Qin D., Plattner, G.-K., Tignor, M., Allen, S.K., Boschung, J., Nauels, A., Xia, Y., Bex, V., Midgley, P.M. (eds.)]. Cambridge University Press, Cambridge, United Kingdom and New York, NY, USA, 1535 pp. doi:10.1017/CBO9781107415324.

Jankowski, K.L., Törnqvist, T.E., Fernandes, A.M., 2017. Vulnerability of Louisiana's coastal wetlands to present-day rates of relative sea-level rise. *Nature Communications*, 8, p.14792.

Ji, L., Zhang, L., Wylie, B., 2009. Analysis of dynamic thresholds for the normalized difference water index. *Photogrammetric Engineering & Remote Sensing*, 75(11), pp.1307-1317.

Ji, X., Li, Y., Luo, X., He, D., 2018. Changes in the lake area of Tonle Sap: Possible linkage to runoff alterations in the Lancang River?. *Remote Sensing*, 10(6), p.866.

Jones, K., Lanthier, Y., van der Voet, P., van Valkengoed, E., Taylor, D., Fernández- Prieto, D., 2009. Monitoring and assessment of wetlands using Earth Observation: The GlobWetland project. *Journal of Environmental Management*, 90(7), pp.2154-2169.

Kane, R., 2009. Periodicities, ENSO effects and trends of some South African rainfall series: an update. *South African Journal of Science*, 105, pp.199-207.

Keddy, P., 2000. *Wetland ecology*. Cambridge, UK: Cambridge University Press.

- Kirwan, M., Temmerman, S., 2009. Coastal marsh response to historical and future sea-level acceleration. *Quaternary Science Reviews*, 28(17-18), pp.1801-1808.
- Klemas, V., 2011. Remote sensing techniques for studying coastal ecosystems: An overview. *Journal of Coastal Research*, 27, pp.2-17.
- Klein, R.J., Nicholls, R.J., Thomalla, F., 2003. Resilience to natural hazards: How useful is this concept?. *Global Environmental Change Part B: Environmental Hazards*, 5(1), pp.35-45.
- Kotze, D.C., Breen, C., Nxele, I., Kareko, J., 2009. WET-Management Review: The impact of natural resource management programmes on wetlands in South Africa. Water Research Commission Research Report No. TT335/09. Water Research Commission, Pretoria.
- Kraaij, T., Hanekom, N., Russell, I.A., Randall, R.M., 2008. Agulhas National Park - State of Knowledge. South African National Parks.
- Krishnamurthy, P., Lewis, K., Choularton, R., 2018. Climate impacts on food security and nutrition: a review of existing knowledge. [online] Met Office and WFP's Office for Climate Change, Environment and Disaster Risk Reduction. Available at: <https://www.wfp.org/content/climate-impacts-food-security-and-nutrition-review-existingknowledge> [Accessed 6 Nov. 2018].
- Kumbier, K., Cabral Carvalho, R., Vafeidis, A.T., Woodroffe, C.D., 2017. Modelling inundation extents of the June 2016 storm surge in estuarine environments using static and dynamic approaches.
- Lambert, C.P., Walling, D.E., 1987. Floodplain sedimentation: A preliminary investigation of contemporary deposition within the lower reaches of the River Culm, Devon, UK. *Geografiska Annaler: Series A, Physical Geography*, 69(3-4), pp.393-404.
- Law, A., Gaywood, M.J., Jones, K.C., Ramsay, P., Willby, N.J., 2017. Using ecosystem engineers as tools in habitat restoration and rewilding: beaver and wetlands. *Science of the Total Environment*, 605, pp.1021-1030.
- Lewison, R., 2007. Population responses to natural and human-mediated disturbances: assessing the vulnerability of the common hippopotamus (*Hippopotamus amphibius*). *African Journal of Ecology*, 45(3), pp.407-415.

Liang, K., Yan, G., 2017. Application of Landsat Imagery to Investigate Lake Area Variations and Relict Gull Habitat in Hongjian Lake, Ordos Plateau, China. *Remote Sensing*, 9(10), p.1019.

Li, W., Du, Z., Ling, F., Zhou, D., Wang, H., Gui, Y., Sun, B., Zhang, X., 2013. A comparison of Land surface water mapping using the normalized difference water index from TM, ETM+ and ALI. *Remote Sensing*, 5(11), pp.5530-5549.

Lumbierres, M., Méndez, P.F., Bustamante, J., Soriguer, R., Santamaría, L., 2017. Modeling biomass production in seasonal wetlands using MODIS NDVI land surface phenology. *Remote Sensing*, 9(4), p.392.

Malherbe J., Engelbrecht F.A., Landman W.A., 2013. Projected changes in tropical cyclone climatology and landfall in the Southwest Indian Ocean region under enhanced anthropogenic forcing. *Climate Dynamics*, 40 (11-12), pp.2867-2886.

Martinez, M.L., Taramelli, A., Silva, R., 2017. Resistance and resilience: Facing the multidimensional challenge in coastal areas. *Journal of Coastal Research*. 77, pp1-6.

McCarthy, T., Cooper, G., Tyson, P., Ellery, W., 2000. Seasonal flooding in the Okavango Delta, Botswana- recent history and future prospects. *South African Journal of Science*, (69), pp.25-33.

McFeeters, S.K., 1996. The use of the Normalized Difference Water Index (NDWI) in the delineation of open water features. *International journal of remote sensing*, 17(7), pp.1425-1432.

Mensik, J.G., Pavaglio, F.L., 2004. Biological integrity, diversity, and environmental health policy and the attainment of refuge purposes: a Sacramento National Wildlife Refuge case study. *Natural Resources Journal*, pp.1161-1183.

Millennium Ecosystem Assessment., 2005. Ecosystems and Human Well-being: Current State and Trends. vol. 1. World Resources Institute, Washington, DC.

Mitsch, W., Gosselink, J., 2015. *Wetlands*. 5th ed. John Wiley & Sons.

Mohamed, Y., Savenije, H.H.G., 2014. Impact of climate variability on the hydrology of the Sudd wetland: signals derived from long-term (1900–2000) water balance computations. *Wetlands Ecology and Management*. 22, 191–198.

Mogensen, L.A., Rogers, K., 2018. Validation and Comparison of a Model of the Effect of Sea-Level Rise on Coastal Wetlands. *Scientific reports*, 8(1), p.1369.

Moore, J.W., 2006. Animal ecosystem engineers in streams. *AIBS Bulletin*, 56(3), pp.237-246.

Morioka, Y., Engelbrecht, F., Behera, S., 2015. Potential sources of decadal climate variability over southern Africa. *Journal of Climate*, 28(22), pp.8695-8709.

Morris, J., Sundareshwar, P., Nietch, C., Kjerfve, B., Cahoon, D., 2002. Responses of coastal wetlands to rising sea level. *Ecology*. 83(10), pp.2869-2877.

Muller, S., Muñoz-Carpena, R., Kiker, G., 2011. Model Relevance. In *Climate* (pp. 39-65). Springer, Dordrecht.

Murphy, B.F., Timbal, B., 2008. A review of recent climate variability and climate change in southeastern Australia. *International Journal of Climatology: A Journal of the Royal Meteorological Society*, 28(7), pp.859-879.

Murray, N.J., Phinn, S.R., Clemens, R.S., Roelfsema, C.M., Fuller, R.A., 2012. Continental scale mapping of tidal flats across East Asia using the Landsat archive. *Remote Sensing*, 4(11), pp.3417-3426.

Nel, W., 2009. Rainfall trends in the KwaZulu-Natal Drakensberg region of South Africa during the twentieth century. *International Journal of Climatology*, 29(11), pp.1634-1641.

Neumann, J.E., Yohe, G, Nicholls, R., Manion M., 2000. Sea-level rise and global climate change: A review of impacts to U.S. Coasts. Pew Centre on Global Climate Change. Available from www.c2es.org/document/sea-level-rise-global-climate-change-a-review-of-impacts-tou-s-coasts/. [accessed 4 February 2018].

Nicholls, R., 2004. Coastal flooding and wetland loss in the 21st century: changes under the SRES climate and socio-economic scenarios. *Global Environmental Change*, 14(1), pp.69-86.

Nicholls, R., Hoozemans, F., Marchand, M., 1999. Increasing flood risk and wetland losses due to global sea-level rise: regional and global analyses. *Global Environmental Change*. 9, pp. S69-S87.

Ning, S., Ishidaira, H., Udmale, P., Ichikawa, Y., 2015. Remote sensing based analysis of recent variations in water resources and vegetation of a semi-arid region. *Water*, 7(11), pp.6039-6055.

Niang I, Ruppel O.C., Abdrabo M., Essel, A., Lennard, C., Padgham, J., Urquhart, P., Adelekan, I., Archibald, S., Barkhordarian, A., Battersby, J., Balinga, M., Bilir, E., Burke, M., Chahed, M., Chatterjee, M., Chidiezie, C.T., Descheemaeker, K., Djoudi, H., Ebi, K.L., Fall, P.D., Fuentes, R., Garland, R., Gaye F., Hilmi, K., Gbobaniyi, E., Gonzalez, P., Harvey, B., Hayden, M., Hemp, A., Jobbins, G., Johnson, J., Lobell, D., Locatelli, B., Ludi, E., Otto Naess, L., Ndebele-Murisa, M.R., Ndiaye, A., Newsham, A., Njai, S., Nkem Olwoch, J.M., Pauw, P., Pramova, E., Rakotondrafara, M-L., Raleigh, C., Roberts, D., Roncoli, C., Sarr, A.T., Schleyer, M.H., Schulte-Uebbing L., Schulze, R., Seid, H., Shackleton, S., Shongwe, M., Stone, D., Thomas, D., Ugochukwu, O., Victor, D., Vincent, K., Warner, K., Yaffa, S., 2014. IPCC WGII AR5 Chapter 22. pp 1- 115.

Novitzki, R. P., 1982. Hydrology of Wisconsin wetlands. U.S. Department of the Interior, Geological Survey and University of Wisconsin-Extension, Geological and Natural History Survey. Madison, WI, USA. Information Circular 40.

Oettli, P., Tozuka, T., Izumo, T., Engelbrecht, F., Yamagata, T., 2013. The self-organizing map, a new approach to apprehend the Madden–Julian Oscillation influence on the intraseasonal variability of rainfall in the southern African region. *Climate Dynamics*, 43(5-6), pp.1557-1573.

Ollis, D.J., Snaddon, C.D., Job, N.M., Mbona, N., 2013. Classification system for wetlands and other aquatic ecosystems in South Africa. User Manual: Inland Systems. SANBI Biodiversity Series 22. South African National Biodiversity Institute, Pretoria, South Africa.

Patrick W.H., DeLaune R.D., 1990. Subsidence, accretion, and sea-level rise in south San Francisco Bay marshes. *Limnology and Oceanography*, 35(6): pp.1389–1395.

Philippon, N., Rouault, M., Richard, Y., Favre, A., 2012. The influence of ENSO on winter rainfall in South Africa. *International Journal of Climatology*, 32(15), pp.2333-2347.

Pohl, B., Fauchereau, N., Reason, C., Rouault, M., 2010. Relationships between the Antarctic Oscillation, the Madden–Julian Oscillation, and ENSO, and consequences for rainfall analysis. *Journal of Climate*, 23(2), pp.238-254.

- Poulter, B., Halpin, P., 2008. Raster modelling of coastal flooding from sea-level rise. *International Journal of Geographical Information Science*, 22(2), pp.167-182.
- Ramirez, J.A., Lichter, M., Coulthard, T.J., Skinner, C., 2016. Hyper-resolution mapping of regional storm surge and tide flooding: comparison of static and dynamic models. *Natural Hazards*, 82(1), pp.571-590.
- Reason, C.J.C., Jagadheesha, D., Tadross, M., 2003. A model investigation of inter-annual winter rainfall variability over southwestern South Africa and associated ocean-atmosphere interaction. *South African journal of science*, 99(1-2), pp.75-80.
- Reason, C., Landman, W., Tennant, W., 2006. Seasonal to decadal prediction of southern African climate and its links with variability of the Atlantic Ocean. *Bulletin of American Meteorological Society*, 87(7), pp.941-955.
- Reed, D., 2002. Sea-level rise and coastal marsh sustainability: geological and ecological factors in the Mississippi delta plain. *Geomorphology*, 48(1-3), pp.233-243.
- Riddell, E., Everson, C., Clulow, A., Mengistu, M., 2013. The hydrological characterisation and water budget of a South African rehabilitated headwater wetland system. *Water SA*, 39(1), pp 57-66.
- Robock, A., 2000. Volcanic eruptions and climate. *Reviews of Geophysics*, 38(2), pp.191-219.
- Rodríguez, J.F., Saco, P.M., Sandi, S., Saintilan, N., Riccardi, G., 2017. Potential increase in coastal wetland vulnerability to sea-level rise suggested by considering hydrodynamic attenuation effects. *Nature communications*, 8, p.16094.
- Rokni, K., Ahmad, A., Selamat, A., Hazini, S., 2014. Water feature extraction and change detection using multi-temporal Landsat imagery. *Remote Sensing*, 6(5), pp.4173-4189.
- Rogers, K., Saintilan, N., Copeland, C., 2012. Modelling wetland surface elevation dynamics and its application to forecasting the effects of sea-level rise on estuarine wetlands. *Ecological Modelling*. 244, pp.148-157.

Scheiter, S., Gaillard, C., Martens, C., Erasmus, B., Pfeiffer, M., 2018. How vulnerable are ecosystems in the Limpopo province to climate change?. *South African Journal of Botany*, 116, pp.86-95.

Schuerch, M., Rapaglia, J., Liebetrau, V., Vafeidis, A., Reise, K., 2001. Salt marsh accretion and storm tide variation: An example from a Barrier Island in the North Sea. *Estuaries Coasts*, 35(2), pp. 468-500.

Schulze, R.E., 1997. South African Atlas of Agrohydrology and Climatology. Water Research Commission Report No TT82/96, Pretoria.

South Africa., 2007. South Africa 1:50 000 sheet 3420CA & CC Bredasdorp. Fourth edition. (Map). Cape Town: Chief Directorate of National Geospatial Information.

Short, F., Kosten, S., Morgan, P., Malone, S., Moore, G., 2016. Impacts of climate change on submerged and emergent wetland plants. *Aquatic Botany*, 135, pp.3-17.

Smith, R.A.J., Rhiney, K., 2016. Climate (in) justice, vulnerability and livelihoods in the Caribbean: The case of the indigenous Caribs in northeastern St. Vincent. *Geoforum*, 73, pp.22-31.

Snowling, S.D., Kramer, J.R., 2001. Evaluating modelling uncertainty for model selection. *Ecological modelling*, 138(1-3), pp.17-30.

South Africa 2002. *South Africa 1:50 000 sheet 3419 DB&DD Elim*. Fourth edition. (Map). Cape Town: Chief Directorate of National Geospatial Information.

Temmerman, S., Govers, G., Wartel, S., Meire, P., 2004. Modelling estuarine variations in tidal marsh sedimentation: Response to changing sea level and suspended sediment concentrations. *Marine Geology*, 212(1-4), pp.1-19.

Teng, J., Jakeman, A.J., Vaze, J., Croke, B.F., Dutta, D., Kim, S., 2017. Flood inundation modelling: A review of methods, recent advances and uncertainty analysis. *Environmental Modelling & Software*, 90, pp.201-216.

- Titus, J., 1991. Greenhouse effect and coastal wetland policy: How Americans could abandon an area the size of Massachusetts at minimum cost. *Environmental Management*, 15(1), pp. 39-58.
- Tulbure, M.G., Broich, M., 2013. Spatiotemporal dynamic of surface water bodies using Landsat time-series data from 1999 to 2011. *ISPRS Journal of Photogrammetry and Remote Sensing*, 79, pp.44-52.
- Tooth, S., McCarthy, T., 2007. Wetlands in drylands: geomorphological and sedimentological characteristics, with emphasis on examples from southern Africa. *Progress in Physical Geography*, 31(1), pp.3-41.
- Tooth, S., 2018. The geomorphology of wetlands in drylands: Resilience, non-resilience, or...?. *Geomorphology*, 305, pp.33-48.
- Tyson, P., 1981. Atmospheric circulation variations and the occurrence of extended wet and dry spells over Southern Africa. *Journal of Climatology*, 1(2), pp.115-130.
- Tyson, P., Preston-Whyte, R., 2000. The weather and climate of southern Africa. Cape Town: Oxford University Press.
- Tyson, P.D., Cooper, G.R.J., McCarthy, T.S., 2002. Millennial to multi-decadal variability in the climate of southern Africa. *International Journal of Climatology*, 22(9), pp.1105-1117.
- United Nations., 2003. Project document: Agulhas Biodiversity Initiative (ABI). New York: United Nations Development Programme Global Environmental Facility.
- Van Goor, M., Zitman, T., Wang, Z., Stive, M., 2003. Impact of sea-level rise on the morphological equilibrium state of tidal inlets. *Marine Geology*, 202(3-4), pp.211-227.
- Vilina, Y., Cofre, H., 2000. "El Niño" effects on the abundance and habitat association patterns of four Grebes species in Chilean wetlands. *Waterbirds*, pp.95-101.
- Vogel, C., 2000. Climate and climatic change: causes and consequences. In: R. Fox and K. Rowntree, ed., *The Geography of South Africa in a Changing World*, 1st ed. Oxford University Press, pp.284-303.

Vousdoukas, M.I., Mentaschi, L., Voukouvalas, E., Verlaan, M., Jevrejeva, S., Jackson, L.P., Feyen, L., 2018. Global probabilistic projections of extreme sea levels show intensification of coastal flood hazard. *Nature communications*, 9(1), p.2360.

Wang, Y., Huang, F., Wei, Y., 2013, June. Water body extraction from LANDSAT ETM+ image using MNDWI and KT transformation. In *Geo-informatics (GEOINFORMATICS), 2013 21st International Conference on* (pp. 1-5). IEEE.

Wang, G., Wang, M., Lu, X., Jiang, M., 2016. Surface elevation change and susceptibility of coastal wetlands to sea level rise in Liaohe Delta, China. *Estuarine Coastal Shelf Science*. 180, pp. 204-211.

Wei, X., Liu, W., Zhou, P., 2013. Quantifying the relative contributions of forest change and climatic variability to hydrology in large watersheds: a critical review of research methods. *Water*, 5(2), pp.728-746.

Xu, H., 2006. Modification of normalised difference water index (NDWI) to enhance open water features in remotely sensed imagery. *International Journal of Remote Sensing*, 27(14), pp.3025-3033.

Yaffee, S., 1999. Three Faces of Ecosystem Management. *Conservation Biology*, 13(4), pp.713-725.

Zanter, K., 2017. Landsat Collection 1 Level 1 Product Definition. United States Geological Survey

Zanter, K., 2018. Landsat 7 (L7) Data user's handbook. United States Geological Survey

Zedler, J., Kercher, S., 2005. Wetland resources: status, trends, ecosystem services and restorability. *Annual Review of Environment and Resources*, 30(1), pp.39- 74.

Zhang, Y., Li, W., Sun, G., King, J., 2018. Coastal wetland resilience to climate variability: A hydrologic perspective. *Journal of Hydrology*, 568, pp.275-284.